博士論文（要約）

Global gene expression analysis on the formation of pearl sac and pearl by allografting in *Pinctada fucata*

（*Pinctada fucata* 同種間移植による真珠袋および真珠形成過程の網羅的遺伝子発現解析）

マリオム

Global gene expression analysis on the formation of pearl sac and pearl by allografting in *Pinctada fucata*

（*Pinctada fucata* 同種間移植による真珠袋および真珠形成過程の網羅的遺伝子発現解析）

A
Thesis submitted to
Graduate School of Agricultural and Life Sciences
The University of Tokyo
in partial fulfillment of the requirements
for the degree of

Doctor of Philosophy (PhD)
in
Department of Aquatic Bioscience

By
Mariom
August 2019

DECLARATION

I, Mariom, hereby declare that the thesis entitled "**Global gene expression analysis on the formation of pearl sac and pearl by allografting in *Pinctada fucata***" is an authentic record of the work done by me and that no part thereof has been presented for the award of any degree, diploma, associateship, fellowship or any other similar title.

31 May 2019

Mariom

Laboratory of Aquatic Molecular Biology and Biotechnology

Department of Aquatic Science,

Graduate school of agriulturural and life sciences,

The university of tokyo

DEDICATION

In the name of "Almighty Allah", most gracious, most merciful

This thesis has been dedicated to my lovely daughter
'Samiha Mahnoor Alam'

-the best gift and inspiration of my life

ACKNOWLEDGEMENTS

The author wishes to acknowledge all commend and gratitude to "Almighty Allah", the great, gracious, merciful and supreme ruler of the universe, who enabled her to complete the research work successfully for the degree of Doctor of Philosophy (PhD) in the University of Tokyo.

The author expresses her abstruse indebtedness and sincerest gratitude to her reverend academic advisor and research supervisor, Associate Professor Dr. Shigeharu Kinoshita, Laboratory of Aquatic Molecular Biology and Biotechnology, Department of Aquatic Bioscience, The University of Tokyo, for his scholastic supervision, valuable suggestions, solitary instructions, constructive criticism, constant encouragement and kind cooperation in carrying out this research. The author also expresses her deepest sense of gratitude to the Head of the laboratory, Professor Dr. Shuichi Asakawa for his indefatigable supervision, pleasant manner, admirable patience, friendly advice and fruitful criticism to improve the thesis. The author owes to them not only for the study but also for extending their help in many other aspects during her stay in Japan. A supervisor like Kinoshita sensei is really very rare. The author will never forget him.

Special heartfelt gratitude is extended to Assistant Professor, Dr. Kazutoshi Yoshitake for his valuable suggestions, kind cooperation, affectionate and constructive criticism throughout the entire period of this particular research work. Their regular guidance and supervision helped tremendously to improve the technical and scientific knowledge of the author in the field of aquatic molecular biology and biotechnology.

The author also would like to express her heartfelt eternal gratitude, enthusiastic appreciation and immense indebtedness to Professor Dr. Shugo Watabe for his reviewing, frequent assistance and tremendous attention, valuable comments and suggestions towards further improving the thesis. The author would like to give special thanks to Professor Dr. Shigeki Matsunaga and Associate Professor Dr. Michio Suzuki for their meticulous reviewing and valuable comments and suggestions.

The author feels proud to express her immense indebtedness and deep regards to Dr. Yoji Igarashi for his endless support and kind cooperation during the course of the research work. The author also would like to extend her special grateful thanks to all the members of the Laboratory of Aquatic Molecular Biology and Biotechnology for their reinforcement, constant encouragement and assistance during the study. The author is pleased to extend her gratitude to the staff of the OICE for their enthusiastic endeavor and mutual aid, strong support, fruitful advices and kind co-operation during the study period.

The author also wishes to take the great privilege to acknowledge the Mikimoto pearl farm, Mie for providing with experimental facilities and assistance to conduct this research work. Special grateful thanks is expanded to Dr. Kiyohito Nagai and Dr. Kaoru Maeyama for their wholehearted guidance and continuous support.

The author owes special debts of gratitude to her beloved parents, parents-in-law, brothers, brother and sister-in-laws for their endless love and blessings, inspiration and encouragements, valuable advices and a lot of sacrifice in all respect throughout the study period that paved the way of her time in this University. Special heartfelt thanks goes to her life partner Md. Khurshed Alam (Sagor) and her daughter Samiha Mahnoor Alam for their continuous support and sacrifice to move the study to a successful end that makes the dream come true.

Finally, the author wishes to take the opportunity to acknowledge the Ministry of Education, Culture, Sports, Science and Technology, Japan for awarding her with the MUNBUKAGAKUSHO Scholarship (MEXT) without which this study would have not been possible.

The Author
May 2019

CONTENTS

Abbreviations

$CaCO_3$	:	Calcium carbonate
CRISPR	:	Clustered regularly interspaced short palindromic repeats
DEGs	:	Differentially expressed genes
DSB	:	Double strand break
EGFR	:	Epidermal growth factor receptor
EPF	:	Extrapallial fluid
EPS	:	Extrapallial space
FGFR	:	Fibroblast growth factor receptor
HDR	:	Homology-directed repair
HMA	:	Heteroduplex mobility assay
HSP	:	Heat shock protein
IF	:	Inner fold of the mantle
MAPK	:	Mitogen activated protein kinase
MF	:	Middle fold of mantle
NC	:	Nacreous layer
NHEJ	:	Non-homologous end joining
OE	:	Outer epithelium
OF	:	Outer fold of the mantle
P	:	Periostracum
PAM	:	Protospacer adjacent motif
PAMs	:	Pathogen associated molecular profiles
PBS	:	Phosphate buffered saline
PCA	:	Principal component analysis
PCR	:	Polymerase chain reaction
PG	:	Periostracal groove
PL	:	Pallial line
PM	:	Pallial muscle
PN	:	Pallial nerve
PR	:	Prismatic layer
RT	:	Reverse transcriptase
SEM	:	Scanning electron microscope

SMP	:	Shell matrix proteins
SNP	:	Single nucleotide polymorphism
SNV	:	Single nucleotide variants
TLRs	:	Toll-like receptors
TPM	:	Transcripts per million

LIST OF TABLES

LIST OF FIGURES

Summary

Global gene expression analysis on the formation of pearl sac and pearl by allografting in *Pinctada fucata*

（*Pinctada fucata* 同種間移植による真珠袋および真珠形成過程の網羅的遺伝子発現解析）

The bivalve mollusk, *Pinctada fucata* is renowned worldwide for its ability of producing high quality spherical pearl and accounts for more than 90% of seawater pearl production. Pearls are the result of mollusk's capability to produce calcified shell materials in response to an injury to the mantle tissue. Mollusk shell is mainly composed of calcium carbonate ($CaCO_3$) crystals (>90% w/w) surrounded by an organic matrix (0.01% to 5% w/w) of proteins, lipids and polysaccharides. As in shell biomineralization, pearl formation is also regulated by the extracellular organic matrix secreted by the mantle tissue of mollusk.

Mantle grafting is the commonly practiced method for producing spherical pearl. The process involves a surgical implantation where a small piece (3 × 3 mm) of mantle tissue is excised from a suitable donor oyster and then implanted into the gonad of a host oyster along with an inorganic nucleus. Once transplanted, the outer epithelial cells of the graft start to proliferate and differentiate to give rise a monolayer of secretory epithelium around the nucleus termed as 'pearl sac'. The newly formed pearl sac gradually secretes various matrix proteins onto the nucleus in order to produce a lustrous pearl. Therefore, it is very reasonable to claim that, pearl sac formation is the critical step of pearl culture which eventually determines the success of culture.

Under normal condition, outer epithelium of mantle is a stable and mitotically inactive tissue, whereas the inner epithelial cells, contrarily, proliferate intermittently for the renewal of the tissue. Upon a mantle injury, the outer epithelial cells multiply actively to regenerate the injured site. The pearl sac formation simply resembles the wound healing process that occurs after a mantle injury. During mantle grafting, the external epithelial cells of the graft become active soon after surgical implantation and start to proliferate into a pearl sac. Other components of the graft, such as inner epithelial cells, muscles fibres and connective tissue eventually disappear. It is assumed that, the outer epithelium contains proliferating stem cells, but the feature of those cells is unclear. So, identification of genes involved in epithelial cell proliferation and differentiation is of utmost important to understand the mechanisms of pearl formation.

Shell or pearl biomineralization is a highly controlled biological process regulated by the cascades of a substantial number of genes. Though the mechanism of pearl formation has been studied largely, but the complex physiological process by which pearl sac and pearl is formed has not been properly understood yet. Using an RNAseq approach, here,

we aimed to reveal the genes involved in the development of pearl sac and pearl, and the sequential expression patterns of different shell matrix proteins (SMPs) secreted from the pearl sac during different stages of pearl formation. We also examined the pearl layers to scrutinize the microstructural characterization of the surface depositions on pearls.

1. Genes expressed during the proliferation of mantle epithelial cells into pearl sac

To describe the genes engaged in pearl sac formation, we performed RNA sequencing of mantle graft and the later pearl sac at different stages of pearl formation. During grafting experiments for three months, we collected nine samples: donor mantle epithelial cells, donor mantle pallium, donor mantle pallium on grafting, and mantle pallium each from the host at 24 hour, 48 hour, 1 week, 2 weeks, 1 months and 3 months post grafting. In the wound healing process, pearl sac was developed by two weeks of culture as indicated by the up-regulated Gene Ontology (GO) terms relevant to epithelial cell proliferation and differentiation. Kyoto Encyclopedia of Genes and Genomes (KEGG) pathway analysis showed that, immune genes were highly expressed ($P < 0.05$) between 0 h – 24 h in a donor dependent-manner and 48 h – 1 w in a host dependent-manner.

We screened out a number of genes including *JAG1, RFX3, STRC, FGFR2, SAV1, RAC1, DMD, RGMA, PTK7, MAF, MEF2A, SFRP5, TGM1, FZD1, GRHL2, TEAD1, PRKDC, LAMC1, EGFR, CASP8, CDC42, RSPO2, MTSS1, MATN1, SULF1, SPG20* and *LRP6* that may be involved in the proliferation and differentiation of mantle epithelial cells into pearl sac. Furthermore, it is the first time that, we identified some stem cell marker genes including *ABCG2, SOX2, MEF2A, HES1, MET, NRP1, ESR1, STAT6, PAX2, FZD1* and *PROM1* that were expressed differentially during pearl sac development. RT-PCR data showed ubiquitous expression of these stem cell marker genes in *P. fucata*, which further proposed their cell proliferation-related functions in different tissues. Additionally, qPCR results demonstrated that all these genes were highly expressed in mantle tissue suggesting their potential role in the proliferation of mantle epithelium into pearl sac. Furthermore, *PAX2* and *FZD1* were expressed higher in mantle compared to other tissues such as gonad and muscle.

2. Gene expression profiles at different stages of pearl formation during 3 months pearl culture

More than 200 molluscan biomineralization-related genes that contribute to the formation of shell and pearl have been identified till date. In this study, we screened out 192 genes likely involved in pearl biomineralization by blast search against a list of reference biomineralization genes prepared beforehand. It has been clearly defined that, the biomineralization genes are being secreted by the pearl sac developed from donor mantle graft, not by the host gonad tissue. So, the identified biomineralization-related genes in our study were expressed in the pearl sac, i.e., in the donor mantle epithelium.

Though the mantle tissue is primarily responsible for shell/pearl biomineralization, recent studies has also been reported that oyster hemocytes can mediate shell

biomineralization by secreting and transporting $CaCO_3$ crystals to the site of mineralization. Therefore, the interaction observed between donor mantle graft and surrounding host hemocytes immediately after grafting is very essential for the proper development of pearl sac and pearl.

Principal component analysis (PCA) precisely elucidates that the mineralization process during the first 3 months of culture is regulated differently. Further hierarchical clustering of 192 biomineralization-related genes showed clearly different expression profiles between the earlier (before 1 week) and later stages (1 week to 3 months) of pearl grafting. Detailed expression analysis of the major SMPs demonstrated that most of the prismatic layer forming SMPs were first up-regulated and then gradually down-regulated, indicating their involvement in the development of pearl sac and the onset of pearl mineralization. Most of the nacreous layer forming SMPs were up-regulated after the formation of pearl sac with the highest expression at 1 month, suggesting the completion of the nacreous layer formation. Nacrein, MSI7 and shematrin involved in both layer formation were highly expressed during 0 h – 24 h, down-regulated up to 1 week and then up-regulated again after maturation of pearl sac. Actually, these SMPs control and mediate the CaCO3 crystal formation. However, the genes highly expressed in the pearl sac may not be highly expressed in the mantle pallium. Therefore, the expression profiling of the SMPs can be used as a marker of the shell and pearl formation

3. Microstructural characterization of pearl layers recapitulates the mineralization sequence of pearl

Clear morphological differences were observed among the pearls obtained at 1 month and 3 months of culture. Surface examination of 1 month pearls revealed the variation in the initial mineralization among the pearls. Moreover, the nacre deposition at the early stage of pearl formation was not uniform throughout the surroundings of a given pearl. But at 3 months, the pearl surface became smoother and more regular with a pearl luster.

Scanning electron microscopy (SEM) demonstrated that an initial organic layer was deposited onto the nucleus surface before the secretion of prismatic and nacreous layers. But, the thickness of the organic material layer was variable among different pearls and even in different parts of the same pearl. Thus the initial mineralization of pearl is not simply the reappearance of the nacreous structures, rather it is more complex. The metabolic changes that occur in the mantle epithelial cells during its differentiation into a pearl sac may result in the formation of a new mineralizing sequence that is comparable to the structure of the shell. However, the prismatic layer of pearl is more diversified compared to the regular brick-wall like structures of nacre that develops later on it. Unlike the canonical mollusk shell, prismatic layer in pearl was composed of both aragonite and calcite prisms, organic materials and some unknown compounds.

The study recapitulates the mineralization sequence of pearl, where a heterogeneous prismatic layer is secreted first and followed by nacreous layer. Additionally, SEM

imaging confirmed the deposition of nacreous layer around the nucleus by 1 month that we predicted from our gene expression study.

Conclusion

The findings of the present study conclude two consecutive stages during the 3 months pearl culture. One is the initiation of pearl sac formation as part of the wound healing process in response to the oyster defense mechanism (before 1 week post grafting). Another is the maturation of pearl sac and deposition of organic matrices on the bare nucleus (2 week to 3 months). We figured out the key genes including some stem cell marker genes engaged in proliferation and differentiation of mantle epithelial cells into pearl sac. We also described the notable immune genes and pathways that provide insight into the increased understanding of the host immune reaction in response to accepting a graft.

The expression pattern of the key genes involved in the development of pearl sac and pearl elucidated that immune and cell proliferation related-genes were mostly enriched during earlier stages (before 2 weeks), whereas biomineralization genes were expressed in later stages (2 weeks to 3 months) of pearl grafting. The expression profiling of 192 biomineralization genes indicates that first 3 months of pearl biogenesis are very crucial when the pearl sac forms and secretes significant amount of nacre for making a lustrous pearl. Microstructural characterization of pearls explains the order of mineralization where a periostracum-like layer is secreted first before the deposition of the heterogeneous prismatic layer and the outermost nacreous layer onto the nucleus. CRISPR/Cas9 mediated gene editing suggests that it can be a simple but efficient tool for gene editing in pearl oyster towards improving the quality of cultured pearl.

The improved understanding of the molecular mechanism underlying the formation of pearl sac and pearl obtained from this study will provide a basis for future research towards upgrading the pearl culture practice and pearl quality. The study also gives some valuable information for identifying the functional genes implicated for pearl sac formation. However, further functional analyses are needed to verify the functions of the identified stem cell marker genes in pearl sac development.

List of Publications

The content of this thesis have been published as follows:

Mariom, S. Take, Y. Igarashi, K. Yoshitake, S. Asakawa, K. Maeyama, K. Nagai, S. Watabe and S. Kinoshita 2019. Gene expression profiles at different stages for formation of pearl sac and pearl in the pearl oyster *Pinctada fucata*. **BMC Genomics 20: 240**.

CHAPTER 1

General Introduction

1.1 General Background

1.1.1 The pearl oyster

The term 'pearl oyster' is generally applied to the marine bivalve mollusks from the genera *Pinctada* and *Pteria* under the feathered oyster family Pteriidae, (Skelton and Benton, 1993). Being members of a distinct family pearl oysters are not closely related to the true oysters (Ostreidae). *Pteria* spp. are usually used for producing half pearl or blister pearl (mabe pearl) in the Gulf of California, Mexico, Southeast Asia, Australia and in some Pacific island nations (Beer and Southgate, 2000; Kiefert et al., 2004; Ruiz-Rubio et al., 2006). *Pinctada* genus is well known throughout the world for the production of white or black round pearls of high commercial value. It is native to the Indo-Pacific region including Red sea, Persian Gulf, coastal waters of India, Western Pacific ocean, China, Korea and Japan. (Gervis and Sims, 1992; Matlins, 2001; Choi and Chang, 2003; Mohamed et al., 2006; Kripa et al., 2007; Strack, 2008; Wada and Temkin, 2008). Besides the pearl oysters, some other mollusks such as the freshwater mussels under the family Unionidae and Margaritiferidae, also yield pearls of commercial value (Zhu et al., 2019).

Presently, the oysters mainly used for producing spherical pearl are the *Pinctada fucata* (Akoya), *Pinctada maxima* (silver lipped), and *Pinctada margaritifera* (black lipped), along with freshwater mussels *Hyriopsis cumingii* (Southgate and Lucas, 2008; Torrey and Sheung, 2008). The Akoya pearl oyster *P. fucata* is one of the smallest pearl producing oysters, which is widely used to produce akoya pearls specially in China and Japan having a high market value (Kripa et al., 2007; Southgate and Lucas, 2008). Akoya pearls are renowned for their lustrous white colour with cream and pink overtones. *P. maxima* is the largest pearl oyster species that is used for the production of golden and silver South Sea pearls mainly in Indonesia, northern Australia, Philippines,

Malaysia and Myanmar (Southgate and Lucas, 2008). This species also accounts for the production of the largest cultured pearls. *P. margaritifera* is the second largest of the pearl oysters that is mainly cultured for black or Tahitian pearls in French Polynesia and the Cook Islands (Southgate and Lucas, 2008; Wada and Temkin, 2008).

1.1.2 Shell or pearl biomineralization

Biomineralization is a process in which inorganic ions orderly accumulate and deposit on the intracellular or extracellular matrix under the guidance of bio-macromolecules in living organisms (Lowenstam, 1981; Lowenstam and Weiner, 1989; Paine and Snead, 1997, Kröger et al., 2002; Hoang et al., 2003). Two major biomineralization products in nature are the mollusk shell and pearl. Molluscan exoskeleton (shell) is one of the most abundant biominerals that provides structural support, protection from predators and stressors, and contributes to physiological homeostasis (Crenshaw, 1972; Furuhashi et al., 2009; Haszprunar and Wanninger, 2012). Mollusk shell is mainly composed of calcium carbonate ($CaCO_3$) crystals (more than 90% by mass) with a framework of organic material (0.01% to 5% by mass) (Lowenstam and Weiner, 1989; Zhang and Zhang, 2006; Furuhashi et al., 2009). Though the organic macro-molecules typically constitute less than 5% (w/w) of the biomineralized shell, they play a central role in the nucleation, orientation, polymorphism, morphology, and organization of $CaCO_3$ crystallites in the shell (Belcher et al., 1996; Kong et al., 2009). The organic matrices in mollusk shell contain proteins, lipids, and polysaccharides such as chitin (Furuhashi et al., 2009). However, the basic structure and characteristic feature of the shell is common to all mollusk.

The pearl oyster *P. fucata* is a well-studied species in terms of shell or pearl biomineralization due to its commercial value in pearl farming. The shell of *P. fucata*

consists of a thin outermost organic layer, the periostracum, and two mineralized layers - the outer prismatic layer and the inner nacreous layer (Fig. 1.1) (Saruwatari et al., 2009; Furuhashi et al., 2009). The periostracum is a highly cross-linked proteinaceous layer that covers the external surface of the shell. It is assumed to act as a barrier between the extrapallial space and the outer environment (Saleuddin and Petit, 1983). It forms first and serves as an initial matrix for the calcified layers that subsequently deposits on it (Taylor and Kennedy, 1969; Nakahara and Bevelander, 1971; Checa, 2000). The prismatic layer is composed of calcite crystals, whereas the nacreous layer is made up of aragonite crystals (Furuhashi et al., 2009). Both the mineral layers are embedded in an organic matrix framework and these organic–inorganic microstructures give the molluscan shell huge mechanical strength and toughness (Taylor and Kennedy, 1969; Kamat et al., 2000; Okumura et al., 2012).

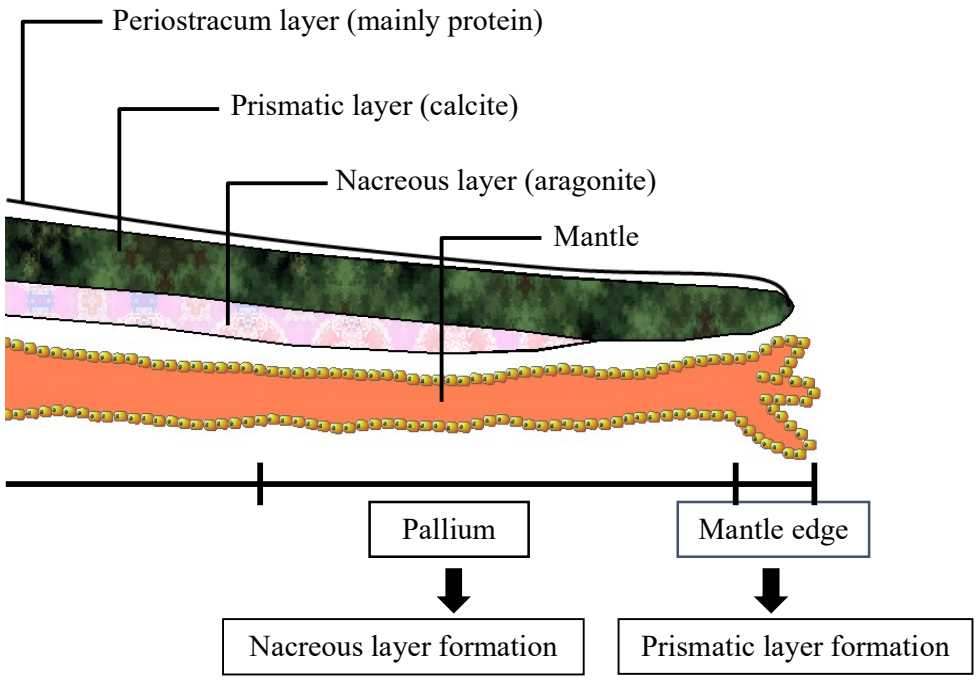

Figure 1.1. Schematic diagram of the cross-section of shell showing different shell layers in *P. fucata* (adapted from Kinoshita et al., 2011). Prismatic layer is secreted by mantle edge and nacreous layer is secreted by mantle pallium.

Shell formation is a highly controlled biological process that allows the mollusk to build their shells even in environments unfavorable for mineral precipitation (Carter, 1980; Ries et al., 2009; Beniash et al., 2010; Dickinson et al., 2013). In mollusk, mantle tissue is responsible for the formation of shell. The outer epithelial cells of the mantle secrete organic matrix called as shell matrix proteins (SMPs) and inorganic ions into the extrapallial space (EPS), the space between the shell and mantle, hence forming the extrapallial fluid (EPF) (Zhang and Zhang, 2006; Joubert et al., 2010). Thus mantle tissue supplies the periostracum and calcified layers with the inorganic ions and organic matrices necessary for mineralization of the shell through the EPF (Petit et al., 1980; Waller, 1980).

The oyster mantle is divided into three zones: mantle pallium, mantle edge and mantle centre (Fig. 1.2) (Chellam et al., 1991; Garcia-Gasca et al., 1994). Different parts of mantle contain regions of specialized epithelial cells that secrete a particular $CaCO_3$ polymorph for shell development. Thus, the periostracum is secreted from the groove of mantle and the prismatic layer is secreted by the outer epithelium of the mantle edge (Garcia-Gasca et al., 1994, Marie et al., 2012). Nacreous layer, on the other hand, is secreted by the mantle pallium and mantle centre (Fougerouse et al., 2008; Marie et al., 2012). Therefore, the outer epithelial cells of mantle play the key roles in the production and regeneration of a shell. In case of a shell damage or injury, the mantle starts to reform the shell in cooperation with the immune system (Watabe, 1983; Mount et al., 2004).

Pearls are the result of mollusk's capability to produce calcified shell materials in response to an injury to the mantle tissue through the secretions of mantle (Kawakami, 1952; Taylor and Strack, 2008). Unlike mollusk shell, the formation of pearl is an

accidental occurrence within the normal life cycle of a mollusk. During shell mineralization different cells secrete different shell layers, whereas during pearl formation the same cells secrete both the prismatic and nacreous layer (Marie et al., 2012).

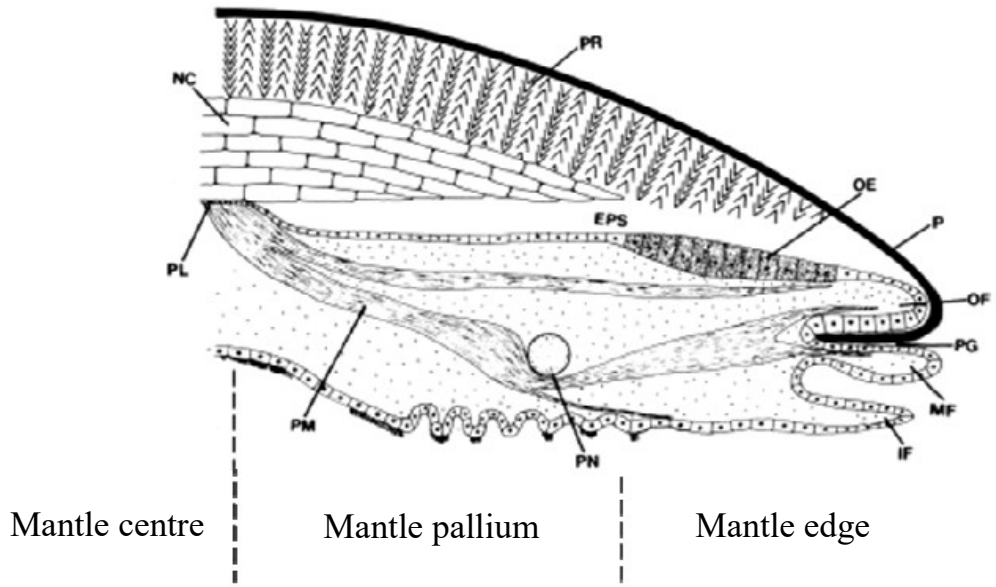

Figure 1.2. Diagrammatic cross-section of the growing mantle attached to a shell showing its different parts (Fougerouse et al., 2008). Mantle is divided into three regions namely, mantle edge, mantle pallium and mantle centre. PR: Prismatic layer, NC: nacreous layer, EPS: extrapallial space, MF: middle fold of mantle, OE: outer epithelium of the mantle, OF: outer fold of the mantle, IF: inner fold of the mantle, P: periostracum, PG: periostracal groove, PL: pallial line, PM: pallial muscle, PN: pallial nerve.

1.1.3 Pearl formation process

Pearls have always been objects of great value and have been used for adornment and as a symbol of material wealth throughout the human history. A pearl is a biological product produced naturally by certain oysters, mussels or clams in response to an irritant (Dakin, 1913; Taylor and Strack, 2008). Pearl is quite different than any other gems such

as diamond as it is produced inside the living animals by themselves. It is commonly known as the 'queen of jewels' (Ward, 1995).

Pearl is formed inside the mollusk when a foreign particle usually a parasite or sand particle finds its way into the animal and gets caught in the soft tissue of the mollusk (Fig. 1.3) (Dakin, 1913). This particle acts as the nucleus of the pearl from a very early stage. To get rid of the irritant, the mollusk starts to coat the foreign body with layers of nacre as a defense mechanism, and over time, a pearl begins to form (Taylor and Strack, 2008) (Fig. 1.3). Nacre is secreted by the epithelial cells of the mantle and is deposited until an iridescent pearl is formed (Kawakami, 1952). The unique luster of pearls comes from this nacre, which is also referred as the mother-of-pearl. Nacre is mainly composed of polygonal aragonitic tablets, a crystalline forms of calcium carbonate that also forms the interior layer of the mollusk shell (Watabe, 1965; Wada, 1968; Gregoire, 1972). Pearls can be of different colours depending on the natural pigment of the nacre and the shape of the pearl depends on the original shape of the irritant.

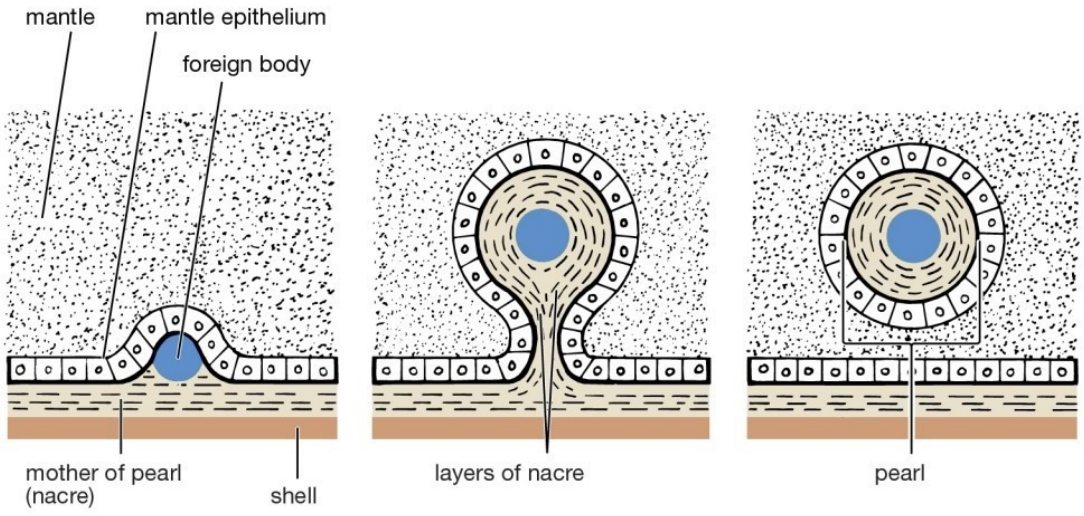

Figure 1.3. Diagram showing the formation of pearl in wild when a foreign body gets caught between the shell and mantle of the mollusk (Adapted from Dakin, 1913).

1.1.4 Mantle grafting and proliferation of mantle epithelial cells into a pearl sac

Pearl production in nature is an unpredictable and uncontrolled event which has been progressively overcome by human intervention through the pearl culture. Cultured pearls are produced through the modification of the process of natural pearl formation (Kawakami, 1952). The basic technique used to produce spherical pearls is the application of the piece method termed as 'seeding' or 'grafting' (Nagai, 2013). Grafting procedure invented by Mise-Nishikawa and improved by Mikimoto and his company at the beginning of the twentieth century is still used today to form beautiful and lustrous pearl (Taylor and Strack, 2008; Nagai, 2013).

Pearl culture begins with the collection and raising of donor and recipient oysters. Mantle grafting is the fundamental step in cultured pearl production. The grafting process involves a surgical implantation in which a tiny piece of mantle tissue (approximately 3 × 3 mm in size) termed as 'graft' is dissected out from a suitable donor oyster and transplanted with a spherical inorganic bead/nucleus into the pearl pouch of the recipient or host oyster (Fig. 1.4) (Kawakami, 1952; Taylor and Strack, 2008). Depending on the size and health condition of the oyster, one donor can be used for up to 25 host oysters mantle graft (Scoones, 1990). The grafting process induces an immunological reaction. Soon after implanting, the recipient oyster starts healing the wound as part of their immune defense by encapsulating the transgraft and the bead with surrounding hemocytes (Funakoshi, 2000). In the wound healing process, the granular hemocytes phagocytose tissue debris, whereas the agranular hemocytes secrete extracellular matrices (Suzuki et al., 1991; Suzuki and Funakoshi, 1992, Mount, et al., 2004; Ivanina et al., 2017; Huang et al., 2018). Once inserted into the receiving oyster, the external epithelial cells of the mantle graft multiply to form a thin mineralizing epithelium around the nucleus termed as 'pearl sac' in 30 to 50 days (Fig. 1.4 and 1.5)

(Machii, 1968; Awaji and Suzuki, 1995; Cochennec-Laureau et al, 2010). The process of pearl sac formation simply resembles the wound healing process that occurs after a mantle injury (Pauley and Heaton, 1969; Armstrong et al., 1971; Sminia et al., 1973). Other components of the graft, such as inner epithelial cells, muscle fibres and connective tissues eventually disappear (Machii, 1968; Cochennec-Laureau et al., 2010). The pearl sac subsequently starts to deposit a concentric layers of $CaCO_3$ polymorphs in the form of nacre onto the nucleus (Fig. 1.5) (Kawakami, 1952; Chen and Qian, 2009, Du et al., 2010). This is the starting point for the future pearl. The oysters are then reared for 15 to 18 months to get the final pearl with a sufficiently thick layer of nacre (0.8 mm).

The nucleus also plays a key-role in pearl formation. As it is manufactured from mollusk shells, it contains a small percentage of organics which can remarkably influence the quality of the final pearl (Cochennec-Laureau et al., 2010; Schmitt et al., 2018).

A period of 'conditioning' or pre-operative treatment is generally followed to prepare the oysters for implantation. The rate of survival and nucleus retention of the implanted oysters depends on many factors such as size and age of oysters, size of nucleus, grafting method and so on (Yukihira and Klumpp, 2006; Kripa et al., 2007). Proper post-operative care can reduce stress and thus maximize the nucleus and/or graft retention after implantation (Taylor and Strack, 2008).

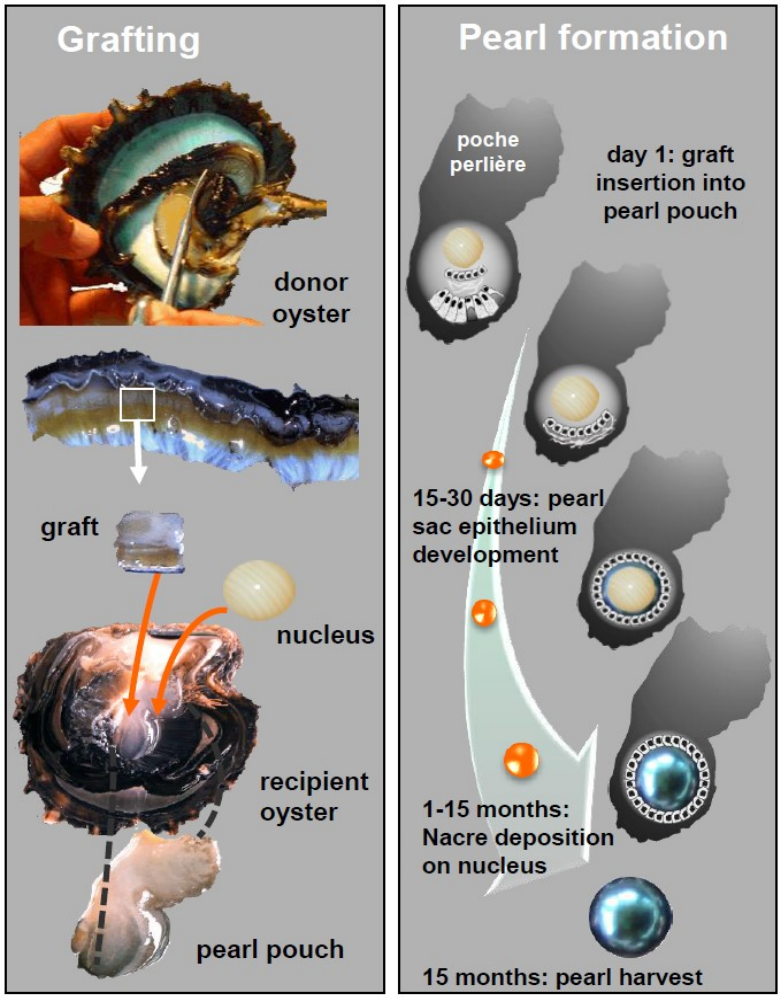

Figure 1.4. The different steps of mantle grafting and pearl formation in the pearl oyster (Gueguen et al., 2013). During the grafting process, a small piece of mantle tissue from the donor oyster (the graft) is inserted into the 'pearl pouch' of the host oyster together with a nucleus. After transplanting, the outer epithelial cells of the graft multiplies and forms a pearl sac around the nucleus. The pearl sac then starts to deposit aragonitic nacreous layers onto the nucleus. A rearing period of about 18 months is needed to harvest the final pearl.

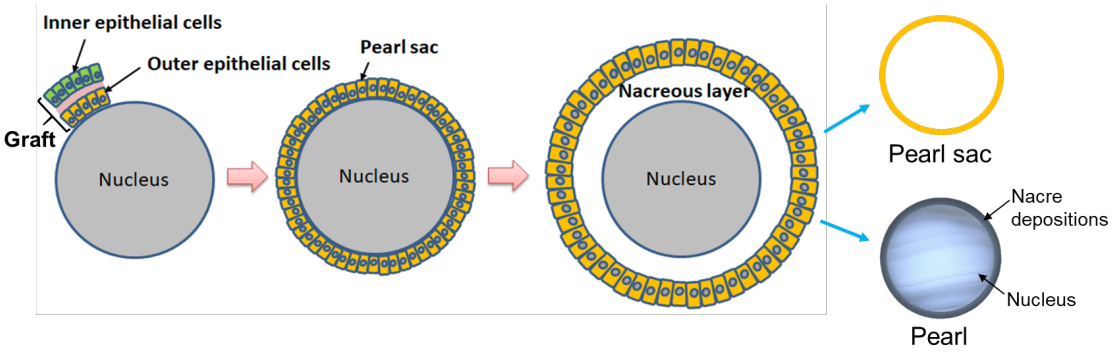

Figure 1.5. Proliferation of mantle epithelial cells into pearl sac during cultured pearl formation. Once implanted, the outer epithelial cells of the mantle graft tend to proliferate and differentiate to give rise a mono-layer of secretory epithelium termed as pearl sac that secretes various proteins to form the nacreous layer surrounding the nucleus.

1.2 Objectives of the study

Molluscan biomineralization is of great research interest and has been extensively studied in the last decades due to the tempting scientific, medicinal and commercial value of shells and pearls. The pearl oyster *P. fucata* is considered as an excellent model for the study of molluscan biomineralization owing to the availability of the draft genome and sequenced transcriptome of this species (Takeuchi et al., 2012; Takeuchi et al., 2016) as well as the availability of the information on the structure, mechanical properties and the mineral composition of the shell (Takeuchi and Endo, 2006; Nogawa et al., 2008; Kinoshita et al., 2011; Liu et al., 2015a; Li et al., 2016a). Although, these resources provide abundant information on shell architecture, ultrastructure and morphogenesis, but due to the complicated nature of molluscan biomineralization, it has not been fully realized so far (Furuhashi et al., 2009).

The mineralization process that occurs during the formation of shell and pearl is very similar (Taylor and Strack, 2008; Cuif et al., 2011). Though the mechanism of pearl formation in *Pinctada* has been studied extensively, the complex physiological process by which pearl sac and pearl is developed has not been well-understood yet. Moreover, the genes involved in pearl sac development and immune response are truly limited. Therefore, identification of functional genes in pearl sac will help to further understand the mechanism of pearl formation and immune response of the host oyster after grafting operation.

The present study was undertaken to achieve the following objectives:

a) To unravel the genes involved in the development of pearl sac and the immunological changes that occur upon graft transplantation in the pearl oyster *P. fucata*,

b) To screen out the biomineralization-related genes and their expression profiling at different stages for the formation of pearl sac and pearl in *P. fucata*,

c) To scrutinize the internal microcrystal biomineralization of pearls mediated by the pearl sac epithelium in *P. fucata*.

d) To develop an easy and efficient method of genome editing in the bivalve mollusk *P. fucata* using CRISPR/Cas9 system.

1.3. Summary/outline of the thesis

The thesis is composed of general introduction, three research chapters and general discussion. The research followed a chronological approach. First chapter (Chapter I) provides a general background of the study. Chapter 2 explains the molecular process involved in the formation of pearl sac through mantle grafting as an immunological response of the host oysters. It also describes the genes involved in the formation of pearl sac and the major immune related genes that expressed during pearl sac formation. Chapter 3 describes the expression profiling of all the genes that expressed during first three months of pearl development. Chapter 4 illustrates the microstructural characterization of the surface depositions on pearls obtained from chapter 2. The last chapter (Chapter 5) integrates and interprets all the finding obtained from the study and draws a conclusion and suggestions for further study.

CHAPTER 2

Transcriptome analysis reveals stem cell marker genes expressed during the proliferation of mantle epithelial cells into pearl sac in the pearl oyster, *Pinctada fucata*

First part of this chapter has been published as:

Mariom, S. Take, Y. Igarashi, K. Yoshitake, S. Asakawa, K. Maeyama, K. Nagai, S. Watabe and S. Kinoshita, 2019. Gene expression profiles at different stages for formation of pearl sac and pearl in the pearl oyster *Pinctada fucata*. **BMC Genomics 20: 240**.

Abstract

In pearl farming, a piece of mantle tissues excised from a donor oyster is implanted into a host oyster along with an inorganic nucleus. The outer epithelial cells of the mantle graft proliferate to form a pearl sac which gradually secretes various matrix proteins surrounding the nucleus that results into a lustrous pearl. Therefore, it is very reasonable to claim that pearl sac formation is the most important step of pearl culture that ultimately determines the success of culture. Using an RNAseq approach, we aimed to unravel the genes involved in the development of pearl sac during pearl formation. During grafting experiments for three months, we collected nine samples (donor mantle epithelial cells, donor mantle pallium, donor mantle pallium on grafting, and mantle pallium each from the host at 24 hour, 48 hour, 1 week, 2 weeks, 1 month and 3 months post grafting). Kyoto encyclopedia of genes and genomes (KEGG) pathway analysis showed that immune genes were highly expressed ($P < 0.05$) between 0 h – 24 h in a donor dependent-manner and 48 h – 1 w in a host dependent-manner. In the wound healing process, pearl sac was developed by two weeks of culture as indicated by the up-regulated Gene Ontology (GO) terms relevant to epithelial cell proliferation and differentiation. Moreover, the GO terms related to epithelial cell proliferation were down-regulated after two weeks of grafting. It is the first time that, we identified some stem cell marker genes including ABCG2, SOX2, MEF2A, HES1, MET, NRP1, ESR1, STAT6, PAX2, FZD1 and PROM1 that were expressed differentially during the formation of pearl sac. These results provide valuable information in understanding the molecular mechanism of pearl sac formation in *P. fucata*. However, further functional analyses are needed to confirm the roles of the identified genes in pearl sac formation.

2.1 Introduction

The bivalve mollusk, *Pinctada fucata* is well known throughout the world for its ability of producing high quality pearl and accounts for more than 90% of seawater pearl production (Southgate and Lucas, 2008). Artificial pearl production using this species was first industrialized in late 1890s in Japan (Nagai, 2013).

In pearl culture, a small piece of mantle tissue is dissected from a donor oyster and then transplanted into the gonad of a host oyster along with an inorganic bead (termed as 'nucleus') for nucleated-pearl production (Kawakami, 1952; Taylor and Strack, 2008). The outer surface of this mantle graft is covered by a monolayer of ciliated columnar epithelial cells with basal nuclei that undergoes proliferation and differentiation into a layer of secretory epithelium encircling the nucleus called 'pearl sac' (Aoki, 1966; Machii, 1968). The outer epithelium should contain proliferative stem cells that differentiate into pearl sac afterwards, but the features of those cells are unclear. After successful implantation, the growth and development of pearl sac depends on the interactions between donor graft cells and those of host gonad tissues. The graft tissue firmly clings to the gonad tissue with the proliferation of the epithelial cells and forms a pearl sac in course of time (Kishore and Southgate, 2016). The cells of the pearl sac obtain nourishment from the surrounding haemolymph (Chellam, 1991). Usually, it takes about 1 to 4 weeks to complete the development of pearl sac depending on several conditions like water temperature (Kawakami, 1953), season (Machii and Nakahara, 1957), sex of host oyster (Eddy et al., 2015), species (Awaji and Suzuki, 1995; Scoones, 1996; Kishore and Southgate, 2016) and so on. The epidermal cells (secretory epithelium) of the fully grown pearl sac gradually secrete and deposit various matrix proteins surrounding the nucleus that eventually results in the formation of a lustrous pearl (Kawakami, 1952; Aoki, 1966). The mineralization process that occurs during the

formation of cultured pearl is very similar to that of inner shell biomineralization regulated by the mantle (Kawakami, 1952; Taylor and Strack, 2008). Therefore, it is very reasonable to claim that pearl sac formation is the most important step of pearl culture that ultimately determines the success of culture.

Moreover, the surgical implantation practiced in pearl grafting can induce the immune reaction in host oyster to some extent in response to receiving a transplant and the oyster survival (Huang et al., 2015a; Wei et al., 2017a). Therefore, it is very important to explore the key genes involved in the immunological changes that occur upon graft transplantation. A transcriptome study in *P. martensii* detected some immune-related genes including HSP90, toll-like receptors (TLRs) and lysozyme from the pearl sac after 180 days of implantation (Zhao et al., 2012). Very recently, some studies examined the immune reaction of the pearl oyster hemocyte upon allografting (Wei et al., 2017a; Wang et al., 2017) and xenografting (Wei et al., 2017b) by transcriptome analysis. Some studies also explained that the process of the pearl-sac formation during pearl culture is identical to the wound healing process that occurs after a mantle injury (Armstrong et al., 1971; Awaji and Machii, 2011). However, the immunological reaction that appears in the donor mantle graft and in the host oyster during the subsequent stages of pearl sac formation is still unclear. Accordingly, increased understanding of the host immune response upon accepting a transplant is required to further improve the effectiveness of pearl culture technique.

With the development of versatile and cost-effective next generation sequencing technology, RNA sequencing has been extensively used in the genomic research of various organisms (Mortazavi et al., 2008; Qian et al., 2014). It allows a broad genome coverage with unbiased quantification of transcript expression in order to identify

important genes or pathways involved in various biological processes with their expression profiling (Mazzitelli et al., 2017; Huang et al., 2015b). In the present study, we therefore aimed to identify the genes playing a critical role in the formation of pearl sac using high-throughput transcriptome profiling. Moreover, we identified some stem cell marker genes differentially expressed during pearl sac development. Simultaneously, we screened out the key genes involved in the immunological changes that occur during pearl sac formation.

2.2 Materials and Methods

2.2.1 Experimental animal and mantle grafting

About 2 years old healthy pearl oysters, *P. fucata*, were used as donor and recipient for mantle grafting experiment. Mantle was dissected out from three donor oysters and a strip of mantle tissue was excised from mantle pallium for graft preparation and transplanted into 42 recipient oysters. Graft transplantation was performed by a skilled technician at the Mikimoto pearl farm, Mie, Japan. Two host oysters for each sampling received graft from the same donor (Fig. 2.1a). During grafting experiments for three months, we collected nine samples i.e. donor mantle epithelial cells (cell), donor mantle pallium (before), donor mantle pallium on grafting but before transplantation (0 h), 24 h, 48 h, 1 w, 2 w, 1 m, and 3 m post grafting) (Fig. 2.1b-c) and preserved in RNAlater® solution (Ambion, USA) at -80°C until RNA extraction. Mantle epithelial cells were separated as described by Awaji and Machi (2011). Due to the difficulty of separating pearl sac completely the pearl sac samples were contaminated with host gonad tissues especially 1 w, 2 w, 1 m, and 3 m samples.

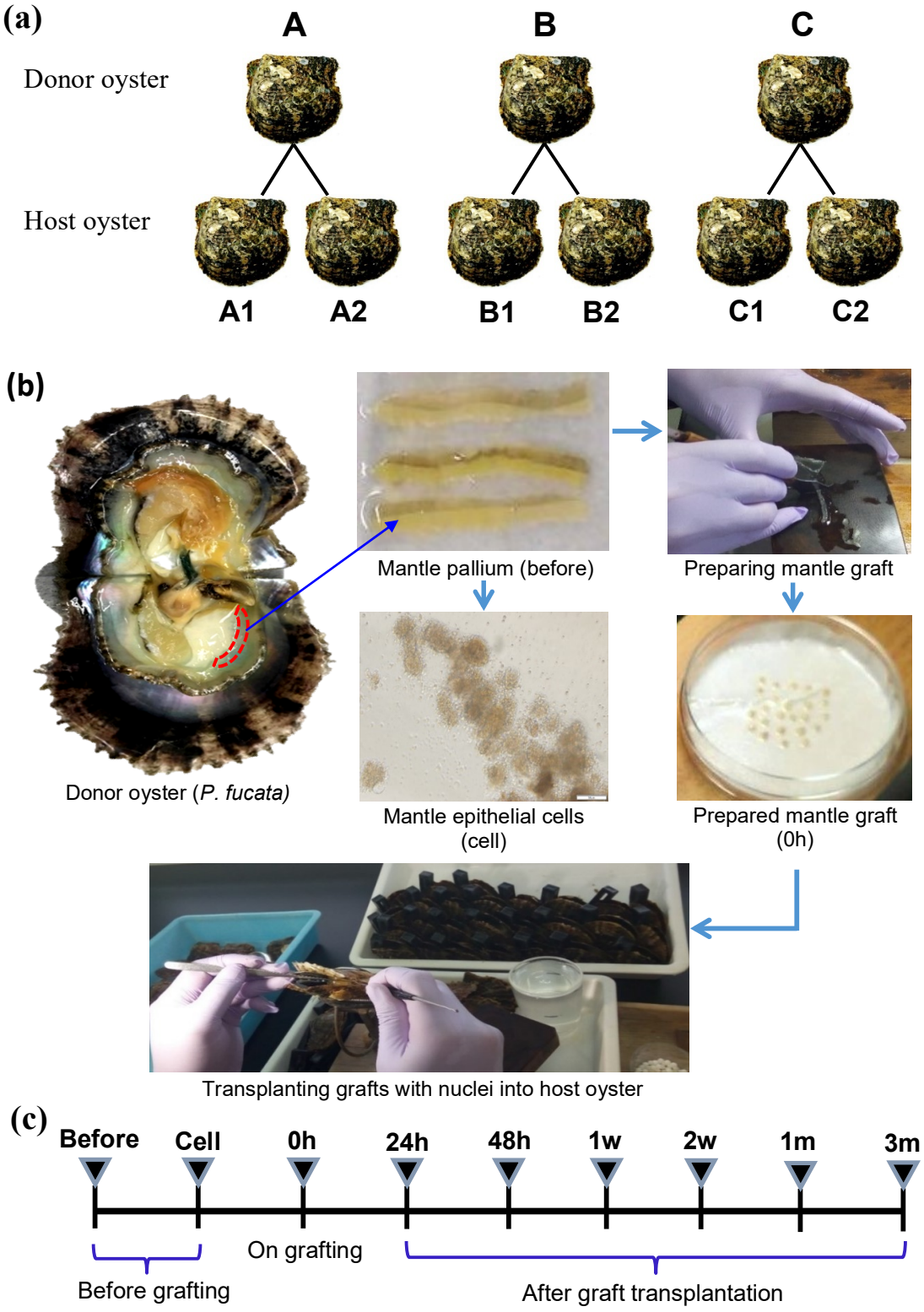

Figure 2.1. Experimental design for mantle grafting. (a) donor and host oysters used for grafting, (b) grafting process, and (c) sampling schedule. Briefly, a pallial zone of mantle was excised from the pearl oysters and sterilized. The pallium strips were then used to

prepare the grafts as well as to collect the epithelial cells, separately. “h” for hour, “w” for week and “m” for month.

2.2.2 RNA extraction and cDNA library preparation

Total RNA was extracted from the RNA later preserved samples with the RNeasy Mini Kit (QIAGEN, Hilden, Germany) according to the manufacturer’s instructions. RNA quality and integrity were assessed on an Agilent 2200 Tapestation (Agilent Technologies, CA, USA) using RNA ScreenTape. RNA concentrations were measured by Qubit® 2.0 Fluorometer RNA assay kit (Life Technologies, CA, USA).

A total of 2 µg RNA per sample was used as input materials for mRNA sample preparations. Sequencing libraries were generated using the TruSeq Stranded mRNA Library Prep Kit (Illumina, USA) following the manufacturer's recommendations. Briefly, mRNA was purified from total RNA and fragmented before first strand and second strand cDNA syntheses. The first-strand cDNA was synthetized with the mRNA fragments using SuperScript II Reverse Transcriptase and random hexamer primers. Then the second-strand cDNA was synthetized using DNA polymerase I. Index adapters were then added to identify sequences for each sample in the final data. The quality of the libraries was assessed on the Agilent Bioanalyzer 2200 system. Finally, the libraries were paired-end sequenced on an Illumina Hiseq 4000 platform at BGI, Japan, and 100 bp paired-end reads were generated.

2.2.3 RNA-seq data analysis

Raw sequences were transformed into clean reads after removing the adapter sequences and low-quality reads (Q < 20). The resulting clean reads were then *de novo* assembled using Trinity version 2.4.0 with standard settings (Grabherr et al., 2011) and pseudo-

aligned to the reference *P. fucata* genome using Kallisto (Bray et al., 2016). Assembled contigs were annotated by Trinotate for a BLAST search against the Swiss-Prot, RNAMMER, GO, COG, Pfam, and KEGG, and by in-house script for a BLAST search against NCBI NT. The quantified reads were then used to determine the differential gene expression of 2 groups of samples with a threshold criteria FDR < 0.01 and log2 ratio > 1. Statistical analysis software R was used for preprocessing and the bioconductor package DESeq2 (Love et al., 2014) and sleuth (Pimentel et al., 2017) were used for differential gene expression analysis of RNAseq data. The total up- and down-regulated DEGs at seven time combinations (before – 0 h, 0 h – 24 h, 24 h – 48 h, 48 h – 1 w, 1 w – 2 w, 2 w – 1 m and 1 m – 3 m) were used for subsequent GO and KEGG pathway enrichment analyses.

The GO annotations were functionally classified by GOEAST web-based software (http://omicslab.genetics.ac.cn/GOEAST/index.php) (Zheng and Wang, 2008) for gene function distributions and the GO terms with a corrected *P* -value < 0.05 were considered significantly enriched by the differentially expressed genes. KOBAS 3.0 software was used to screen out the differentially expressed immune genes statistically enriched ($P < 0.05$) in KEGG immune pathways (Xie et al., 2011). The hypergeometric test was used to identify the significant KEGG pathways and the *P*-value was corrected by the Benjamini and Hochberg method.

2.3 Results

2.3.1 Transcriptome sequence assembly

The results of statistical analysis of sequencing data are summarized in Table 2.1 and Table 2.2. After filtering, the total number of clean reads was 925.35 million. The quality assessment of the sequencing data showed that the distribution of quality Q20 was more than 95% in each sample and the GC content was 39.04% – 50.37%. Again, 65.52% of the clean reads were successfully quantified with Kallisto (Bray et al., 2016) to obtain transcript counts and abundances (Table 2.1).

Table 2.1 Statistical analysis of transcriptome sequencing data.

Parameters	Counts
Total clean reads	925,349,740
Total clean bases	92,534,974,000
Q20	> 95.13%
GC count	39.04% – 50.37%
Quantified reads ($\times 10^6$)	813.77
Quantification ratio	65.52%

Table 2.2. Statistical analysis of transcriptome sequencing data for each sample

Sample name	Clean reads	Clean bases	Read length (bp)	Q20 (%)	GC content	Quantified reads ($\times 10^6$)	Quantification ratio (%)
Before_A	17,164,384	1,716,438,400	100	98.32	43.20%	16.73	67.75
Before_B	10,026,656	1,002,665,600	100	98.20	43.32%	10.15	68.77
Before_C	12,059,064	1,205,906,400	100	98.24	42.67%	12.18	68.50
0h_A	9,811,942	981,194,200	100	98.17	44.64%	9.74	68.34
0h_B	9,412,514	941,251,400	100	98.22	45.18%	9.27	68.14
0h_C	10,398,038	1,039,803,800	100	98.40	44.86%	11.02	70.54
24h_A1	10,355,918	1,035,591,800	100	98.20	43.00%	10.24	68.09
24h_A2	7,867,464	786,746,400	100	98.44	43.25%	8.08	71.73
24h_B1	8,870,314	887,031,400	100	98.61	42.38%	8.73	72.15
24h_B2	7,403,436	740,343,600	100	98.63	43.34%	22.58	67.36
24h_C1	23,143,452	2,314,345,200	100	98.23	40.50%	9.53	71.33
24h_C2	12,869,554	1,286,955,400	100	98.05	41.23%	13.01	68.30
48h_A1	7,112,274	711,227,400	100	98.62	42.38%	7.39	69.98
48h_A2	6,976,730	697,673,000	100	98.50	41.03%	9.48	68.07
48h_B1	9,891,620	989,162,000	100	98.42	40.95%	6.99	68.82
48h_B2	9,625,184	962,518,400	100	98.35	42.74%	9.19	69.26
48h_C1	9,008,866	900,886,600	100	98.33	41.43%	9.82	68.42
48h_C2	5,665,372	566,537,200	100	98.69	42.34%	5.97	70.70
1w_A1	48,419,298	4,841,929,800	100	95.58	41.15%	40.27	61.44
1w_A2	23,539,310	2,353,931,000	100	96.39	41.38%	21.27	64.77
1w_B1	36,485,718	3,648,571,800	100	96.32	41.45%	32.36	64.06
1w_B2	17,106,708	1,710,670,800	100	95.67	44.09%	14.51	64.41
1w_C1	5,467,236	546,723,600	100	97.90	50.37%	3.83	64.10
1w_C2	30,277,428	3,027,742,800	100	96.51	41.59%	27.64	64.71
2w_A1	34,149,422	3,414,942,200	100	96.46	41.18%	28.76	62.37
2w_A2	69,600,066	6,960,006,600	100	96.03	40.42%	61.38	63.54
2w_B1	32,927,364	3,292,736,400	100	97.05	41.53%	29.5	64.44
2w_B2	26,223,104	2,622,310,400	100	96.49	40.58%	22.49	63.11
2w_C1	38,238,402	3,823,840,200	100	96.50	42.09%	31.83	62.69
2w_C2	55,393,672	5,539,367,200	100	95.13	41.81%	45.3	62.51
1m_A1	45,558,068	4,555,806,800	100	95.67	40.62%	39.64	62.91
1m_A2	26,248,864	2,624,886,400	100	97.31	41.29%	22.59	63.00
1m_B1	25,934,080	2,593,408,000	100	96.55	40.29%	21.51	61.10
1m_B2	32,196,990	3,219,699,000	100	96.97	44.01%	25.97	62.89
1m_C1	25,541,512	2,554,151,200	100	96.38	40.22%	19.85	58.60

1m_C2	32,021,402	3,202,140,200	100	96.35	40.85%	26.87	61.33
3m_A1	23,359,108	2,335,910,800	100	95.64	40.84%	19.25	60.50
3m_A2	24,171,408	2,417,140,800	100	96.33	42.24%	18.64	58.99
3m_B1	30,337,036	3,033,703,600	100	96.66	41.62%	23.83	60.16
3m_B2	11,595,252	1,159,525,200	100	96.56	40.22%	8.99	58.99
3m_C1	1,231,312	123,131,200	100	97.30	39.04%	1.2	66.43
3m_C2	22,436,394	2,243,639,400	100	96.39	40.34%	17.84	59.91
Cell_A	7,382,306	738,230,600	100	98.34	44.65%	7.1	68.67
Cell_B	5,825,620	582,562,000	100	98.26	44.03%	5.37	66.89
Cell_C	6,019,878	601,987,800	100	98.48	45.08%	5.88	69.79

2.3.2 Functional annotation and classification of the DEGs between different time groups

To discern the successive changes that occurs during pearl formation upon grafting, we considered seven consecutive time combinations (before – 0 h, 0 h – 24 h, 24 h – 48 h, 48 h –1 w, 1 w – 2 w, 2 w – 1 m and 1 m – 3 m) during three months grafting experiment. The total up- and down-regulated differentially expressed genes (DEGs) were detected at seven mentioned time combinations (Fig. 2.2). The highest number of total DEGs (11,744) was detected at 48 h – 1 w time point of which 4,076 were up-regulated and 7,668 were down-regulated (Fig. 2.2). All the DEGs at mentioned seven time points were then used for subsequent GO enrichment analysis. In GO enrichment analysis, three functional categories were determined: biological process, cellular component and molecular function.

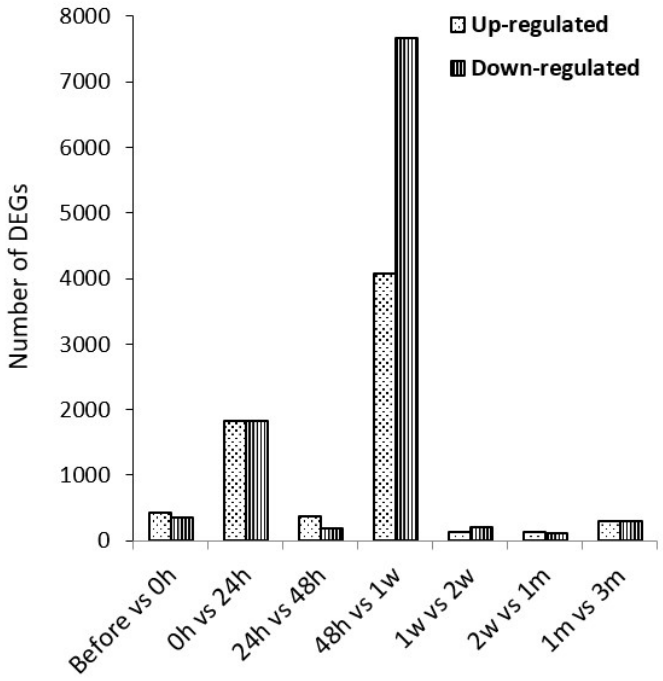

Figure 2.2. The numbers of up-regulated and down-regulated DEGs at different time points of three months grafting experiment. Before and 0 h means pre-transgraft. The others, 24 h – 3 m, mean post-transgraft. "h" for hour, "w" for week and "m" for month.

2.3.3 Differentially expressed genes in immune-related pathways

The immune response that occurs upon grafting process during cultured pearl production plays a vital role in response to oyster survival and regeneration (Wei et al., 2017a). To gain insights into the potential functioning of immune system, we monitored the expression of the key genes in different immune-related pathways throughout the grafting period. According to the results of GO enrichment analysis, most of the immune-related genes were enriched at 0 h – 24 h and 48 h – 1 w time points. At 0 h – 24 h time point, 128 and 188 immune related terms were up- and down-regulated, respectively, whereas at 48 h – 1 w time point, 67 and 216 terms were up- and down-regulated, respectively. Further, we mapped all the DEGs in the KEGG database to

search for the genes involved in significant immune-related pathways. Figure 2.3 explained that immune related pathways were significantly ($P < 0.05$) enriched at 0 h – 24 h and 48 h – 1 w time points which is consistent with the results of GO enrichment analysis. During graft preparation (before – 0 h) most of the immune pathways were down-regulated due to the suppression of immune genes in early donor cells i.e., before samples (Fig. 2.3b). After transplantation, surrounding host hemocytes encapsulate the graft and nucleus making the graft contaminated with host immune cells. Thus 0 h – 24 h comparison elucidating that host immune cells became active at the site of grafting at 24 h (Fig. 2.3). Most of the immune genes were enriched at 48 h – 1 w interpreting the distinction of immune functions between donor (48 h) and host (1 w) cells. From the observation of 48 h – 1 w enrichment, it is complicated to conclude whether donor or host immune cells were more functional at this stage. The up and down-regulated DEGs involved in 21 crucial immune pathways during the process of pearl sac formation were screened out by KEGG pathway analysis and listed in Table 2.3.

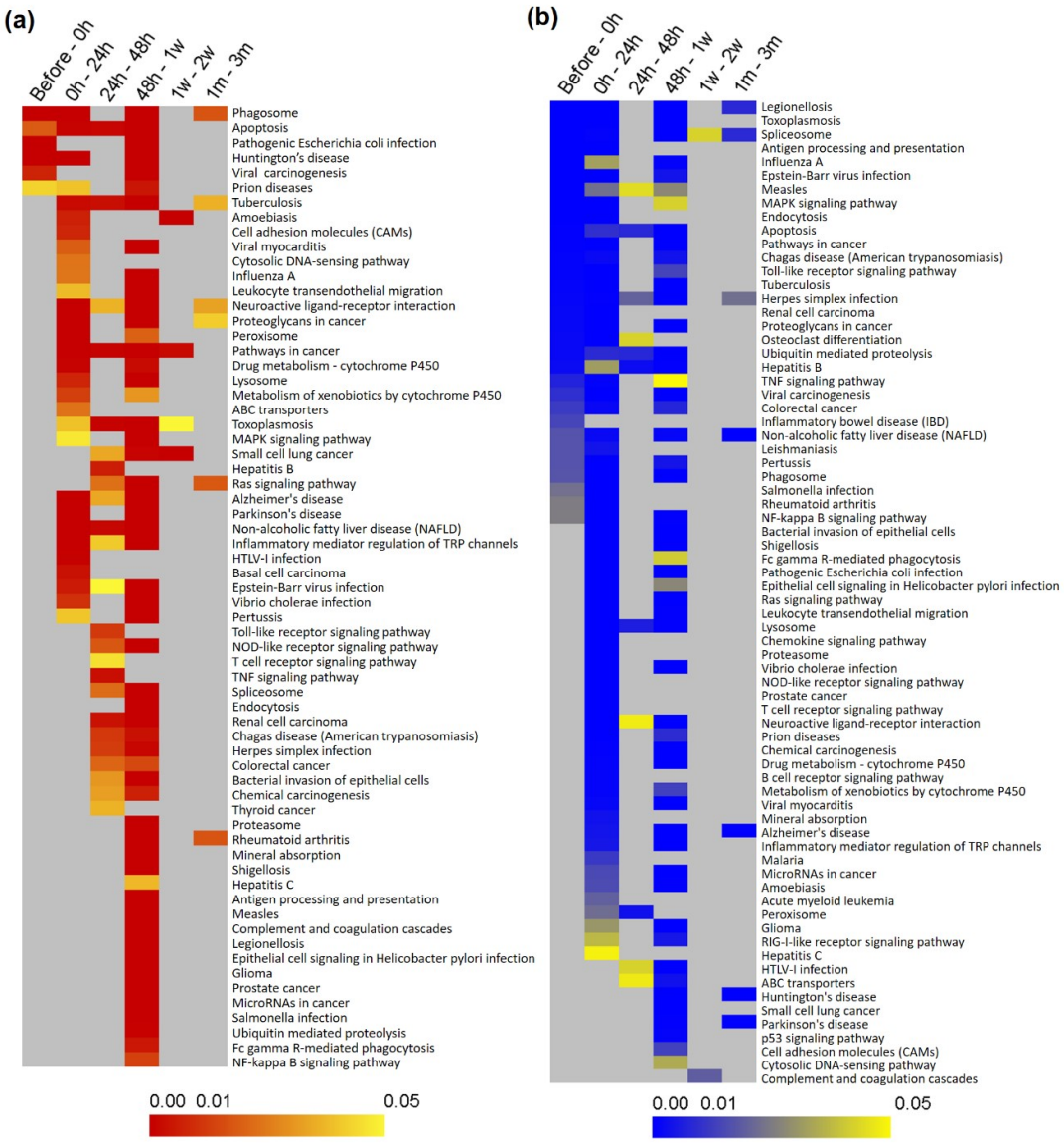

Figure 2.3. Heat maps of KEGG pathway enrichment analysis for immune related DEGs. (a) Up-regulated DEGs. (b) Down-regulated DEGs. Up- or down-regulated DEGs at each time point were submitted to KEGG pathway analysis using Kobas 3.0 web-based software. Columns and rows in the heat maps indicate treatments and enriched pathway terms, respectively. Sample names are displayed above the heat maps. Color scales indicate *P* values of enrichment tests and gray cells represent an empty value or a value > 0.05.

Table 2.3. Up-regulated and down-regulated DEGs significantly ($P < 0.05$) involved in KEGG immune pathways

KEGG immune pathway	Up-regulated DEGs	Down-regulated DEGs
Phagosome	COOA1, CALR, MRC1, ACT5C, TLR1, S61A2, PLC, SC61A, TLR2, ITB1, C209C, NOXA1, CO7A1, CYSP1, TLR4, VA0D1, RAC1, VATL, TBA3, VATA, VATG, TOLL8, ACT, CATL, ACTB1, VATE, TBB4B, CY24A, ACT3A, VATB, CO3, RAB5C, C209E, DYHC1, RABF1, CATL1, SC61B, TBA1, VA0D, HGS, TBA2, VTC1A, ACTB, TBA3E, RAB7, MPRD, TOLL, MARCO, HGS, S22BB, S61G1, TBB1	VA0D1, TSP4, ACT, VATL, RAB7, RAC1, PK3C3, VAS1, VATG, CY24B, CY24A, VATB, RAB5C, RABF1, VPP1, TLR13, CATL, NOXA1, HGS, TBA2, VATA, EEA1, TBB, TSP4, ACT2, ACT1, TBB4B, PLCL, TLR2, FYV1, CO7A1, MRC2, ACTC, TLR1, ITB1, MRC1, CALR, TSP3, ACT3, DYHC2, CATL1, DYHC1, PLC, TLR22, TBA1, ACT10, LAMP2, NOS1
Apoptosis	M3K14, JUN, HTRA2, CYC, PARP1, ACT5C, P85A, AIFM1, PARP3, CYSP1, CATL1, TBA3, ACT, CATL, ACTB1, CATZ, GA45G, ACT3A, PERF, BIRC3, CFAD, CATC, ITPR1, GA45A, CPR1, IF2A, TBA1, BIRC2, PIAP, Y068, ACTB, TBA3E, TBA2, IAP, CASP8	TBA2, CATL, MK01, CASP8, TRAF2, NFKB1, PIAP, ACT, BIRC5, NF70, ACT2, PIDD1, LMNB1, DAXX, LMNA, ATM, PARP2, BIR, ACT1, M3K14, HTRA2, CYC, ITPR3, ACTC, YMD2, BIR7B, ITPR, TNF10, MP2K1, BIR7A, ACT3, ITPR2, CYSP1, IKKA, CATL1, Y068, AIFM1, CASP2, PARP4, P85A, PK3CB, TBA1, ACT10, CASP7
Cell adhesion molecules (CAMs)	UNC89, LACH, NLGNX, NCAM1, BSCN, PTPRM, ITB1, CAD15, CEL, ACNT1, ACOX3, IDHP, XDH, UCPA, SODC	PTPRF, LYAM2, NLGNX, ITA2, LACH, CEL, CD180, IL6RB, ITA1, STAN, NRG, ITB1, NLGNY, GSLG1, CAD15, NEO1, NCAM2, LADD, ACES, UNC89
Peroxisome	SODM, XDH, CATA, PEX14, DCMC, SOX, PEX6, SODC, IDHP, MSOX	XDH, DCMC, FACR1, UCPA, NLTP, DHB4, DECR2
Drug metabolism - cytochrome P450	SNO1, CP2C8, ADH1, GSTT1, GST7, GST1, SCR11, GST6, CP2DE, CP2BJ, CP3AT, FMO5, CP3AA, GST2, AOFA, GSTA3	GST3, C8D11, CP2BB, CP3AE, MGST2, SNO1, CP3AA, CP2G1, FMO5, CP3AB, ADH1, ADH7, CP2CN, CP2J6, CP3A9, GSXL4, ADHX, GSTM1, GSTT1, GST7, CP2BJ, GSTUQ, GST6, CP3A5, GSXL8, CP2DE

Lysosome	PTHD3, CYSP1, PPGB, ARSB, CD63, AP3D1, LYAG, HEX, SPHM, VA0D1, VATL, CDIP1, ASAH1, CATL, SCRB2, CATZ, GLCM, NAGAB, PPT1, NPC2, NRAM2, ASM, NPC1, CFAD, CTNS, AP1B1, CATC, CATL1, ASPG, CPR1, VA0D, MPRD, FUCO	VPP1, AP3B1, LITAF, VA0D1, NRAM2, NPC1, CLH2, PAG15, S17A5, VATL, NRAMA, CATL, VAS1, GALC, PPGB, HEXB, AP4B1, ANTR2, ARSB, FUCO, AP3D1, LIPG, CATL1, SORT, LAMP2, CYSP1, LYAG, SL172, MPRI, AP3B2
Toxoplasmosis	CYC, P85A, TLR2, ITB1, LAMB1, BIRC7, LAMA1, HSP7C, 1HSP70, HSP74, PIAP, PPIA, GNAI, HSP72, BIR7A, MP2K6, BIRC2, BIRC3, Y068, BIR7B, HSP71, IAP	XIAP, HSP72, HSP74, TLR13, HSP70, CASP8, HSP71, BIR7A, MP2K6, NFKB1, MK01, LDLR, PIAP, GNAI, IRAK4, LOX5, AOSL, TLR2, PPIF, LAMA, BIR, LAMB1, BIR7B, YMD2, ITA1, TRAF6, ITB1, MK14, IKKA, CYC, LAMA1, LAMC1, Y068, P85A, TLR22, PK3CB
MAPK signaling pathway	M3K14, JUN, ARRB1, FGFR4, FLNA, MKNK1, PA24A, FGFR1, DUS7, RGRF2, HSP7C, HSP70, HSP74, CCG3, STK3, RAP1, RAC1, RAP1B, HSP72, HSP71, DUS10, EGFR, MP2K6, GA45A, PAK1, NLK, GA45G, CDC42, PAK3	JUN, HSP72, HSP74, HSP70, YR831, HSP71, SVH2, TRAF2, RAP1, EGFR, NFKB1, RAP1B, KAPC, RAC1, MK01, CDC42, TAU, PAK1, MP2K6, FGFR2, TAOK1, MAPK2, TAOK3, RRAS2, M3K4, PTPRR, MP2K1, DAXX, KS6AA, M3K14, CA2D2, DUS3, SOS1, KPC1, MPIP2, TRAF6, M3K1, FGFR3, MK14, CAC1D, CANB1, M3K3, IKKA, GRP3, GRB2, PP2C2, NF1, FGFR4, PTN5, M3K13, BRAF, KAPC1, EVI1, RGRF2, SRF
Ras signaling pathway	CDC42, P85A, VGFR1, CALM, SEA, RAP1, EGFR, CALL5, NMDE2, RGL1, RAB5C, RABF1, RHO, PAK1, PA2, PAK3, TNR16, ANGP4, RAC1, RAP1B	RHO1, SVH2, RAL, RAP1, EGFR, NFKB1, RAP1B, KAPC, RHO, RAC1, MK01, CDC42, RAB5C, RABF1, CALM, PAK1, PAK3, EXOC2, FGFR2, RRAS2, MP2K1, CALMS, JAK, ILPR, SOS1, TBK1, ABL1, PLCG1, PLD1, IGF1R, HGF, ETS2, PK3CB, PLPL9, VGFR1, FGFR3, ANGP4, KSYK, IKKA, GRP3, FGFR, ANGP2, MET, NF1, AFAD, FGFR4, P85A, GRB2, KAPC1, RGRF2, KPC1
Inflammatory mediator regulation of TRP channels	TRPA1, ADCY1, ADCY9, P85A, TNNC, ADCY5, PA24A, CP2J2, CALMF, PE2R4, CALM, CALL5, MP2K6, PP12, ITPR1	CALM, MP2K6, PE2R4, LOX12, KAPC, GNAS, TRPA1, ITPR3, CALMS, PLCG1, CP2H2, ITPR, MK14, PLPL9, KPCD, PK2, ITPR2, ADCY5, ADCY9, PP1B, P85A, PIP1, PK3CB, ASIC2, KAPC1, KPC1, PLCB4

Spliceosome	THOC2, RBP1, DDX42, HSP7C, HSP70, HSP74, SRSF1, BX42, SRSF4, HSP72, SRS1A, SRSF5, HSP71, RBM22, SYF1	HSP72, HSP74, HSP70, RBP1, DDX42, HSP71, CTBL1, SRSF4, DBP2, CDC5L, SF3B6, THOC2, DDX46, DHX8, HNRPU, SF3B1, AQR, SMD1, PPIL1, PRP4, PRP16, ACINU, SR140, TCRG1, DEAHC, SRR55, RBMX, RBM25, PRP8, U520, U2AF2
TNF signaling pathway	P85A, CASP8, JUN, BIRC2	JUN, CASP8, MP2K6, MK01, TRAF2, NFKB1, TRAF3, FBP1, MMP12, M3K14, MP2K1, CASP7, BIR7A, IKKA, P85A, TRAF5, PK3CB, DNM1L, MK14, BIR, BCL3
Toll-like receptor signaling pathway	P85A, CASP8, JUN	TLR13, CASP8, JUN, MP2K6, MK01, TLR21, RAC1, NFKB1, TRAF3, IRAK4, MP2K1, TLR2, TRAF5, TRAF6, TBK1, TLR22, PK3CB, TLR1, IKKA, MK14, P85A
NOD-like receptor signaling pathway	BIRC2, CASP8, ENPL, HSP83, HS90B, HS90A, ENPL1, IAP, BIRC3	MK01, CASP8, HSP83, HS90B, NFKB1, HS90A, PPIP1
Endocytosis	HSP7C, SEA, HSP74, PDC6I, HGS, EGFR, ARPC3, ALXA, SPG20, RHO, AP2S1, RAA2A, HSP70, CHM2B, EHD1, ARF1, SNX2, CHM1B, VPS35, HSP72, ADRB2, RAB5C, HSP71, CDC42, ARF, ARPC5, RAB7, VPS4A, RABF1, PML, VPS4B	HSP72, HSP74, HSP70, EEA1, HSP71, RAB10, CLH2, RHO1, SVH2, ARPC5, RAB7, EGFR, LDLR, VPS29, SPG20, ARPC3, RHO, ARF1, WASL, PDC6I, CDC42, ARC1A, RAB5C, CAPZA, ARF, RAB8A, RABF1, ARPC4, VPS4B, HGS, WASC5, ARF2, EPN2, ARPC2, STAM1, VPS4A, FGFR2
Antigen processing and presentation	HSP7C, HSP70, HSP74, B2MG, GRP78, CATL, CALR, HSP83, HSP72, CYSP1, HS90B, HSP97, CATL1, PDIA3, HSP71, HS90A	HSP72, HSP74, HSP70, HSP71, HSP97, CATL, GRP78, HSP83, HS90B, HS90A,
Ubiquitin mediated proteolysis	UBC12, RBX2, RBX1, BIR7A, UBCD6, BIR7B, UBCD1, ELOC, PIAP, BIRC2, IAP, PML, BIRC3	UBC12, XIAP, RBX1, UB2Q2, BIR7A, FBX4, UBCD1, UBA1, CUL1, PIAP, FBXW7, WWP2, UBC9, BIRC6, SAE1, APC7, CDC16, KEAP1, PIAS2, TRI18, APC1, UBR5, DET1, RHBT1, BIR, SMUF2, TRIPC, BIR7B, YMD2, UBE2U, BRCA1, HERC4, UBE3B, HERC1, TRAF6, M3K1, CD205, CUL4A, DDB1, FBX2, APC10, APC4, NED4L

Fc gamma R-mediated phagocytosis	ACTP, CDC42, ARPC5, GELS1, RAC1, ARPC3, PAK3, PAK1	ARPC5, VAV3, ARPC3, GELS1, RAC1, MK01, CDC42, ARC1A, PAK1, ARPC4, WASL, ARPC2, KPCD, WUN, PK2, ASAP1, PLCG1, MP2K1, PLD1, P85A, WASF3, PK3CB, BIN1, AMPH, KPC1, PLPL9
NF-kappa B signaling pathway	Y068, PARP1, BIRC2, PIAP, IAP, BIRC3	XIAP, PARP1, TLR1, TLR13, TRAF2, BLNK, NFKB1, TRAF3, MALT1, IRAK4, PIAP, UBC9, YMD2, PIDD1, ATM, DDX58, BIR, TRAF5, DCL3B, PLCG1, TRAF6, RB6I2, BIR7B, M3K14, BIR7A, KSYK, IKKA, CSK2B, Y068
Metabolism of xenobiotics by cytochrome P450	SCR11, GST6, ADH1, GSTT1, GST7, DHDH, GST1, CP2BJ, CP3AT, CP3AA, GST2, GSTA3	CP2B4, DHI1L, GST3, C8D11, CP2BB, CP3AE, MGST2, CP3AA, GSTM1, ADH1, CP3AB, GSTT1, GST7, CP3A5, GSTUQ, DHDH, CP1A1, ADHX, ADH7, GST6, CP3A9
Complement and coagulation cascades	PPN, A1AT, KCP3, FIBB, F13A, CO3, KCP1, FIBG, FIBA	KCP1, KCP3

2.3.4 Differentially expressed genes related to epithelial cell proliferation and differentiation

In the course of wound healing process, the outer epithelial cells of the mantle graft proliferate and differentiate into pearl sac (Awaji and Machii, 2011). So, to know the genes engaged in pearl sac development, we focused on epithelial cell proliferation and differentiation-related GO terms. GO analysis revealed that epithelial cell proliferation and differentiation-related terms were embellished in the biological process category. Among them, we found 21 up-regulated and 35 down-regulated terms relevant to epithelial cell proliferation and differentiation were significantly ($P < 0.05$) enriched during pearl sac formation (before to 2 w) (Fig. 2.4). It was also observed that epithelial cell proliferation and differentiation-related genes were enriched during the first two weeks of graft transplantation (Fig. 2.4). After that, there was no significantly up-regulating term pertinent to epithelial cell proliferation (Fig. 2.4a). Moreover, epithelial cell proliferation related terms were down-regulated after two weeks of grafting (Fig. 2.4b). These results suggest that the pearl sac formation was completed after two weeks of graft transplantation. The DEGs significantly ($P < 0.05$) up-regulated (34) and down-regulated (88) during the development of pearl sac are listed in Table 2.4 and Table 2.5.

Epithelial stem cells may be a source of proliferative epithelial cells to form the pearl sac. We observed some stem cell marker genes i.e. *SOX2, MEF2A, HES1, MET, NRP1, ESR1, STAT6, PAX2, FZD1, PROM1* and *ABCG2* that were expressed significantly during the formation of pearl sac (Table 2.4).

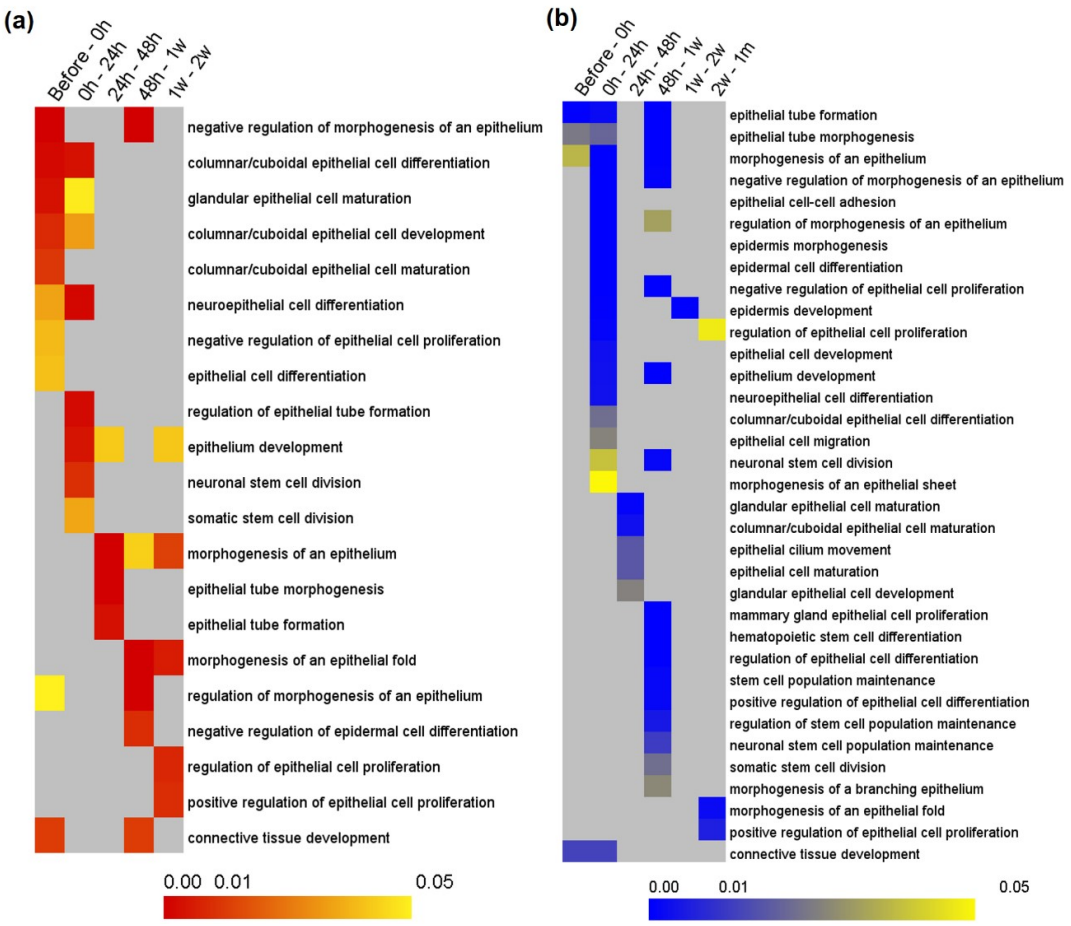

Figure 2.4. Heat maps of GO enrichment analysis for epithelial cell proliferation and differentiation-related DEGs. (a) Up-regulated DEGs. (b) Down-regulated DEGs. Up or down-regulated DEGs at each time point were submitted to GO enrichment analysis using GOEAST web-based software (http://omicslab.genetics.ac.cn/GOEAST/index.php). The results of GO enrichment analysis are displayed in Additional file 2: Table S2. Biological function in GO terms involved in epithelial cell proliferation and differentiation were selected to display in heat maps according to the statistical significance ($P < 0.05$). Columns and rows in the heat maps indicate treatments and enriched biological process GO terms, respectively. Sample names are displayed above the heat maps. Color scales indicate P values of enrichment tests and gray cells represent an empty value or a value > 0.05.

Table 2.4. Genes significantly ($P < 0.05$) enriched in epithelial cell proliferation and differentiation related GO terms

GO term	Up-regulated DEGs	Down-regulated DEGs
Negative regulation of morphogenesis of an epithelium	*SULF1*	*SULF1, LRP6*
Columnar/cuboidal epithelial cell differentiation	*JAG1, RFX3, STRC*	*JAG1, FGFR2, SAV1, RAC1*
Glandular epithelial cell maturation	*RFX3*	*RFX3*
Columnar/cuboidal epithelial cell development	*RFX3, STRC*	-
Columnar/cuboidal epithelial cell maturation	*RFX3*	*RFX3*
Neuro-epithelial cell differentiation	*STRC, JAG1*	*JAG1, RAC1*
Negative regulation of epithelial cell proliferation	*TSC2, FBXW7, PTPRK, SULF1, MTSS1*	*PTPRK, TSC2, FBXW7, MTSS1, SULF1, PTPRM, LRP6, SAV1, XDH*
Epithelial cell differentiation	*EHF, TGM1, RFX3, STRC, JAG1, MTSS1, MYO1E*	-
Regulation of epithelial tube formation	*PTK7, SFRP5, FZD1, LRP6*	-
Epithelium development	*RFX3, DMD, RGMA, PTK7, MAF, MEF2A, SFRP5, TGM1, FZD1, GRHL2, TEAD1, PRKDC*	*TSC2, EHF, RUNX1, JAG1, RAB10, FGFR2, EP300, ENAH, CASP8, CDC42, MTSS1, LRP4, MMP12, LRP6, NRP1, ILK, IPMK, PAK1, SAV1, CLIC4, RAC1, MYO1E, EGFR, TBX1, LBX1*
Neuronal stem cell division	*FGFR1, LRP6*	*RAB10, FGFR2, LRP6*
Somatic stem cell division	*FGFR1, LRP6*	*LRP6, FGFR2, ASPM, DOCK7*
Morphogenesis of an epithelium	*CASP8, CDC42, RSPO2, MTSS1*	*TBX1, RAB10, CASP8*
Epithelial tube morphogenesis	*CASP8, RSPO2, MTSS1*	*TBX1, CASP8*
Epithelial tube formation	*CASP8*	*CASP8*
Morphogenesis of an epithelial fold	*EGFR, AR*	*EGFR*
Regulation of morphogenesis of an epithelium	*SFRP5, WNT2B, LRP6, AR, SULF1, ESR1, RAC1*	*FGFR2, SULF1, LRP6, RAC1*

Negative regulation of epidermal cell differentiation	*MSX2, DLL1, HES1*	-
Regulation of epithelial cell proliferation	*LAMC1, PTPRK, EGFR*	*PTPRK, TSC2, FBXW7, FGFR2, MTSS1, SULF1, PTPRM, MMP12, LRP6, NRP1, SAV1, XDH, EGFR, TBX1*
positive regulation of epithelial cell proliferation	*LAMC1, EGFR*	*LAMC1, EGFR*
connective tissue development	*MATN1, SULF1, SPG20, LRP6*	*MATN1, SULF1, SPG20, LRP6,*
epithelial cell-cell adhesion	-	*CDC42*
epidermis morphogenesis	-	*RUNX1, FGFR2, CDC42*
epidermal cell differentiation	-	*JAG1, CDC42, SAV1, CLIC4, RAC1*
epidermis development	-	*RUNX1, JAG1, FGFR2, CDC42, LRP4, SAV1, CLIC4, RAC1, EGFR*
epithelial cell development	-	*FGFR2, CDC42, CLIC4, RAC1, MYO1E*
epithelial cell migration	-	*MYH9, NRP1*
morphogenesis of an epithelial sheet	-	*JAG1, MMP12, LRP6*
epithelial-mesenchymal cell signaling	-	*CDC42*
epithelial cilium movement	-	*RFX3*
epithelial cell maturation	-	*RFX3*
glandular epithelial cell development	-	*RFX3*
mammary gland epithelial cell proliferation	-	*STAT6, ESR1, MED1*
hematopoietic stem cell differentiation	-	*XRCC5, ACE, TAL1, SRF, ERCC2*
regulation of epithelial cell differentiation	-	*XDH, SMO, DMBT1, PROM1, SOX2, APC, PAX2, VDR, NODAL, MED1, CAV1, RFX3, XDH, EZH2, KEAP1*
stem cell population maintenance	-	*SMC3, RIF1, SOX2, APC, PCM1, SKI, MED27, RTF1, SMC1A, NODAL, MED21, VPS72, GATA2, SRRT, LEO1, SRRT, FGFR3*

positive regulation of epithelial cell differentiation	-	*DMBT1, PROM1, SOX2, APC, PAX2, VDR, MED1, RFX3*
regulation of stem cell population maintenance	-	*SMO, CNOT1, PAX2, CNOT2, TAL1, NODAL, CNOT3*
neuronal stem cell population maintenance	-	*SOX2, PCM1, SRRT*
morphogenesis of a branching epithelium	-	*TCF21, LRP6, SALL1, SLIT2, PKD1, FGFR2, MET, FOXD3, LAMA1, SOX2, DLG1, WNT4, PAX2, VDR, ESR1, TBX20, IHH, GRB2, RBM15, MED1, MKS1, FOXA2, SRF*

Table 2.5. Gene symbol with full gene name

Gene symbol	Full gene name
ACE	Angiotensin-converting enzyme
APC	Adenomatous polyposis coli protein
AR	Androgen receptor
ASPM	Abnormal spindle-like microcephaly-associated protein
CASP8	Caspase-8 subunit p10
CAV1	Caveolin-1
CDC42	Cell division control protein 42 homolog
CLIC4	Chloride intracellular channel protein 4
CNOT1	CCR4-NOT transcription complex subunit 1
CNOT2	CCR4-NOT transcription complex subunit 2
CNOT3	CCR4-NOT transcription complex subunit 3
DLG1	Disks large homolog 1
DLL1	Delta-like protein 1
DMBT1	Deleted in malignant brain tumors 1 protein
DMD	Dystrophin
DOCK7	Dedicator of cytokinesis protein 7
EGFR	Epidermal growth factor receptor
EHF	ETS homologous factor
ENAH	Protein enabled homolog
EP300	Histone acetyltransferase p300
ERCC2	TFIIH basal transcription factor complex helicase XPD subunit
ESR1	Estrogen receptor

EZH2	Histone-lysine N-methyltransferase EZH2
FBXW7	F-box/WD repeat-containing protein 7
FGFR1	Fibroblast growth factor receptor 1
FGFR2	Fibroblast growth factor receptor 2
FGFR3	Fibroblast growth factor receptor 3
FOXA2	Hepatocyte nuclear factor 3-beta
FOXD3	Forkhead box protein D3
FZD1	Frizzled-1
GATA2	Endothelial transcription factor GATA-2
GRB2	Growth factor receptor-bound protein 2
GRHL2	Grainyhead-like protein 2 homolog
HES1	Transcription factor HES-1
IHH	Indian hedgehog protein
ILK	Integrin-linked protein kinase
IPMK	Inositol polyphosphate multikinase
JAG1	Protein jagged-1
KEAP1	Kelch-like ECH-associated protein 1
LAMA1	Laminin subunit alpha-1
LAMC1	Laminin subunit gamma-1
LBX1	Transcription factor LBX1
LEO1	RNA polymerase-associated protein LEO1
LRP4	Low-density lipoprotein receptor-related protein 4
LRP6	Low-density lipoprotein receptor-related protein 6
MAF	Transcription factor Maf
MATN1	Cartilage matrix protein
MED1	Mediator of RNA polymerase II transcription subunit 1
MED21	Mediator of RNA polymerase II transcription subunit 21
MED27	Mediator of RNA polymerase II transcription subunit 27
MEF2A	Myocyte-specific enhancer factor 2A
MET	Hepatocyte growth factor receptor
MKS1	Meckel syndrome type 1 protein
MMP12	Macrophage metalloelastase
MSX2	Homeobox protein MSX-2
MTSS1	Metastasis suppressor protein 1
MYH9	Myosin-9
MYO1E	Unconventional myosin-Ie

NODAL	Nodal homolog
NRP1	Neuropilin-1/Protein kinase C-binding protein NELL1
PAK1	Serine/threonine-protein kinase PAK 1
PAX2	Paired box protein Pax-2
PCM1	Methyl-CpG-binding domain protein 1
PEX13	Peroxisomal membrane protein PEX13
PKD1	Polycystin-1
PRKDC	DNA-dependent protein kinase catalytic subunit
PROM1	Prominin-1
PTK7	Inactive tyrosine-protein kinase 7
PTPRK	Receptor-type tyrosine-protein phosphatase kappa
PTPRM	Receptor-type tyrosine-protein phosphatase mu
RAB10	Ras-related protein Rab-10
RAC1	Ras-related C3 botulinum toxin substrate 1
RBM15	Putative RNA-binding protein 15
RFX3	Transcription factor RFX3
RGMA	Repulsive guidance molecule A
RIF1	Insulin-like peptide INSL6/Telomere-associated protein RIF1
RSPO2	R-spondin-2
RTF1	RNA polymerase-associated protein RTF1 homolog
RUNX1	Runt-related transcription factor 1
SALL1	Sal-like protein 1
SAV1	Protein salvador homolog 1
SFRP5	Secreted frizzled-related protein 5
SKI	Ski oncogene
SLIT2	Slit homolog 2 protein
SMC1A	Structural maintenance of chromosomes protein 1A
SMC3	Structural maintenance of chromosomes protein 3
SMO	Smoothened homolog
SOX2	Transcription factor SOX-2
SPG20	Spartin
SRF	Serum response factor
SRRT	Serrate RNA effector molecule homolog
STAT6	Signal transducer and activator of transcription 6
STRC	Stereocilin
SULF1	Extracellular sulfatase Sulf-1

TAL1	T-cell acute lymphocytic leukemia protein 1
TBX1	T-box transcription factor TBX1
TBX20	T-box transcription factor TBX20
TCF21	Transcription factor 21
TEAD1	Transcriptional enhancer factor TEF-1
TGM1	Protein-glutamine gamma-glutamyltransferase K
TSC2	Tuberin
VDR	Vitamin D3 receptor
VPS72	Vacuolar protein sorting-associated protein 72 homolog
WNT2B	Protein Wnt-2b
WNT4	Protein Wnt-4
XDH	Xanthine dehydrogenase/oxidase
XRCC5	X-ray repair cross-complementing protein 5

2.3.5 Comparison of enrichment studies between DESeq2 and sleuth calculated DEGs

In the first part of the study (KEGG immune pathways and GO cell proliferation), we used the DEGs calculated from DESeq2 (Love et al., 2014). In order to compare the enrichment results, we again calculated DEGs using sleuth (Pimentel et al., 2017) to ascertain whether any differences exists in enrichment studies between these two calculations. However, the number of DEGs obtained from sleuth was comparatively lower than that obtained from DESeq2. Also sleuth could not detect any DEGs at 24 h – 48 h, 2 w – 1 m and 1 m – 3 m time combinations. We used both DESeq2 and sleuth estimated DEGs separately for KEGG pathway enrichment analysis. In spite of having variations in the number of DEGs, immune genes were mostly enriched at 0 h – 24 h and 48 h – 1 w time points in both cases (Fig. 2.3 and Fig. 2.5). Moreover, there was no apparent changes in the pathways that were significantly up- or down-regulated verifying that the interpretation of our result was not influenced much due to the selection of software like DESeq2 or sleuth.

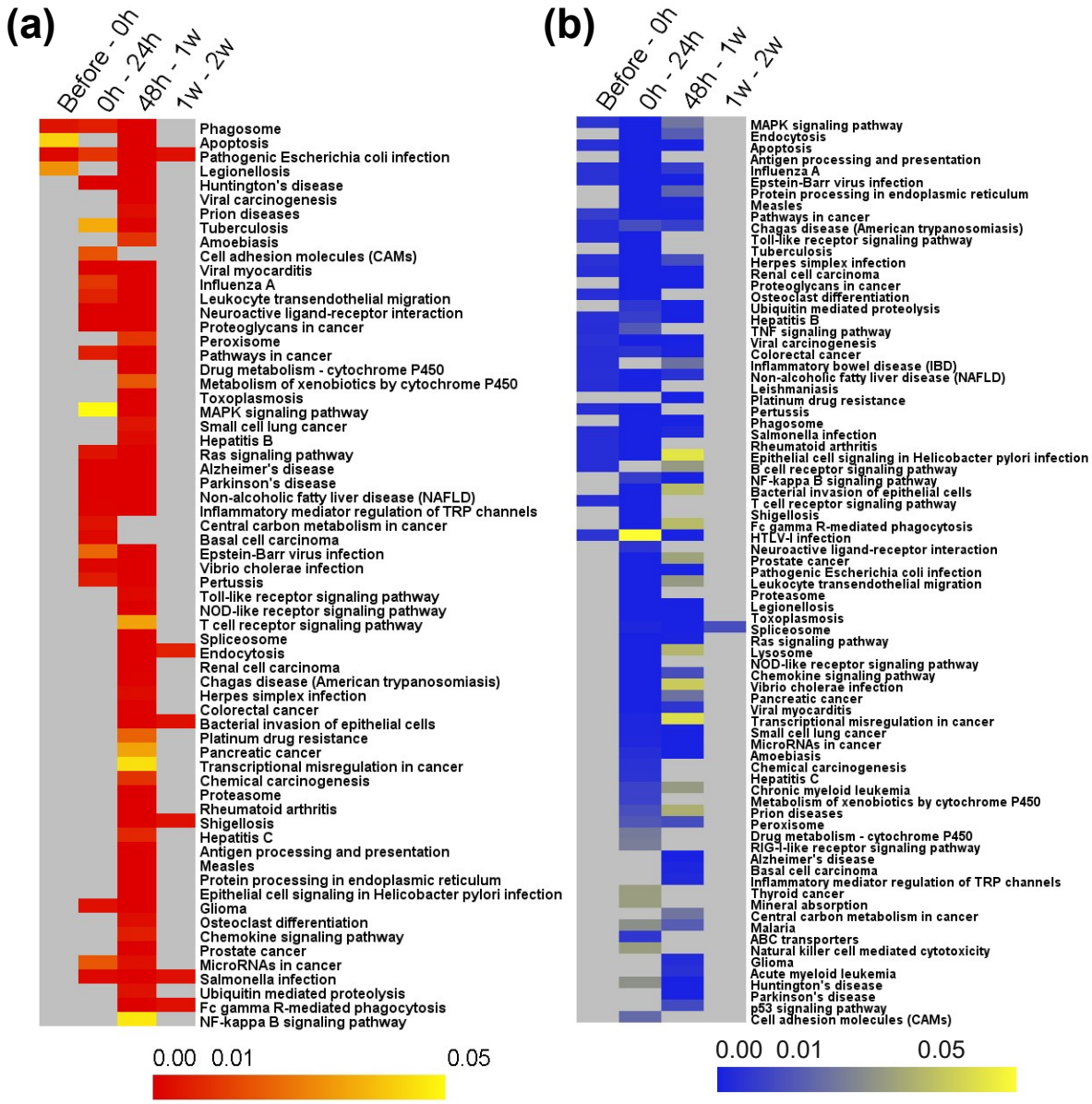

Figure 2.5. Heat maps of KEGG pathway enrichment analysis for immune related DEGs estimated by sleuth. (a) Up-regulated DEGs. (b) Down-regulated DEGs. Up- or down-regulated DEGs at each time point were submitted to KEGG pathway analysis using Kobas 3.0 web-based software. Columns and rows in the heat maps indicate treatments and enriched pathway terms, respectively. Sample names are displayed above the heat maps. Color scales indicate *P* values of enrichment tests and gray cells represent an empty value or a value > 0.05.

2.4 Discussion

We identified all the DEGs at different time combinations during grafting and conducted a series of bioinformatic analysis to screen out the key genes and pathways closely related to immune function and epithelial cell proliferation. The highest number of DEGs was obtained during 48 h – 1 w time point. At 48 h after graft implantation many important biological functions like immune reactions, cell proliferations and various metabolic pathways were up-regulated which might be resulted in the maximum number of DEGs assigned at 48 h – 1 w. However, it is very difficult to summarize whether this is because of the up-regulation of many processes or due to the differences in gene expression between donor (48 h) and host (1 w) tissues or both.

2.4.1 Differentially expressed genes in immune pathways

Graft implantation process causes the oysters stressed. The increased stress during 48 h of graft transplantation causes increased hemocyte infiltration in the wound site (Awaji and Suzuki, 1995). The host oysters showed immune response during the early stages of grafting as indicated by the up-regulation of many immune functions (Fig. 2.3).

Toll-like receptors (TLRs) are fundamental components of innate immunity playing a significant role in defense against pathogen both in vertebrates (Roach et al., 2005; Takeda and Akira, 2005) and invertebrates like fly (Lemaitre et al., 1996), oyster (Zhang et al., 2013; Wang et al., 2018a) and scallop (Wang et al., 2015; Wang et al., 2018b). It is also revealed that many components (TLR, MyD88, TRAF, IKK, NF-κB and so on) in the canonical TLR signaling pathway in the animals from fly to human are rather conserved (Wang et al., 2018b; Ausubel 2005). Though TLRs mediated innate immune responses both in vertebrates and invertebrates share a common ancient ancestry, the domain organization, mode of activation and functions are diverse (Imler and Zheng,

2004; Kanzok et al., 2004). Earlier evidences suggested that, the ancient molluscan TLRs possessed a powerful pattern recognition ability to recognize broader ligands than its mammalian homologues (Wang et al., 2015; Wang et al., 2016a), and mediated the downstream signaling cascades in a MyD88-dependent or MyD88-independent pathways to activate the expression of various immune effectors (Wang et al., 2018b; Wang et al., 2011; Song et al., 2015; Xin et al., 2016). Moreover, two TLRs (ORF06037 and ORF09244) in scallop exhibited a closer phylogenetic relationship to the plasma membrane located TLRs, such as *TLR1*, *TLR2*, *TLR4* and *TLR6* in human and mouse (Wang et al., 2018b). Among eighty three anticipated TLR genes from Pacific oyster *C. gigas* genome, eighty TLRs are predicted to contain the toll/interleukin-1 receptor (TIR) domain and at least six TLRs have been identified to participate in immune response so far (Wang et al., 2018a; Zhang et al., 2015). Thus, higher expressions of TLR signaling pathway at 24 h in our data indicate that host oysters react to the transplanted allograft and induce the immune response (Fig. 2.3a). Differential expression of TLRs like *TLR1* and *TLR6* and their downstream signaling molecules including TNF-alpha and IL-1 has also been observed previously in hemocytes of *P. fucata* 48 h after the nucleus insertion (Wei et al., 2017a). Recently, immune function of *TLR6* has also been identified in Pacific oyster *Crassostrea gigas* which exhibits a broader recognition spectrum (Wang et al., 2016a). Different TLRs enriched in different pathways explain their role in recognizing distinct pathogen-associated molecular profiles (PAMPs) (Table 2.3) (Wang et al., 2016a; Haynes et al., 2001). *TLR1* and *TLR2* were significantly up-regulated at 0 h, whereas *TLR4* at 48 h, indicating that *TLR4* may play a vital role in wound healing and immune response to the inserted nucleus and mantle graft. In a recent study on *P. fucata*, *TLR4* was also found to increase significantly after implantation peaking at day 2 (Wu et al., 2017). *TLR4* is believed to initiate inflammation and tissue injury by responding to

both bacterial endotoxin and multiple endogenous ligands, including heat-shock protein (HSP) (Ohashi et al., 2000). Other key molecules of TLR pathway including *NF-κB1* and tumor necrosis factor receptor-associated factor *TRAF2,3,5* and *6* were also enriched during 0 h – 24 h and 48 h – 1 w in consistence with their role in regulating inflammatory responses (Table 2.3). Among seven identified mammalian TRAF family gene (*TRAF1-7*), *TRAF1,2,3* and *7* have already been confirmed to evolve in immune response in oyster (Huang et al., 2016; Huang et al., 2012a; Fu et al., 2011, Tanguy et al., 2004). The inflammatory functions of *NF-κB1* and TRAF molecules in *P. fucata* were also described earlier (Huang et al., 2012a; Huang et al., 2012b; Jiao et al., 2014). In addition to immune function, NF-κB signaling pathway also involves in shell formation in *P. fucata* by regulating the transcriptional activity of nacrein promoter (Sun et al., 2015).

A member of caspases, *CASP8*, was activated both in donor mantle graft (before – 0 h and 0 h – 24 h) and host oyster (48 h – 1 w) (Fig. 2.3a, Table 2.3). Caspases are well-known for their important roles in apoptosis (Gyrd-Hansen and Meier, 2010; Silke and Meier, 2013; Qu et al., 2014) and inflammation (McIlwain et al., 2013; Riedl and Shi, 2004). Thus the early expression of *CASP8* in apoptosis pathway was most likely implicated for cell death in the wounded graft (Fig. 2.3, Table 2.3). The involvement of *CASP8* in other pathways like TLR/NOD-like receptors signaling indicated its non-apoptotic function (Fig. 2.3, Table 2.3). The dual role of *CASP8* in apoptotic and non-apoptotic activity has also been described previously where *CASP8* bears a significant role in cell death as well as in regulating TLR and NF-κB signaling (Bénédicte et al., 2007). Moreover, the role of *CASP8* in innate immunity has been described in *C. gigas* against virus (Li et al., 2015) and in *C. hongkongenesis* against bacteria (Xiang et al., 2013).

HSPs are the most abundant, ubiquitously expressed, soluble, intracellular proteins and are phylogenetically conserved in all organisms (Tsan and Gao, 2004). HSPs are important in regulating the immune responses like activation of macrophages and dendritic cells and in the production of cytokines and chemokines (Tsan and Gao, 2004; Van et al., 2012). In this study, several HSPs like *HSP70, HSP71, HSP72, HSP74, HSP83, HSP97* and *HSP7C* were found up-regulated at 48 h – 1 w and down-regulated at 0 h – 24 h, suggesting that HSPs may be induced by surgery and graft transplantation (Table 2.3). Host oysters may be more susceptible to the effects of heat or other stress induced by grafting. Recently, the up-regulation of *HSP70* was also detected in *P. fucata* at 0 h – 48 h of allografting (Wei et al., 2017a) and 6 h – 96 h of xenografting (Wei et al., 2017b). The involvement of HSPs in different immune pathways also conclude their simultaneous role in countering environment stress, immune response, inflammatory process and the regulation of apoptosis.

Mitogen-activated protein kinase (MAPK) signaling pathway enriched in 0 h – 24 h and 48 h – 1 w suggests an important role of this pathway in pearl grafting (Fig. 2.3a,b). MAPK cascades with conserved function play a critical role in the regulation of many physiological and biochemical processes including cell proliferation, differentiation, cell growth and death, immune reaction, and environmental adaptation (Krishna and Narang, 2008; Lewis et al., 1998; Zou et al., 2015). In conjunction with the activation of NF-κB and Ras signaling pathway, MAPK activation induces the expression of multiple genes that jointly regulate the inflammatory response (Krishna and Narang, 2008). The DEGs in MAPK signaling pathway detected in this study suggest the cooperation of the MAPK signaling pathway in pearl sac and pearl formation. *EGFR* and *FGFR* are important cell surface receptors that can induce MAPK signaling by activating other kinases. Though the predominant function of *EGFR* is related to cell proliferation and differentiation, it

also plays an important role in innate immunity in mollusk (Sun et al., 2014). Moreover, the up-regulated expression of *EGFR* at 48 h – 1 w and 1 w – 2 w might correlate with wound healing and promotion of cell proliferation and migration (Table 2.3) (Sun et al., 2014). Signal transduction begins with the activation of small GTPases like RAS and RHO family proteins (Avruch et al., 2001; Zhang and Dong, 2005). Other than the MAPKs, RAS and RHO subfamily proteins were also expressed which have substantial roles in MAPK activation (Table 2.3) (Zhang and Dong, 2005). Very little is known about the role of MAPKs in pearl oyster. However, some previous studies suggested the involvement of MAPKs in the innate immunity of *C. hongkongenesis* (Qu et al., 2016; Qu et al., 2017). More recently, a MAP kinase, *MKK4*, was found to be expressed in *P. fucata* 1 day after grafting in response to the nucleus insertion operation indicating its role in host defense mechanism, potentially in protecting the pearl oyster from injury caused by grafting (Zhang et al., 2018).

2.4.2 Differentially expressed genes during epithelial cells proliferation and differentiation

The mantle tissues of mollusk are metabolically and transcriptionally active and play a pivotal role in shell and pearl biomineralization (Clark et al., 2010). After the grafting operation, the donor mantle tissues not only survive but also proliferate to form the pearl sac (Kishore and Southgate, 2016; Awaji and Suzuki, 1995). Therefore, the genes involved in proliferation and differentiation of outer epithelial cells are of utmost important in the course of pearl formation. Before proliferating into pearl sac, the adhesion between the mantle graft tissues and connective tissues of gonad of the host oysters is a prerequisite that eventually affects the success of nucleus implantation and pearl sac formation (Kishore and Southgate, 2016). Thus, the proliferation of connective tissue cells among gonadal follicles during pearl sac formation is very significant and

found up-regulated at 48 h as indicated by the process of 'connective tissue development' (Awaji and Suzuki, 1995). The transplanted grafts were clearly separable at 48 h from the gonad tissues where these were implanted as the development of pearl sac was not initiated by this time (Awaji and Suzuki, 1995). However, after 1 week the transplanted grafts could not be clearly distinguished from the surrounding tissues, indicating that the formation of pearl sac was in progress. The up- and down-regulation of many processes related to epithelial cell proliferation at 1 w – 2 w and 2 w – 1 m, respectively, suggest that the pearl sac formation was completed by 2 weeks. We also observed the most crucial time for pearl sac formation was 1 w – 2 w (Fig. 2.4). An early report on pearl sac formation in *P. fucata* stated that the bead was completely covered with a monolayer of epithelial cells by day 14 (Awaji and Suzuki, 1995) which is in line with the result of the present study. Similarly, pearl-sac formation was observed within 3-7 days after implantation in case of 3 mm nuclei, 4-10 days in the case of 4 mm nuclei and 6-12 days in the case of 5 mm nuclei in *P. fucata* (Velayudhan et al., 1995). Two other studies on *P. margaritifera* also showed that the pearl sac development required 12 to 14 days (Kishore and Southgate, 2016; Cochennec-Laureau et al., 2010). All of these results indicate the importance of the first two weeks of pearl culture after grafting during which pearl sac is generated.

The differential expression of a number of genes including *JAG1, RFX3, STRC, FGFR2, SAV1, RAC1, DMD, RGMA, PTK7, MAF, MEF2A, SFRP5, TGM1, FZD1, GRHL2, TEAD1, PRKDC, LAMC1, EGFR, CASP8, CDC42, RSPO2, MTSS1, MATN1, SULF1, SPG20* and *LRP6* in some important processes related to epithelial cells proliferation and differentiation rationally indicate their implication in the formation of pearl sac (Table 2.4). So far we know, the function of these genes has not been described yet in mollusk except epidermal growth factor receptor (*EGFR*). Being a member of the epidermal

growth factor family, *EGFR* primarily functions in development, growth and tissue regeneration (Herbst, 2004). *EGFR* was found to be expressed specifically in the mantle and the pearl sac of *P. fucata*, interpreting its possible role in pearl formation (Zhu et al., 2015). In the present study, *EGFR* was up-regulated during 48 h – 1 w and 1 w – 2 w time points and then down-regulated at 2 w – 1 m, which definitely clarifies its role in the development of pearl sac (Table 2.4).

Though there is no very substantiating evidence about the stem cells that contribute to pearl sac development, but the outer epithelia in the central zone display the characteristic features of the stem cell, i.e. high proliferation rate and high content of saccharides (Fang et al., 2008). Here, we determined several stem cell marker genes of which *ABCG2, FZD1, HES1, MEF2A* and *ESR1* were up-regulated and *MET, NRP1, STAT6, PAX2, PROM1, ESR1* and *SOX2* were down-regulated (Table 2.4). The differential expression of these genes during the first two weeks of pearl culture definitely suggests that the outer epithelium possesses stem cells which proliferate into pearl sac. Besides, the enrichment of these genes in epithelial cell proliferation and differentiation-related processes clarify their potentiality in the formation of pearl sac. Moreover, Stem cell-specific transcription factor *SOX2* was also very recently identified from proliferating gonad duct of Pacific oyster (Cavelier et al., 2017). The signal transducers and activators of the transcription family gene *STAT* have been reported for *P. fucata* in a previous study, where it was up-regulated upon grafting peaking at day 3 (Huang et al., 2015a). *STAT* is stimulated by nucleus grafting operation and may have different functions, including wound repair and the immune response to the graft (Huang et al., 2015a). These results provide valuable information in understanding the molecular mechanism of pearl sac formation in *P. fucata*.

CHAPTER 3

Expression profiles of biomineralization-related genes at different stages for the formation of pearl sac and pearl in the pearl oyster, *Pinctada fucata*

The content of this chapter has been published as:

Mariom, S. Take, Y. Igarashi, K. Yoshitake, S. Asakawa, K. Maeyama, K. Nagai, S. Watabe and S. Kinoshita 2019. Gene expression profiles at different stages for formation of pearl sac and pearl in the pearl oyster *Pinctada fucata*. **BMC Genomics 20: 240**.

Abstract

The most critical step in the pearl formation during aquaculture is issued to the proliferation and differentiation of outer epithelial cells of mantle graft into pearl sac. This pearl sac secretes various matrix proteins to produce pearls by a complex physiological process which has not been well-understood so far. Here, we aimed to screen out the biomineralization-related genes and unravel the sequential expression pattern of the key genes involved in pearl biomineralization in *Pinctada fucata* at different stages using high-throughput transcriptome profiling. Principle component analysis (PCA) showed clearly different gene expression profiles between earlier (before 1 week) and later stages (1 week to 3 months) of grafting. The expression profiling of 192 biomineralization-related genes demonstrated that most of the shell matrix proteins (SMPs) involved in prismatic layer formation were first up-regulated and then gradually down-regulated indicating their involvement in the development of pearl sac and the onset of pearl mineralization. Most of the nacreous layer forming SMPs were up-regulated at 2 weeks after the maturation of pearl sac. Nacrein, MSI7 and shematrin involved in both layer formation were highly expressed during 0 h – 24 h, down-regulated up to 1 week and then up-regulated again after accomplishment of pearl sac formation. These findings provide valuable information in realizing the molecular mechanism of pearl formation in *P. fucata*.

3.1 Introduction

The unique ability of producing pearl has made the pearl oyster one of the best-studied species in relation to biomineralization. One of the most abundant biomineralization product in nature is the mollusk shell. The pearl oyster shell consists of two distinct layers: inner nacreous layer made of aragonite and outer prismatic layer made of calcite (Sudo et al., 1997). Many studies have been focused on oyster shell formation and revealed that the formation of prismatic and nacreous layer is regulated by the proteins secreted from mantle (Sudo et al., 1997; Suzuki and Nagasawa, 2013; Funabara et al., 2014). Moreover, the prisms and nacre are assembled from very different protein repertoires secreted from different regions of mantle (Marie et al., 2012). Mantle edge is responsible for the secretion of prismatic layer and mantle pallium is responsible for the secretion of nacreous layer (Marie et al., 2012).

To date, a vast number of shell matrix proteins have been identified that play a vital role in the molecular mechanisms underlying the formation of shell and pearl (Funabara et al., 2014; Kinoshita et al., 2011; Gao et al., 2016). On the basis of distribution or gene expression patterns, the organic matrix proteins involved in biomineralization have been classified into three categories: nacreous layer forming gene (e.g. Pearlin, MSI60, linkine, N19, N16, Perlucin-7, dermatopontin, lustrin, pif177, MSI80) prismatic layer forming gene (e.g. Aspein, KRMP, MSI31, MPN88, prismalin-14, cement-like protein, PUSP-20) and both layer forming gene (Nacrein, MSI7, Shematrin, N66) (Awaji and Machii, 2011; Suzuki and Nagasawa, 2013; Funabara et al., 2014). However, all the biomineralization-associated genes are not necessarily involved in the formation of the $CaCO_3$ polymorphs like calcite or aragonite, and of the specific microstructures like prisms or nacre, rather some regulate the expression of the shell or pearl

biomineralization genes (Marie et al., 2012; Li et al., 2017). Some of these genes are involved in the formation of prismatic layer (Takeuchi et al., 2008; Suzuki et al., 2004; Kong et al., 2009; Marie et al., 2012), some in nacreous layer (Marie et al., 2012; Suzuki et al., 2009; Montagnani et al., 2011; Samata et al., 1999; Ohmori et al., 2018), some in both layers (Miyamoto et al., 1996; Zhang et al., 2003; Yano et al., 2006), and the others control and modulate the secretion and expression of these shell or pearl forming genes (Zhao et al., 2014; Gao et al., 2016; Li et al., 2017). For example, some are transcription factor genes which largely influence the expression of some SMP genes (Zhao et al., 2014; Zheng et al., 2015; Gao et al., 2016), some are receptor genes that involve in shell biomineralization by mediating TGFβ/BMP signaling pathway in mollusks (Zhao et al., 2016; Li et al., 2017), and some inhibit the secretion of $CaCO_3$ to control the overgrowth of $CaCO_3$ polymorph (Samata et al., 1999; Zhang et al., 2003). All these components of the shell matrices are synthesized and deposited in a precisely controlled manner. Therefore, the expression profiling of the genes primarily involved in shell or pearl mineralization can provide useful information in discerning the mechanism of pearl formation. However, current knowledge in relation to the expression pattern of these genes is very limited (Wang et al., 2009; Miyazaki et al., 2010; Gu et al., 2016; Li et al., 2017b; Luyer et al., 2019).

Shell matrix proteins (SMPs) are considered to play an important role in crystal nucleation, crystal growth and inhibition, crystal polymorphism, crystal morphology, and atomic lattice orientation (Belcher et al., 1996; Kong et al., 2009; Liu et al., 2012). They act as a basis for the quality of pearl formation. But the fate of the SMPs during pearl development still needs to be exemplified. It is notable that during shell biomineralization prisms and nacre are assembled from very different protein repertories

while in pearl biomineralization the same cells secrete both prism and nacre (Marie et al., 2012).

In spite of having comprehensive studies about the mechanism of pearl formation in *Pinctada*, we still know very little about the genes that expressed in the mantle graft and the later pearl sac and how the grafting process affects gene expression through pearl formation (Machi, 1968; Awaji and Suzuki, 1995; Chen and Qian, 2009; Awaji and Machi, 2011; Eddy et al., 2015). Hence, the goal of the study was to improve the overall understanding of the expression profiles of 192 pearl forming genes secreted from the pearl sac epithelium during the development of pearl. Then, we focused on the detailed expression pattern of the well-known shell matrix proteins (SMPs) during three months grafting experiment.

3.2 Materials and Methods

3.2.1 Experimental animal and mantle grafting

Grafting experiment was described in chapter 2 (Fig. 2.1). Briefly, mantle graft was prepared from 3 donor *P. fucata* and were transplanted into 42 host oysters at the Mikimoto pearl farm, Mie, Japan (Fig. 2.1a,b). All the oysters were about 2 years old and in good condition. After grafting operation, the recipient oysters were reared for 3 months. We collected nine samples i.e., donor mantle epithelial cells (cell), donor mantle pallium (before), donor mantle pallium on grafting but before transplantation (0 h), 24 h, 48 h, 1 w, 2 w, 1 m, and 3 m post grafting) for the gene expression studies (Fig. 2.1c). All the samples were preserved immediately in RNAlater® solution (Ambion, USA) at -80°C until RNA extraction. Pearl sacs at 1 w, 2 w, 1 m and 3 m were contaminated with host gonad tissues due to the difficulty of separating pearl sac completely from the surrounding host gonad tissues.

3.2.2 RNA sequencing and data analysis

Total RNA was extracted from all the collected samples using RNeasy Mini Kit (QIAGEN, Hilden, Germany) according to the manufacturer's protocol. cDNA library was prepared using TruSeq Stranded mRNA Library Prep Kit (Illumina, USA) taking 2 µg of total RNA per sample as input materials as described in chapter 2. After assessing the quality, the libraries were paired-end sequenced (Illumina Hiseq 4000) and 100 bp paired-end reads were generated.

The resulting clean reads were *de novo* assembled using Trinity version 2.4.0 (Grabherr et al., 2011) and pseudo-aligned to the reference *P. fucata* genome using Kallisto (Bray et al., 2016) as described in chapter 2. Assembled contigs were annotated by Trinotate for a BLAST search against the Swiss-Prot, RNAMMER, GO, COG, Pfam, and KEGG, and by in-house script for a BLAST search against NCBI NT. Statistical analysis software R was used for the analysis of RNA-seq data.

3.2.3 Screening of bioineralization-related genes

Biomineralization-related transcripts were screened by searching BLAST (blastn for similar species and tblastx for different species) using CLC Genomics Workbench against a list of reference biomineralization genes prepared beforehand. The list of the reference biomineralization-related genes were processed from the literature search. The transcript with the lowest E-value and the highest bit score was identified as the best homolog of the reference gene. The expression level of gene was represented as transcripts per million (TPM).

3.2.4 Estimation of host contamination rate

In order to calculate donor specific SNVs, RNA-seq sequencing data were mapped with STAR (version 2.5.3a) using 2-pass mapping (Dobin et al., 2013). HaplotypeCaller

module of Genome Analysis Toolkit (version 3.8-0) was used to call SNV and SNVs with the genotype quality less than 10 were removed (McKenna et al., 2010). Then contamination ratio was estimated for each donor based on the sample of 0 h as a reference. For example, in the case of donor A, 0 h donor A sample was compared with all sample data not containing donor A, and donor A specific SNVs that appeared only in 0 h donor A were extracted. The number of reads with donor A specific SNV and the number of other reads were added each other and the percentage of reads with donor A specific SNV at 0 h donor A was taken as 100%. Except 0 h, for the other donor A samples, the contamination rate of the host was calculated by the ratio of the donor A specific SNV reads to 0 h.

3.3 Results

3.3.1 Clustering of samples by whole gene expression patterns

Sample distances were calculated using R and visualized in a heatmap to know the differences in overall gene expression pattern during different stages of pearl formation. Cluster analysis revealed the dissimilarities in gene expression at various stages of pearl grafting as the samples were divided into four distinct groups: cell, before – 0 h, 24 h – 48 h and 1 w – 3 m (Fig. 3.1). The figure illustrated that expression profile in cell was apart from any other groups. The differences in expression in 'cell' might be derived from two possible reasons. The first one is as 'cells' consists of only outer epithelial cells but 'mantle pallium' contains outer epithelial cells, inner epithelial cells, connective tissues and so on. Another is the differences in preparation technique. 'Mantle pallium' is just cut from the mantle whereas, 'cell' is prepared from mantle through a complicated process described in the method. These preparation steps might affect the gene expression in 'cell'. Again, upto 48 h samples, the clusters were 'stage dependent' as the

samples were separated in three different stages (cell, before – 0 h and 24 h – 48 h) (Fig. 3.1). At each stage, the clusters were also 'donor dependent' because the samples/grafts obtained from the same donor were grouped together. For example, in 24 h – 48 h cluster, the host oysters 24h_A1, 24h_A2, 48h_A1 and 48h_A2 received graft from the 'donor A' were grouped together (Fig. 3.1). On the other hand, the expression in 1 w – 3 m samples is 'host dependent' as the cluster for 1 w – 3 m samples is neither stage dependent nor donor dependent (Fig. 3.1). This is because after transplantation, the grafts and the later pearl sacs were contaminated with host gonad tissues especially from 1 week to 3 months samples.

In order to know the rate of contamination of host cells, we therefore detected single nucleotide variants (SNVs) between donor and host transcripts. In case of xenografting from two closely related species where inter-specific sequence differences in homologous biomineralization genes are present, it is possible to discern whether the donor or host cells are transcriptionally active for the relevant gene (McGinty et al., 2012). But due to the lack of data on intra-specific polymorphisms in biomineralization genes, it is impractical to separate the gene transcripts derived from individual oysters used as donors or hosts in allografting. As we performed allografting, hence we only calculated the percentage of donor specific SNVs in each sample (Fig. 3.2) in order to get the actual expression of donor specific transcripts for the studied biomineralization-related genes. But in the calculation, the rate of donor specific SNVs were underestimated since not only '0 h' samples but also 'before' and 'cell' samples were without any contamination with host tissues i.e. donor specific SNV rate should be 100% (Fig. 3.2). Hence, the real donor specific SNVs in all the samples except '0 h' were little more than that showed in figure 1. Additionally, figure 3.2 likewise figure 3.1 described

that 0 h – 48 h samples contained transcripts mainly from donor whereas most of the transcripts in 1 w – 3 m samples were from host.

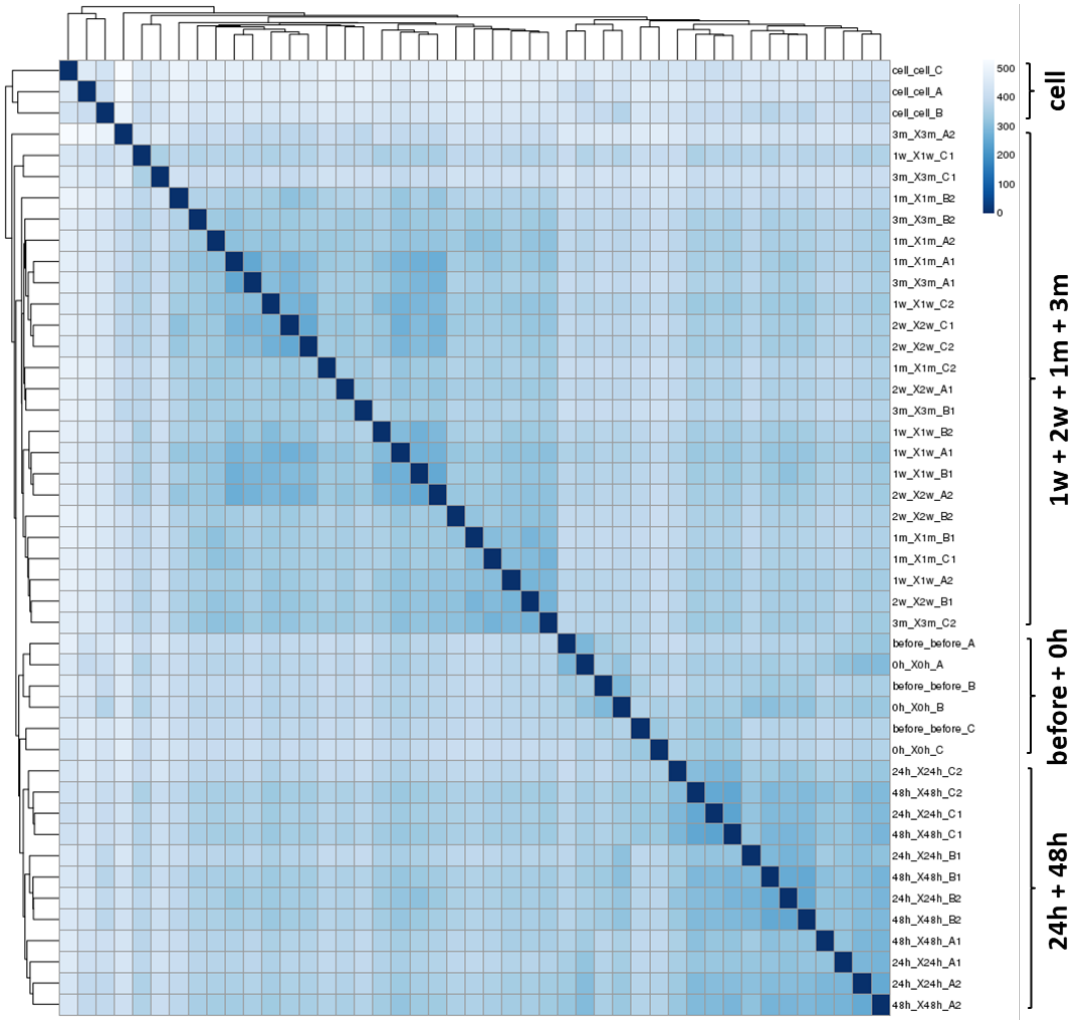

Figure 3.1. Heat map demonstrating whole gene expression profile at different stages of pearl grafting. Hierarchical clustering divided all the samples into four groups (cell, before + 0 h, 24 h + 48 h and 1 w + 2 w + 1 m + 3 m) as indicated on figure. Colour scale indicates the differences in expression.

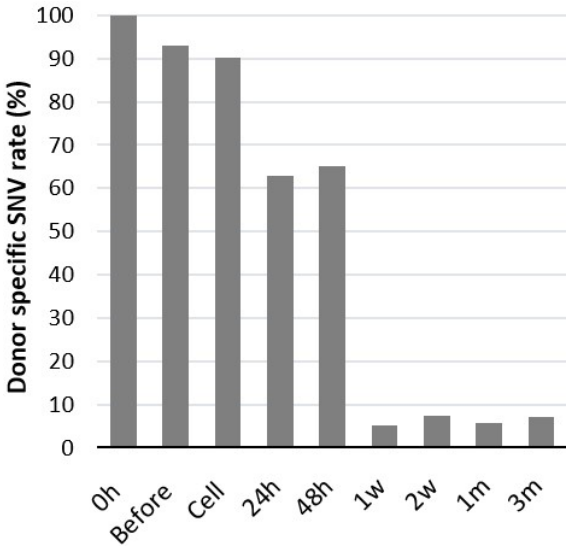

Figure 3.2. Donor specific SNV rate (%) in different samples. The X- and Y-axis illustrate samples at different time points and percentage of SNV, respectively. "h" for hour, "w" for week and "m" for month.

3.3.2 Examination of contamination rate of host transcripts to adjust the expression levels of biomineralization-related genes expressed specifically in the pearl sac

In the next part of the study, we focused on biomineralization-related genes specifically expressed in the mantle epithelial cells. These genes are expressed in donor mantle epithelial cells of pearl sac but not in host tissues surrounding the pearl sac. However, as discussed above, our transcriptome data contained transcripts from contaminated host tissues due to the difficulty of separating pearl sac completely from the surrounding host gonad tissues. For the first time, here we estimated the contamination rate based on the calculated donor specific SNV rate (Fig. 3.2) and then adjusted the expression level (TPM, transcripts per million) of biomineralization-related genes using following equation.

$$Adjusted\ expression\ level = TPM \times \frac{100}{100 - contamination\ rate\ (\%)}$$

Where, $Contamination\ rate\ (\%) = 100 - Donor\ specific\ SNV\ rate\ (\%)$

After adjusting the expression level, we found that the expression pattern of SMPs is comparable to the previous study which substantiate the potentiality of this method (Liu et al., 2012).

3.3.3 Expression profiles of biomineralization-related genes during pearl sac and pearl formation

To date, more than 200 molluscan biomineralization-related genes have been identified that contribute to the formation of the shell and pearl (McGinty et al., 2012; Joubert et al., 2010). Here, we selected 192 biomineralization-related genes from various pearl producing mollusks including *P. fucata* (Table 3.1), and our transcripts were annotated to these reference genes. Then the expression levels of all the 192 genes were adjusted according to the above equation. PCA was performed on the 192 biomineralization-related genes. The results of PCA showed clearly different gene expression profiles between earlier (cell, before, 0 h, 24 h, 48 h) and later stages (1 w, 2 w, 1 m and 3 m) after grafting (Fig. 3.3). Further hierarchical clustering of the 192 genes presented more clear explanation about their expression and contribution during pearl sac and pearl formation (Fig. 3.4). It was evident that one week after graft transplanting the expression of almost all the genes changed drastically and remained comparable upto the end of three months. In the hierarchical clustering, biomineralization-related genes were separated into four groups named group A – D under two major clusters (Fig. 3.4). Most of the genes grouped in cluster 1 showed higher expression during the earlier stages of pearl formation followed by a decrease in the later stages, whereas a reverse trend was observed in gene cluster 2. Table 3.2 listed the genes in different groups and clusters with their recognition in the shell formation.

Table 3.1. Identification of genes reported to be involved in biomineralization in the transcriptome of *Pinctada fucata*

Hit ID	Candidate gene	Accession	E-value	Bit score	Species	Similarity (%)
TRINITY_DN181342_c1_g2_i1	ACCBP1	DQ473430.1	0	1593.66	*Pinctada fucata*	98.69
TRINITY_DN159449_c0_g1_i1	Alkaline phosphatase	AY653739.1	0	1804.66	*Pinctada fucata*	97.83
TRINITY_DN207376_c1_g1_i3	AP-1	KP347629.1	0	2372.72	*Pinctada fucata*	99.18
TRINITY_DN195753_c4_g1_i1	AP-7	AF225916.1	0.70	35.43	*Haliotis rufescens*	42.31
TRINITY_DN157701_c0_g2_i2	AP-24	AF225915.1	0.53	37.27	*Haliotis rufescens*	46.15
TRINITY_DN199219_c6_g1_i1	Aspein	AB094512.1	0	1352.01	*Pinctada fucata*	97.14
TRINITY_DN217445_c7_g1_i1	Predicted: BMP-1	XM_020064487.1	3.27E-124	447.36	*Crassostrea gigas*	74.12
TRINITY_DN211356_c1_g3_i1	Predicted: BMP receptor type 1B	XM_020069073.1	0	545.88	*Crassostrea gigas*	69.61
TRINITY_DN160015_c1_g1_i2	BMP-2	AB176952.2	0	2830.77	*Pinctada fucata*	97.84
TRINITY_DN160015_c1_g1_i1	BMP2/4	AB379969.1	5.36E-154	242.54	*Saccostrea kegaki*	85.98
TRINITY_DN193248_c1_g1_i2	BMP-2B (predicted)	XM_011433252.2	2.77E-174	278.28	*Crassostrea gigas*	93.81
TRINITY_DN207695_c0_g2_i1	BMP-3 (predicted)	XM_011417318.2	0	380.01	*Crassostrea gigas*	71.56
TRINITY_DN202984_c0_g3_i2	BMP-7	KC881250.1	0	5137.28	*Pinctada martensi*	98.61
TRINITY_DN217720_c4_g1_i1	BMP-R2	AJ427420.1	0	640.27	*Crassostrea gigas*	68.62
TRINITY_DN211167_c0_g1_i5	BMSP	AB477349.1	0	346.56	*Mytilus galloprovincialis*	66.29
TRINITY_DN217592_c6_g1_i7	Calcineurin B subunit	EU797511.1	0	1299.71	*Pinctada fucata*	99.59
TRINITY_DN217645_c4_g1_i4	CaM-dependent protein kinase I	EU921667.1	0	1986.80	*Pinctada fucata*	99.03
TRINITY_DN200662_c4_g1_i4	Calcium-dependent protein kinase	AY713401.2	2.11E-44	180.26	*Crassostrea gigas*	57.25
TRINITY_DN129150_c0_g1_i1	Calconectin	DQ352042.1	7.76E-18	76.67	*Pinctada margaritifera*	43.55
TRINITY_DN182688_c2_g1_i1	Calmodulin	AY341376.1	0	654.11	*Pinctada fucata*	99.46
TRINITY_DN194170_c0_g1_i5	Calmodulin-like protein	AY663847.1	0	1263.64	*Pinctada fucata*	99.03

TRINITY_DN212003_c10_g2_i2	Calponin-like protein	AB052656.1	1.75E-58	124.33	*Mytilus galloprovincialis*	59.52
TRINITY_DN207086_c1_g2_i2	Calreticulin	EF551334.1	0	3243.74	*Pinctada fucata*	98.92
TRINITY_DN210861_c3_g2_i11	Carbonic anhydrase II	AB695265.1	3.21E-151	536.89	*Pinctada fucata*	99.67
TRINITY_DN196002_c1_g3_i1	Carbonic anhydrase precursor	AY790884.1	1.17E-67	85.38	*Tridacna gigas*	43.42
TRINITY_DN198845_c0_g6_i1	Cathepsin B	HQ845754.1	0	1016.58	*Pinctada fucata*	97.82
TRINITY_DN185064_c0_g3_i1	Cement-like protein	HE610386.1	5.83E-72	75.76	*Pinctada margaritifera*	53.73
TRINITY_DN194890_c2_g1_i3	Chitin binding protein	KJ930034.2	0	3644.09	*Pinctada martensii*	98.48
TRINITY_DN217609_c10_g1_i5	Predicted: Chitin synthase 1	XM_020066933.1	8.35E-136	383.67	*Crassostrea gigas*	59.32
TRINITY_DN206451_c0_g1_i11	Predicted: Chitinase 3	XM_020069038.1	0	417.12	*Crassostrea gigas*	74.65
TRINITY_DN183439_c6_g1_i1	Predicted: CHST11	XM_011423757.2	2.69E-112	177.94	*Crassostrea gigas*	58.33
TRINITY_DN205761_c0_g3_i3	CLP1 protein	HE610381.1	0	831.80	*Pinctada margaritifera*	94.46
TRINITY_DN161256_c0_g1_i1	C-type lectin 1	FJ812172.1	0	1514.31	*Pinctada fucata*	95.12
TRINITY_DN152363_c0_g2_i1	C-type lectin 2	FJ812173.1	0	796.57	*Pinctada fucata*	98.47
TRINITY_DN192920_c1_g1_i5	Dermatopontin	JQ734542.1	0	1353.81	*Pinctada martensii*	99.22
TRINITY_DN176128_c0_g2_i3	EFCBP	DQ494416.1	1.42E-133	479.18	*Pinctada fucata*	81.80
TRINITY_DN189138_c0_g1_i3	Engrailed	DQ298403.1	7.15E-41	159.61	*Haliotis asinina*	71.43
TRINITY_DN188012_c0_g1_i3	EP protein precursor	AY364453.1	3.46E-11	70.72	*Mytilus edulis*	29.23
TRINITY_DN208997_c0_g2_i3	Fam20c	MF785096.1	0	4053.46	*Pinctada fucata*	97.16
TRINITY_DN171687_c0_g1_i1	Ferritin	GU191936.1	3.75E-93	341.97	*Haliotis rufescens*	84.43
TRINITY_DN213730_c1_g1_i3	Ferritin-like protein	AF547223.1	1.34E-167	592.79	*Pinctada fucata*	98.82
TRINITY_DN177648_c4_g1_i5	GRMP	AF516712.1	2.19E-78	295.24	*Pinctada fucata*	85.94
TRINITY_DN199776_c1_g2_i2	Homeobox protein-4	GU056184.1	1.93E-39	163.27	*Gibbula varia*	82.28
TRINITY_DN172328_c2_g1_i6	Incilarin A	AB003430.1	3.76E-20	75.30	*Incilaria fruhstorferi*	32.50
TRINITY_DN173053_c0_g1_i11	Incilarin C	AB003432.1	3.85E-16	80.34	*Incilaria fruhstorferi*	40.00
TRINITY_DN180235_c0_g1_i13	Jacalin-related lectin PPL2-a	AB425237.1	1.14E-27	78.96	*Pteria penguin*	41.56

TRINITY_DN200752_c5_g1_i1	KRMP-1	DQ114788.1	0	811.00	*Pinctada fucata*	97.69
TRINITY_DN200752_c5_g1_i12	KRMP-2	DQ114789.1	1.38E-177	609.02	*Pinctada fucata*	97.24
TRINITY_DN200752_c5_g1_i6	KRMP-3	DQ114790.1	4.79E-177	623.45	*Pinctada fucata*	97.30
TRINITY_DN155539_c0_g1_i1	KRMP-4	EF183517.1	7.50E-05	48.72	*Pinctada margaritifera*	61.76
TRINITY_DN90541_c0_g1_i2	KRMP-5	EF183518.1	4.14E-04	45.97	*Pinctada margaritifera*	50.00
TRINITY_DN200752_c5_g1_i4	KRMP-6	EF183519.1	6.63E-03	41.85	*Pinctada margaritifera*	51.35
TRINITY_DN179399_c1_g1_i1	KRMP-7	EF192240.1	2.42E-03	42.76	*Pinctada margaritifera*	50.00
TRINITY_DN200752_c5_g1_i13	KRMP-8	EF192241.1	0.641405	34.52	*Pinctada margaritifera*	73.68
TRINITY_DN155539_c0_g1_i2	KRMP-9	EF192242.1	0.348422	35.89	*Pinctada margaritifera*	60.87
TRINITY_DN181079_c1_g1_i2	KRMP-10	EF192243.1	2.76E-06	37.27	*Pinctada margaritifera*	57.69
TRINITY_DN200752_c5_g1_i11	KRMP-11	EF192244.1	0.45	29.48	*Pinctada margaritifera*	69.23
TRINITY_DN166167_c0_g1_i4	Lectin	AB037167.1	3.44E-44	179.77	*Pteria penguin*	50.34
TRINITY_DN181830_c0_g1_i3	Linkine	EF183520.1	9.21E-14	56.51	*Pinctada margaritifera*	44.19
TRINITY_DN216165_c1_g1_i4	L-type voltage-dependent calcium channel beta subunit	EF154452.1	0	1831.71	*Pinctada fucata*	94.91
TRINITY_DN173236_c2_g1_i3	Lustrin A	AF023459.1	6.25E-10	68.88	*Haliotis rufescens*	33.82
TRINITY_DN207119_c2_g1_i7	M45	AF513719.1	2.39E-02	38.64	*Pinctada maxima*	70.00
TRINITY_DN214298_c1_g1_i4	Matrix metalloproteinase	KC881251.3	0	4347.41	*Pinctada martensii*	99.07
TRINITY_DN171392_c5_g1_i1	Metallothionein	KC197172.1	0	798.38	*Pinctada martensii*	97.47
TRINITY_DN188649_c0_g1_i11	Metallothionein-2	KC832833.1	0	834.44	*Pinctada martensii*	98.74
TRINITY_DN134217_c0_g1_i2	ML1A1	DW986183.1	0.82	35.43	*Haliotis asinina*	31.03
TRINITY_DN144665_c0_g1_i1	ML1A2	KX687871.1	0.12	38.64	*Haliotis laevigata*	69.23
TRINITY_DN171687_c0_g1_i1	ML7A7	DW986406.1	1.02E-83	309.90	*Pinctada maxima*	82.25
TRINITY_DN196157_c1_g1_i2	MNRP34	HQ625028	1.27E-97	193.52	Pinctada margaritifera	85.88
TRINITY_DN176504_c1_g1_i8	MPN	HQ259055.1	1.19E-19	73.92	*Pinctada margaritifera*	81.82

TRINITY_DN205004_c2_g2_i13	MPN88	AB295108.1	0	1101.34	*Pinctada fucata*	99.04
TRINITY_DN205004_c2_g2_i8	MPN88-lack6	AB295114.1	0	989.53	*Pinctada fucata*	97.12
TRINITY_DN205004_c2_g2_i4	MPN88-lack7	AB295115.1	0	1064.00	*Pinctada fucata*	98.20
TRINITY_DN177648_c4_g1_i5	MSI7	AB661679.1	0	1032.81	*Pinctada fucata*	92.96
TRINITY_DN187890_c4_g1_i1	MSI25 (hypothetical protein)	AB210136.1	0	1238.40	*Pinctada fucata*	99.57
TRINITY_DN177648_c4_g1_i2	MSI30/MSI2	D86073.1	0	744.27	*Pinctada fucata*	98.59
TRINITY_DN177648_c4_g1_i8	MSI31	AB661680.1	0	1205.94	*Pinctada fucata*	98.84
TRINITY_DN190306_c1_g3_i11	MSI60/insoluble protein	D86074.1	0	1362.83	*Pinctada fucata*	100.00
TRINITY_DN190306_c1_g3_i5	MSI60RP	AB689024.1	0	2203.20	*Pinctada fucata*	97.76
TRINITY_DN181079_c2_g1_i4	MSI80	AB683051.1	0	1734.32	*Pinctada fucata*	96.32
TRINITY_DN170525_c0_g1_i14	MSP-1	AB073617.1	0.24	26.73	*Mizuhopecten yessoensis*	29.63
TRINITY_DN172299_c0_g1_i5	Mucoperlin	AF145215.1	6.88E-06	29.48	*Pinna nobilis*	45.00
TRINITY_DN181604_c4_g2_i5	N14#3.pro	AB023250.1	4.37E-154	547.71	*Pinctada fucata*	86.12
TRINITY_DN181604_c4_g2_i4	N14#7.pro	AB023254.1	1.50E-102	376.39	*Pinctada fucata*	98.17
TRINITY_DN181604_c4_g5_i2	N16-1/N14#1.pro	AB023067.1	2.26E-132	475.57	*Pinctada fucata*	91.59
TRINITY_DN181604_c4_g2_i2	N16-2/N14#2.pro	AB023249.1	8.98E-106	387.21	*Pinctada fucata*	92.16
TRINITY_DN181604_c5_g1_i1	N16-3/N14#4.pro	AB023251.1	5.18E-77	291.63	*Pinctada fucata*	91.26
TRINITY_DN181604_c4_g1_i3	N16-5/N14#5.pro	AB023252.1	1.01E-104	383.60	*Pinctada fucata*	98.20
TRINITY_DN181604_c4_g1_i4	N16-6	AB808591.1	3.47E-73	279.01	*Pinctada fucata*	95.43
TRINITY_DN181604_c4_g5_i1	N16-7	AB781153.1	2.59E-157	558.53	*Pinctada fucata*	97.86
TRINITY_DN213546_c4_g1_i4	N19	AB332326.1	0	845.26	*Pinctada fucata*	91.98
TRINITY_DN213546_c4_g1_i3	N19-2	AB781154.1	3.55E-170	601.81	*Pinctada fucata*	96.20
TRINITY_DN208388_c3_g1_i5	N23	JN995665.1	0	720.83	*Pinctada fucata*	97.20
TRINITY_DN199991_c5_g1_i2	N36/33	FJ913471.1	1.12E-76	226.96	*pinctada maxima*	83.33
TRINITY_DN206875_c1_g7_i1	N44	KC238310.1	0	1703.67	*Pinctada fucata*	98.97

TRINITY_DN199991_c5_g1_i5	N45	FJ913472.1	3.30E-91	336.93	*pinctada maxima*	69.42
TRINITY_DN199991_c5_g1_i7	N66	AB032613.1	4.30E-73	277.37	*pinctada maxima*	71.62
TRINITY_DN190149_c0_g1_i2	N151	AB534773.1	0	1781.21	*Pinctada fucata*	92.54
TRINITY_DN199991_c5_g1_i2	Nacrein	D83523.1	0	2286.15	*Pinctada fucata*	94.21
TRINITY_DN198561_c3_g1_i1	Neuronal calcium sensor-1	DQ099793.2	3.33E-105	382.30	*Lymnaea stagnalis*	80.53
TRINITY_DN188235_c0_g1_i4	NSPI-5	HE610407.1	2.80E-93	322.73	*Pinctada margaritifera*	95.24
TRINITY_DN199049_c3_g2_i1	NUSP-3	HE610403.1	7.41E-42	135.78	*Pinctada margaritifera*	67.06
TRINITY_DN195876_c1_g1_i4	NUSP-6	HE610404.1	1.23E-16	51.93	*Pinctada margaritifera*	100.00
TRINITY_DN196680_c4_g1_i4	NUSP-17	HE610408.1	2.14E-18	76.21	*Pinctada margaritifera*	91.84
TRINITY_DN204711_c0_g3_i1	Paramyosin	XM_020073252.1	2.07E-35	100.50	*Crassostrea gigas*	51.22
TRINITY_DN181604_c4_g5_i2	Pearlin	AB020779.1	4.72E-141	504.43	*Pinctada fucata*	94.19
TRINITY_DN165493_c0_g1_i5	Perlucin	XM_020075162.1	1.73E-30	78.50	*Crassostrea gigas*	49.12
TRINITY_DN193167_c0_g2_i4	Perlucin 7	EF103338.1	5.08E-18	84.92	*Haliotis discus*	32.00
TRINITY_DN188557_c0_g1_i3	Perlwapin-like protein	FS941021.1	0	735.26	*Pinctada fucata*	99.76
TRINITY_DN186079_c0_g6_i2	PfBAMBI	KF280237.1	0	2287.96	*Pinctada fucata*	99.46
TRINITY_DN211356_c1_g3_i1	PfBMPR1B	KF280238.1	0	3339.32	*Pinctada fucata*	99.21
TRINITY_DN195768_c0_g1_i1	PfCB/chitobiase	No accession no. (Kintsu et al., 2017)	0	4352.82	*Pinctada fucata martensii*	98.03
TRINITY_DN183304_c0_g1_i8	PfChi1/chitinase 1	KT956975.1	0	1716.29	*Pinctada fucata*	95.20
TRINITY_DN209015_c0_g1_i2	PfCHS1/chitin synthase	AB290881.1	0	13007.20	*Pinctada fucata*	99.11
TRINITY_DN196988_c5_g1_i3	PfCN/chitinase	No accession no. (Kintsu et al., 2017)	0	2926.35	*Pinctada fucata*	98.92
TRINITY_DN206485_c2_g1_i4	PfDlx	KX889394.1	0	2437.64	*Pinctada fucata*	96.99
TRINITY_DN175424_c7_g4_i6	PFMG1	DQ104255.1	0	1205.94	*Pinctada fucata*	96.34

TRINITY_DN201315_c2_g1_i2	PFMG2	DQ104256.1	0	1243.81	*Pinctada fucata*	97.57
TRINITY_DN205925_c3_g1_i4	PFMG3	DQ104257.1	0	836.25	*Pinctada fucata*	99.79
TRINITY_DN203092_c3_g3_i2	PFMG4	DQ104258.1	5.18E-153	544.10	*Pinctada fucata*	92.27
TRINITY_DN174215_c0_g2_i2	PFMG5	DQ104259.1	0	1232.99	*Pinctada fucata*	99.57
TRINITY_DN175424_c7_g4_i2	PFMG6	DQ104260.1	0	1151.84	*Pinctada fucata*	94.95
TRINITY_DN175424_c7_g4_i6	PFMG7	DQ104261.1	0	1234.79	*Pinctada fucata*	97.15
TRINITY_DN179272_c1_g1_i8	PFMG8	DQ104262.1	0	765.92	*Pinctada fucata*	92.82
TRINITY_DN176888_c0_g1_i10	PFMG9	DQ116436.1	0	648.70	*Pinctada fucata*	93.12
TRINITY_DN187791_c3_g2_i1	PFMG10	DQ116437.1	0	1665.80	*Pinctada fucata*	99.78
TRINITY_DN176813_c0_g5_i1	PFMG11	DQ116438.1	2.02E-172	609.02	*Pinctada fucata*	99.71
TRINITY_DN179530_c0_g1_i3	PFMG12	DQ116439.1	0	1397.09	*Pinctada fucata*	98.27
TRINITY_DN217595_c1_g1_i2	PfMSX	KJ028208.1	0	1076.09	*Pinctada fucata*	99.02
TRINITY_DN176504_c1_g1_i5	Pfp-16 for hypothetical protein	AB210137.1	0	769.52	*Pinctada fucata*	94.30
TRINITY_DN211728_c2_g1_i2	Pf-POU2F1	KM588196.1	0	1400.70	*Pinctada fucata*	97.93
TRINITY_DN190944_c0_g2_i1	Pf-POU3F4	KM519606.1	0	3472.77	*Pinctada fucata*	99.74
TRINITY_DN215982_c3_g1_i4	PfSMAD4	KF307635.1	0	4646.76	*Pinctada fucata*	98.62
TRINITY_DN170595_c0_g1_i2	PfSp8-like protein	KR057959.1	0	2874.05	*Pinctada fucata*	99.69
TRINITY_DN206997_c1_g2_i5	PfTy	AB353113.1	0	872.31	*Pinctada fucata*	95.14
TRINITY_DN206997_c1_g2_i6	PfTy1	AB254132.1	0	1674.81	*Pinctada fucata*	98.35
TRINITY_DN170108_c0_g3_i5	PfTy2	AB254133.1	0	3021.93	*Pinctada fucata*	99.82
TRINITY_DN184627_c5_g2_i3	Pfu000096	AB635374.1	0	641.48	*Pinctada fucata*	91.41
TRINITY_DN181851_c7_g1_i2	PfY2	KY436033.1	0	827.23	*Pinctada fucata*	98.94
TRINITY_DN203725_c1_g3_i4	PfYY-1	KM502551.1	0	2857.82	*Pinctada fucata*	94.40
TRINITY_DN204016_c0_g1_i2	Pif177	AB236929.1	0	5653.04	*Pinctada fucata*	96.99
TRINITY_DN217403_c0_g1_i16	Plasma membrane calcium ATPase	EF121960.1	0	4742.34	*Pinctada fucata*	99.44

TRINITY_DN183439_c6_g1_i2	PmCHST11a	No accession no. (Wang et al., 2017)	0	1009.58	*Pinctada margaritifera*	99.76
TRINITY_DN178806_c0_g2_i1	PmCHST11b	No accession no. (Wang et al., 2017)	2.4E-148	512.43	*Pinctada margaritifera*	62.10
TRINITY_DN175424_c7_g4_i4	PMMG1	FJ386386.1	4.42E-49	195.81	*Pinctada maxima*	56.62
TRINITY_DN205336_c1_g2_i7	PmRunt	KY056582.1	0	4055.26	*Pinctada martensii*	99.39
TRINITY_DN177648_c5_g1_i2	Pmshem-1 for shematrin	AB429365.1	7.16E-14	52.84	*Pinctada maxima*	45.83
TRINITY_DN185411_c1_g6_i2	Pmshem-2 for shematrin	AB429366.1	2.38E-16	46.43	*Pinctada maxima*	62.96
TRINITY_DN185411_c1_g1_i2	Pmshem-3 for shematrin	AB429367.1	9.76E-19	55.59	*Pinctada maxima*	77.42
TRINITY_DN167245_c1_g1_i3	Prisilkin-39	EU921665.1	0	1348.40	*Pinctada fucata*	97.03
TRINITY_DN166624_c0_g1_i1	Prismalin-14	AB159512.1	0	942.65	*Pinctada fucata*	98.89
TRINITY_DN188851_c0_g1_i4	Prismin-1	AB368930.2	0	760.51	*Pinctada fucata*	95.59
TRINITY_DN188851_c0_g1_i8	Prismin-2	AB433980.2	0	753.29	*Pinctada fucata*	95.53
TRINITY_DN168198_c0_g1_i2	PUSP-20	HE610397.1	3.12E-14	49.18	*Pinctada margaritifera*	58.33
TRINITY_DN212649_c5_g1_i4	Putative uncharacterized protein F18	AB254383.1	1.26E-13	78.50	*Crassostrea nippona*	69.77
TRINITY_DN175549_c3_g1_i8	Regucalcin	XM_011432550.2	1.1E-111	175.65	*Crassostrea gigas*	65.35
TRINITY_DN190072_c1_g1_i5	SCP-a	AB036700.1	5.43E-65	122.03	*Mizuhopecten yessoensis*	72.73
TRINITY_DN190072_c1_g1_i6	SCP-b	AB036703.1	2.57E-64	119.74	*Patinopecten yessoensis*	75.81
TRINITY_DN216002_c5_g1_i2	SERCA isoform A	EF488285.1	0	3400.64	*Pinctada fucata*	97.99
TRINITY_DN216002_c5_g1_i4	SERCA isoform C	EF488287.1	0	3287.02	*Pinctada fucata*	98.07
TRINITY_DN185064_c0_g3_i5	SGMP1	AB689023.1	0	2556.66	*Pinctada fucata*	98.71
TRINITY_DN185411_c1_g6_i2	Shematrin-1	AB244419.1	0	1142.82	*Pinctada fucata*	98.48
TRINITY_DN177648_c4_g1_i8	Shematrin-2	AB244420.1	0	1254.63	*Pinctada fucata*	97.56
TRINITY_DN177648_c4_g1_i2	shematrin-2alpha	KC505166.1	3.82E-20	96.37	*Pinctada maxima*	74.55
TRINITY_DN177648_c4_g1_i5	Shematrin-2beta	KJ664800.1	0	1101.34	*Pinctada fucata*	93.68

TRINITY_DN169993_c1_g1_i12	Shematrin-3	AB244421.1	0	1718.09	*Pinctada fucata*	97.15
TRINITY_DN170282_c7_g1_i5	Shematrin-4	AB244422.1	0	1101.34	*Pinctada fucata*	97.97
TRINITY_DN183917_c0_g1_i2	Shematrin-5	AB244423.1	0	2051.72	*Pinctada fucata*	95.49
TRINITY_DN175642_c0_g1_i2	Shematrin-6	AB244424.1	0	2145.49	*Pinctada fucata*	99.34
TRINITY_DN164158_c0_g2_i1	Shematrin-7	AB244425.1	0	1885.81	*Pinctada fucata*	97.99
TRINITY_DN177648_c4_g1_i8	Shematrin-8	EF160119.1	3.86E-76	289.83	*Pinctada margaritifera*	71.53
TRINITY_DN185411_c1_g6_i4	Shematrin-9	EF160120.1	8.99E-34	81.71	*Pinctada margaritifera*	42.68
TRINITY_DN216531_c3_g4_i2	SPARC	AB600273.1	0	1200.53	*Pinctada fucata*	99.70
TRINITY_DN184022_c1_g1_i13	SPI (serine proteinase inhibitor)	FS941243.1	6.95E-167	589.19	*Pinctada fucata*	96.89
TRINITY_DN215287_c2_g3_i1	TFG beta signaling pathway factor	EU137731.1	0	1415.13	*Pinctada fucata*	99.13
TRINITY_DN216470_c6_g1_i4	Tissue inhibitor of matrix metalloproteinase	KC881249.1	0	1553.99	*Pinctada martensii*	99.88
TRINITY_DN203374_c0_g1_i3	Tyr-1	KC870906.1	0	4931.70	*Pinctada martensii*	98.39
TRINITY_DN172129_c8_g1_i1	Tyrosinase	DQ112679.1	0	1487.26	*Pinctada fucata*	98.60
TRINITY_DN189000_c7_g1_i4	Tyrosinase-2	HE610378.1	0	284.24	*Pinctada margaritifera*	74.83
TRINITY_DN191267_c0_g3_i3	Veliger mantle 1	DQ328317.1	3.19E-05	51.47	*Haliotis asinina*	41.03
TRINITY_DN208660_c1_g2_i6	Voltage-dependent L-type calcium channel alpha-1 subunit	AF484081.1	1.57E-166	305.78	*Lymnaea stagnalis*	91.73

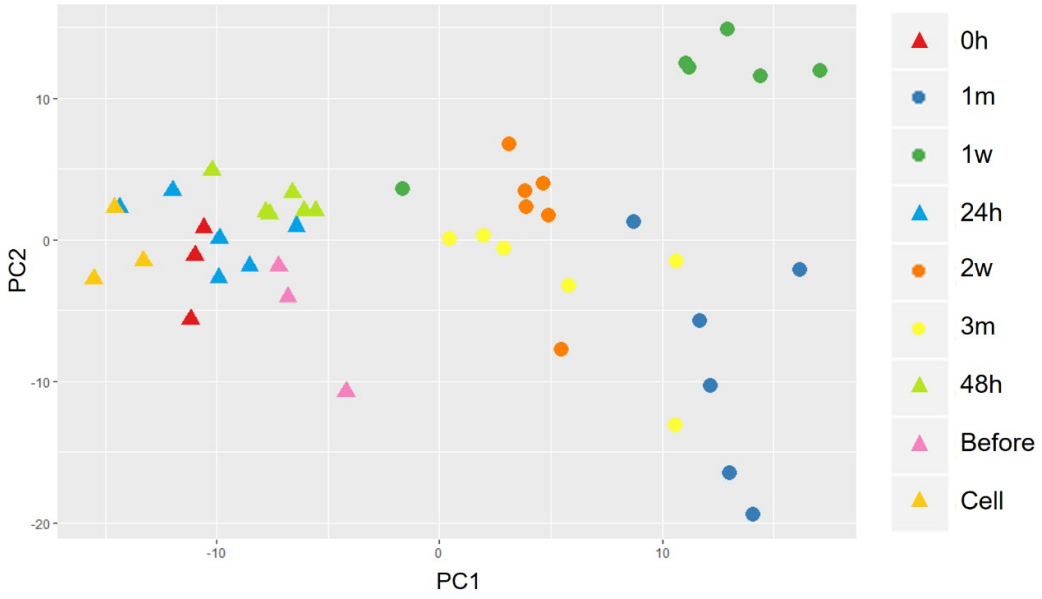

Figure 3.3. Principle component analysis (PCA) of biomineralization-related gene expression profiles at different phases of pearl grafting. The X- and Y- axes represent PC1 and PC2 respectively. Different colors of data points indicate different time points (cell, before, 0 h, 24 h, 48 h, 1 w, 2 w, 1 m and 3 m). All the samples were clustered in two separate groups as indicated by two different shapes: triangle for cell, before and 0 h to 48 h; round for 1 w to 3 m.

Shell matrix proteins (SMPs) are secreted from mantle epithelial cells and regulate calcium carbonate crystal formation, resulting in the development of the shell and pearl (Taylor and Strack, 2008). Difference in the composition of SMPs is important to determine nacre or prismatic layer characteristics. Therefore, expression patterns of SMPs can be used as a marker of the shell and pearl formation. We investigated the relative expression patterns of 28 representative SMPs from 192 biomineralization-related genes having well-defined implications for quality pearl production that are involved in the formation of prismatic layer (10), nacreous layer (14) and both layer (4) (Table 3.2). Many of the prismatic layer and both layers forming genes were clumped in the upper part of the gene cluster 1 (group A and B) and exhibited higher expression

during the earlier stages (Fig. 3.4, Table 3.2). Besides, many nacreous layer forming genes gathered at the lower part of the cluster 1 (group C) and were expressed highly throughout the experiment except in 1 week samples (Fig. 3.4, Table 3.2). In cluster 2, most of the genes exhibited lower or no expression during the earlier stages and higher expression in the later stages. Some of the nacreous layer and both layers forming genes were organized in gene cluster 2 (Fig. 3.4, Table 3.2).

3.3.4 Detailed expression analysis of shell matrix proteins at different stages of pearl sac and pearl formation

Expression levels of respective SMP genes at different stages are illustrated in Fig. 3.5, 3.6 and 3.7. Among the ten prismatic layer forming genes, eight genes were significantly up-regulated during earlier stages and down-regulated in the later stages of pearl development (Fig. 3.5a-h); whereas, prisilkin-39 and calmodulin showed different expression patterns from those of other prismatic layer forming genes (Fig. 3.5i,j). In earlier periods, there was little or no expression of prisilkin-39 except the peak at 24 h, then it was expressed increasingly from 1 w to 3 m, showing the second peak at 1 m (Fig. 3.5i). Calmodulin was observed up-regulating with its highest peak at 1 w before starting to decline to the end (Fig. 3.5j). However, KRMP and MSI31 gene expression levels were apparently higher compared to others (Fig. 3.5b,d).

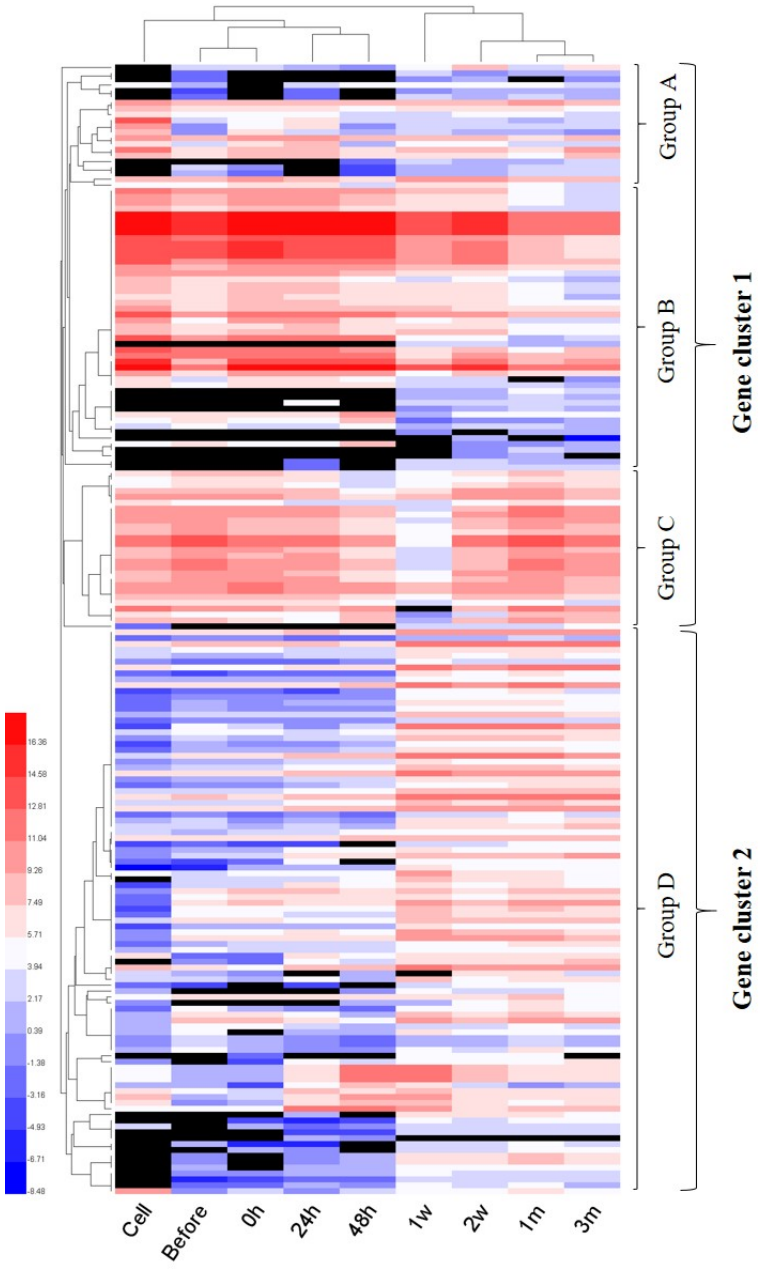

Figure 3.4. Heat map illustrating the expression patterns of 192 biomineralization-related genes across various steps of pearl sac and pearl formation. Each column contains the measurements for gene expression change for a single sample. Relative gene expression is indicated by colour: high-expression (red), median-expression (white) and low-expression (blue). Black cells represent very little or no expression. Genes and samples with similar expression profiles are grouped by hierarchical clustering (left and top trees). These 192 genes are listed in Table 3.2 sequentially.

Table 3.2. Gene clusters obtained from the expression analysis of 192 biomineralization-related genes (genes were listed sequentially from Figure 3.4)

Gene cluster 1	Group A	ACCBP1[b], Alkaline phosphatase, ML1A2, Calmodulin[p], Tyrosinase[p], 000058 mRNA for hypothetical protein, AP-24[n], PfTy[p], PfTy1[b], KRMP-10[p], Shematrin-7[b], Shematrin-5[b], Shematrin-2beta[b], Shematrin-3[b], PFMG5[b], Prismin-2[p], C-type lectin 2, Incilarin A, PmCHST11b[n], PfCB/chitobiase[p], Tyr-1
	Group B	Aspein[p], Cement-like protein[p], SGMP1, PfCN, GRMP[b], MSI7[b], Shematrin-2[b], Shematrin-8[b], Pmshem-3 for shematrin, Pmshem-2 for shematrin, Shematrin-1[b], Shematrin-9[b], PFMG10[b], MPN88[p], Prismalin-14[p], PUSP-20[p], MSI30/MSI2[p], shematrin-2alpha[b], CLP1 protein, MPN[b], Pfp-16 for hypothetical protein, Pmshem-1 for shematrin, Shematrin-6[b], Prismin-1[p], Tyrosinase-2[p], KRMP-1[p], Lustrin A[n], KRMP-3[p], 000118 mRNA for prism uncharacterized shell protein 18 like, KRMP-2[p], MSI31[p], KRMP-7[p], MPN88-lack6, MPN88-lack7, KRMP-4[p], Perlucin[n], Prisilkin-39[p], Regucalcin, KRMP-8[p], KRMP-11[p], N14#3.pro[n], , 000200 mRNA for hypothetical protein, KRMP-5[p], KRMP-6[p], KRMP-9[p], N16-3/N14#4.pro[n], Calconectin, C-type lectin 1
	Group C	Chitin binding protein, PfCHS1[n], N19-2[n], NSPI-5[n], 000081 mRNA for Glycine-rich protein 2 like, NUSP-6[n], Linkine[n], MSI25 (hypothetical protein), NUSP-3[n], N19[n], Pif177[n], MSI60/insoluble protein[n], MSI60RP[n], NUSP-17[n], N16-1/N14#1.pro[n], N16-7[n], Pearlin[n], MRNP34[n], MSI80[n], N36/33, Nacrein[b], N45, N66[b], N14#7.pro[n], N16-6[n], N16-2/N14#2.pro[n], Lectin
Gene cluster 2	Group D	AP-1, MSP-1, N151, PfBAMBI, BMP-2, BMP-R2, M45, N44, Pf-POU2F1, Cathepsin B, Dermatopontin[n], BMP-1B, Calcium/calmodulin-dependent protein kinase I, PfBMPR1B, Homeobox protein-4, BMP-2B, Paramyosin, BMP-7[b], Calcineurin B subunit, Chitinase 3, L-type voltage-dependent calcium channel beta subunit, Putative uncharacterized protein F18, PfMSX[n], TFG beta signaling pathway factor, Calreticulin[p], PfSMAD4, PfDlx[n], PfYY-1, 67kD laminin receptor precursor, Plasma membrane calcium ATPase, Ferritin-like protein, PfY2, 000031 mRNA for hypothetical protein, 000145 mRNA for hypothetical protein, Chitin synthase 1[b], SPI (serine proteinase inhibitor), PfSp8-like protein 1, Matrix metalloproteinase, Metallothionein-2, 000194 mRNA for hypothetical protein, SERCA isoform C, Perlwapin-like protein[n], Pfu000096, BMP-1, SCP-a, SCP-b, Calponin-like protein, Neuronal calcium sensor-1, Calcium-dependent protein kinase, SERCA isoform A, Voltage-dependent L-type calcium channel alpha-1 subunit isoform c, Carbonic anhydrase II, SPARC, Veliger mantle 1, Pf-POU3F4, Metallothionein, PFMG11[b], PFMG2[b], N16-5/N14#5.pro[n], PFMG9[b], Calmodulin-like protein, BMP-4, Jacalin-related lectin PPL2-a, PFMG3[p], Carbonic anhydrase precursor, N23[n], PFMG8, Fam20c[n], EFCBP, CHST11[n], PmCHST11a[n], Incilarin C, EP protein precursor, PfChi1/chitinase 1, PFMG1, PFMG6[b], PMMG1[n], PFMG7[b], PmRunt[n], PFMG4[b], PFMG12, Tissue inhibitor of matrix metalloproteinase, AP-7[n], BMP-3, PfTy2[p], BMSP, ML1A1, Engrailed, 000066 mRNA for hypothetical protein, Ferritin, ML7A7, Mucoperlin[n], Perlucin 7[n], Wnt-1, Wnt-6, Shematrin-4[b]

*Different superscript letters indicate genes that are involved in the formation of different shell layers. 'p': prismatic layer forming gene, 'n': nacreous layer forming gene and 'b': both layer forming gene.

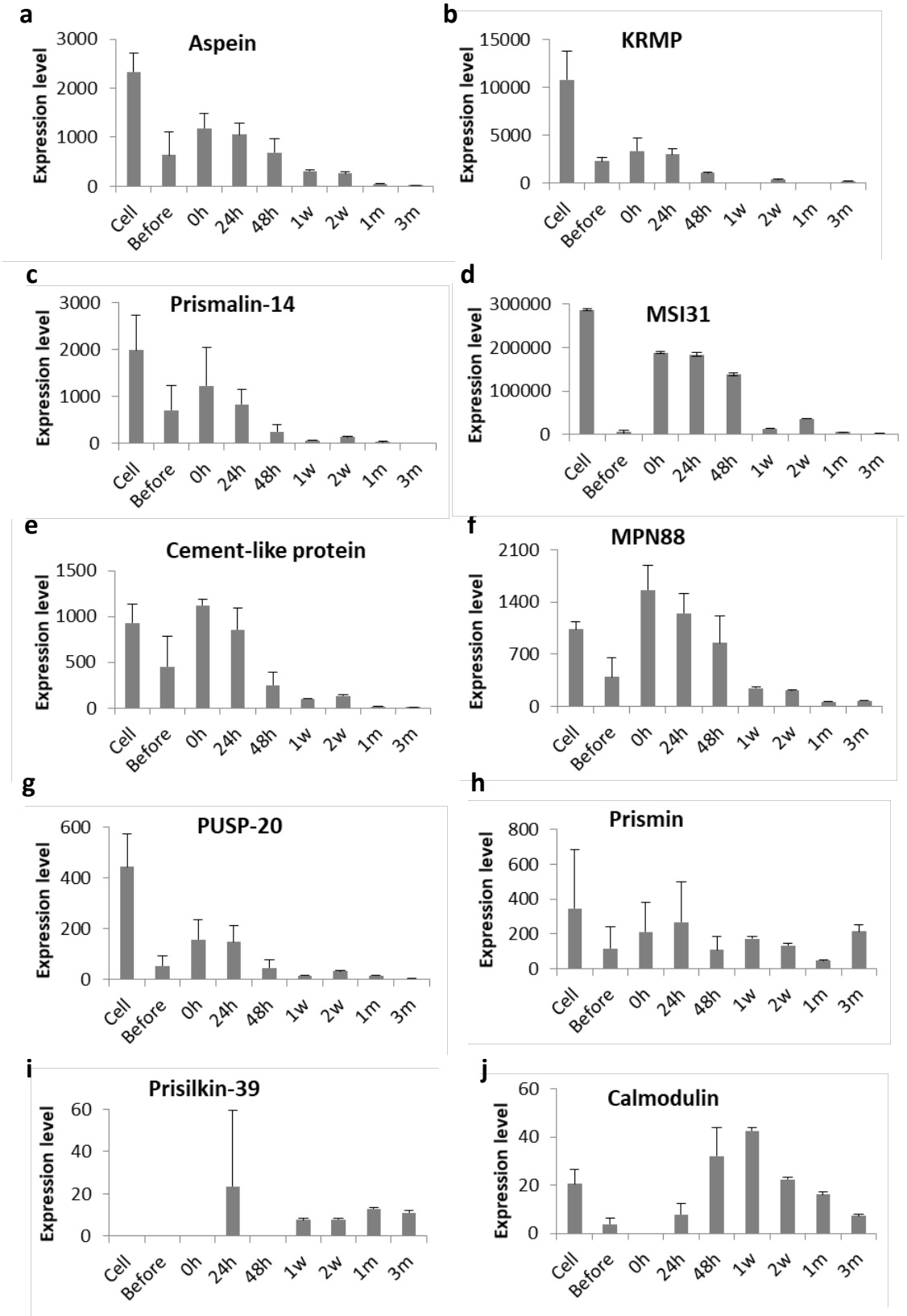

Figure 3.5. Expression patterns of shell matrix proteins (SMPs) involved in the formation of prismatic layer (a-j) at various time points of pearl sac and pearl

development. Expression levels are indicated by adjusted TPM values (transcripts per kilobase million).

Most of the nacreous layer forming SMPs showed higher expression before graft transplantation and then down-regulation upto 1 w, after that up-regulation again upto the end with a maximum expression at 1 m (Fig. 3.6a-i). Mucoperlin, perlucin-7, perlwapin-like protein, lustrin A and dermatopontin, showed little or no expression since 48 h and then started rising significantly (Fig. 3.6j-n). Perlucin-7 and perlwapin-like protein reached the maximum expression at 1 w (Fig. 3.6k,l), whereas lustrin A and dermatopontin at 2 w and 1 m, respectively (Fig. 3.6m,n). NUSP-3 and mucoperlin displayed the highest expression at 3 m (Fig. 3.6i,j). The expression of MSI60 was significantly higher than those of other nacre forming genes (Fig. 3.6c). Both layers forming genes like nacrein, MSI7, N66 and shematrin-1 showed almost similar trend in expression with many nacreous layer forming genes (Fig. 3.7a-d). They were up-regulated during earlier periods with a higher expression within 0 h – 24 h, then down-regulated upto 1 w and up-regulated again after 1 w. Expressions of MSI7 and shematrin-1 were relatively higher (Fig. 3.7b,d).

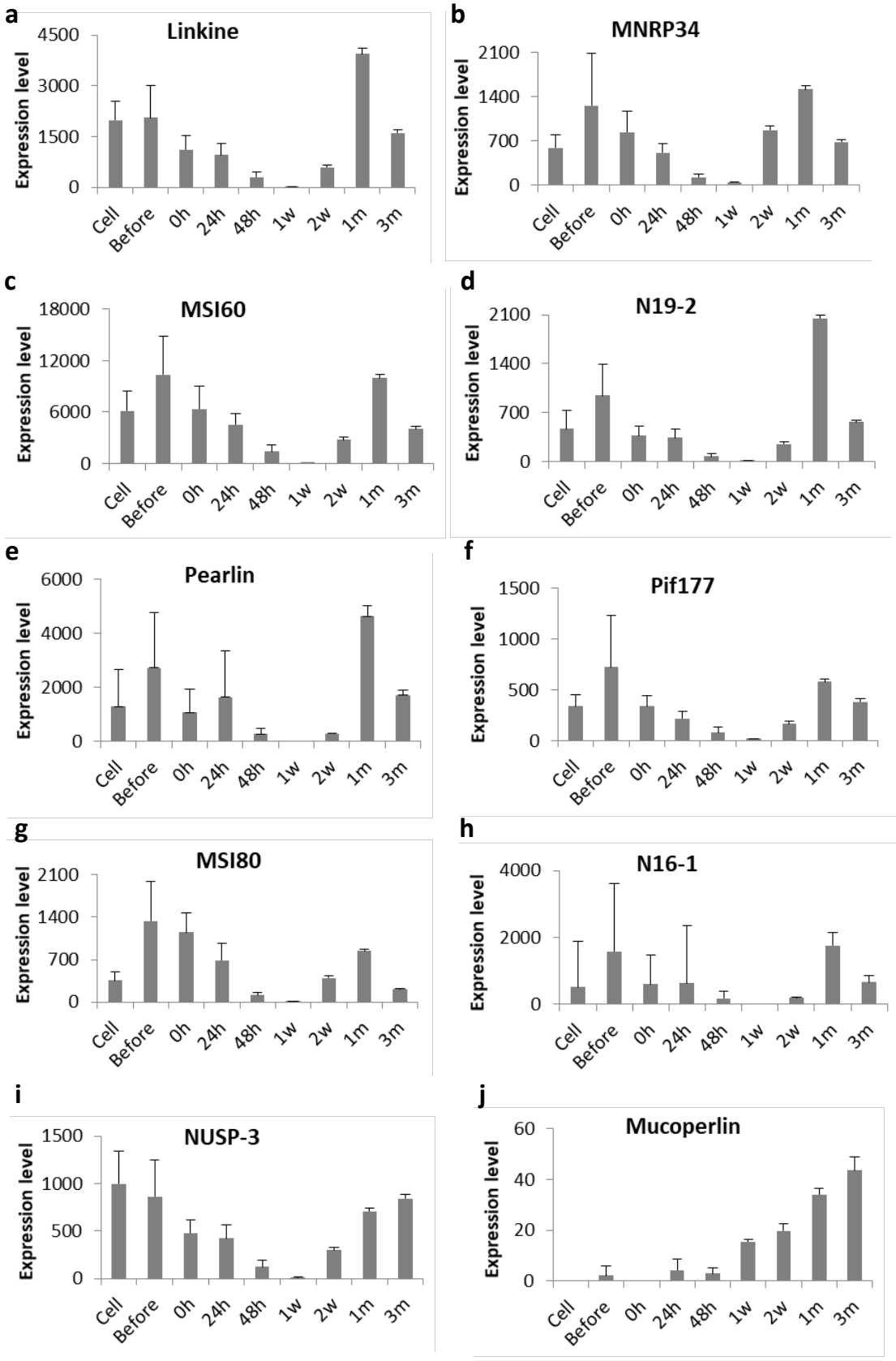
a
Linkine
Expression level
4500
3000
1500
0
b
MNRP34
2100
1400
700
c
MSI60
18000
12000
6000
d
N19-2
e
Pearlin
f
Pif177
1500
1000
500
g
MSI80
h
N16-1
4000
2000
i
NUSP-3
j
Mucoperlin
60
40
20
Cell
Before
0h
24h
48h
1w
2w
1m
3m

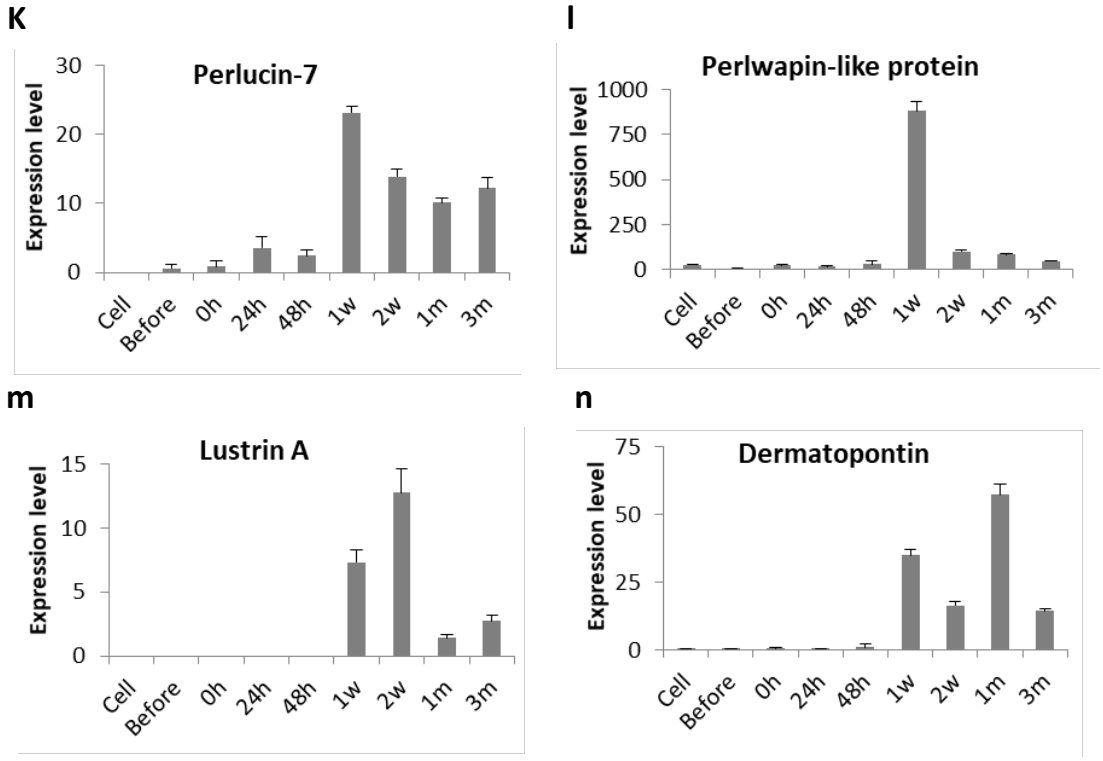

Figure 3.6. Expression patterns of shell matrix proteins (SMPs) involved in the formation of nacreous layer (a-n) at various time points of pearl sac and pearl development. Expression levels are indicated by adjusted TPM values (transcripts per kilobase million).

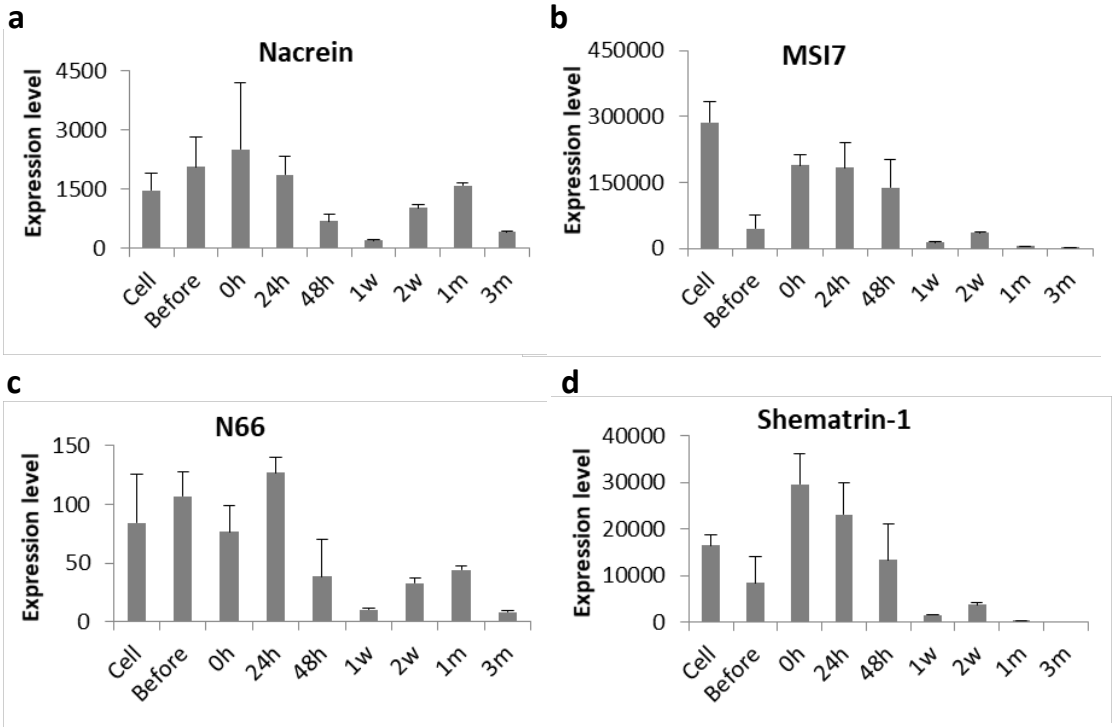

Figure 3.7. Expression patterns of shell matrix proteins (SMPs) involved in the formation of both layer (a-d) at various time points of pearl sac and pearl development. Expression levels are indicated by adjusted TPM values (transcripts per kilobase million).

3.4 Discussion

3.4.1 Gene expression profiles during the formation of pearl sac and pearl

The gene expression profiling describes clearly distinct pattern between earlier and later stages of pearl formation (Fig. 3.3). During the preliminary stages of pearl grafting immune and cell proliferation related-genes were mostly enriched whereas in later stages biomineralization genes (Fig. 3.8).

Shell or pearl biomineralization is a complex process that is strictly controlled by the cascades of a considerable number of genes. Though the mantle tissue of mollusk is primarily responsible for shell biomineralization, it has also been reported that oyster

hemocytes can mediate shell biomineralization by binding calcium ion as well as forming $CaCO_3$ crystals (Mount et al., 2004; Li et al., 2016; Huang et al., 2018). More recently, some studies also concluded that in addition to mineral transportation, hemocytes contribute to the secretion of the extracellular matrix required for shell biomineralization in bivalve (Ivanina et al., 2017; Ivanina et al., 2018). Therefore, the interaction between the epithelial cells of donor mantle and host hemocytes is very essential for the proper development of pearl sac and pearl (Awaji and Machii, 2011). However, the specific role of hemocytes in pearl biomineralization is still obscure.

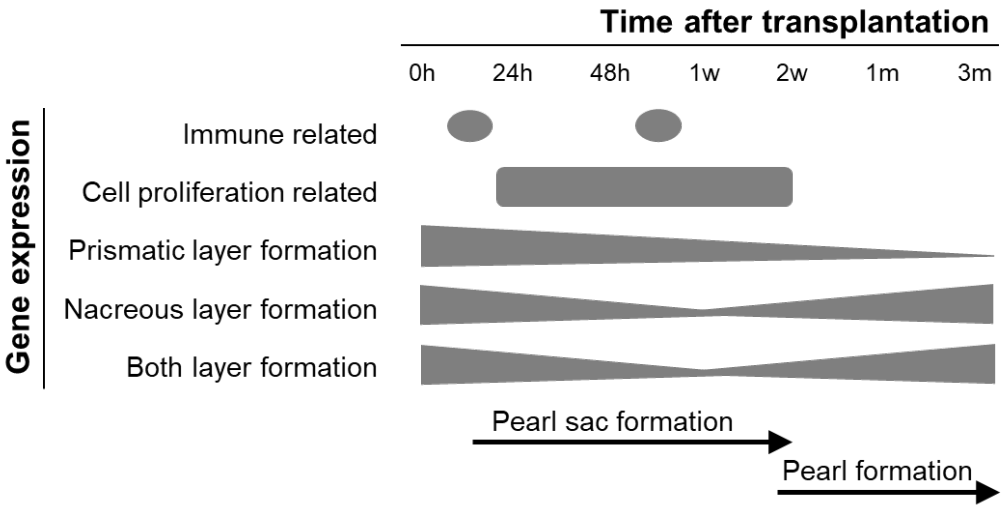

Figure 3.8. Summary of the study showing gene expression pattern during the pearl sac and pearl formation.

It has already been clarified that the biomineralization genes are being expressed by the pearl sac developed from donor mantle graft (McGinty et al., 2012; Masaoka et al., 2013; Tayale et al., 2012; Ky et al., 2018). The identified biomineralization-related genes in this study were expressed in the pearl sac, i.e. in the donor mantle cells. Hierarchical clustering considering only biomineralization-related transcripts precisely deciphers that the mineralization process during the first 3 months of culture is regulated differently

(Fig. 3.4). All along the first 2 days after transplantation gene expression remains more or less constant followed by a drastic change after 1 week either positively or negatively. Most of the prismatic layer forming genes showed higher expression in earlier stages, whereas nacreous layer forming genes were mainly enriched in later stages (Fig. 3.4). This result recapitulates the mineralization sequence, where prismatic layer is formed first and then nacreous layer is deposited. Additionally, the expression pattern of major SMPs revealed the concurrent release of aragonite and calcite during the early stage of mineralization (Fig. 3.5, 3.6). The nacreous layer then forms on the top of the prismatic layer (Liu et al., 2012).

Each of the SMPs evolves a specific function in constructing the shell/pearl microstructure either in the form of prism or nacre. Aspein is involved in prismatic calcite formation (Gao et al., 2016; Takeuchi et al., 2008), while the framework protein prismalin-14 mediates chitin and calcium carbonate crystals (Suzuki et al., 2004). Another framework protein shematrin facilitates calcification of the prismatic microstructure (Yano et al., 2006), whereas MSI7 inhibits the calcite formation (Zhang et al., 2003). An acidic matrix protein, pif, can induce the nucleation of aragonite crystals and has been reported to regulate the formation of nacreous layer (Suzuki et al., 2009). MSI60 with several characteristic domains constitutes the baseline of the nacreous layer (Sudo et al., 1997; Inoue et al., 2011). Pearlin, after being fixed to substrate, induces the formation of aragonite crystals (Suzuki and Nagasawa, 2013). It has been reported that both N16 and N19 can inhibit the crystallization of calcite and therefore are essential to modify the morphology of CaCO3 crystals and orient nacre growth (Samata et al., 1999; Ohmori et al., 2018; Yano et al., 2007).

The relative expression levels of SMPs seem crucial in controlling the quality of the pearl. Most of the studied prismatic layer forming genes including aspein, KRMP, prismalin-14, MSI31, cement-like protein, MPN88 and PUSP-20 were highly expressed before the maturation of pearl sac, but the level of expression decreased with time of culture (Fig. 3.5a-g). After the complete maturation of pearl sac, their expression levels were relatively low. Presumably, it takes 15 to 20 days to complete the formation of the prismatic layer around the nucleus until when the nacreous layer formation was not started yet (Liu et al., 2012). Compared to others prismin, prisilkin-39 and calmodulin were expressed higher even after the formation of pearl sac, possibly indicating their roles in the regulation of crystal growth (Fig. 3.5h-j). Prisilkin-39 showed a similar pattern of expression with a previous shell notching experiment where the first peak was observed on day 2 before start decreasing followed by an increase on day 7 (Fig. 3.5i) (Zheng et al., 2015). Having the dual function, prisilkin-39 is involved both in constructing the chitinous framework and in regulating the crystal growth during the prismatic layer mineralization (Kong et al., 2009). Moreover, the up-regulation of these prismatic layer forming genes during the earlier stages of pearl formation indicates their possible contribution to the development of pearl sac. In a recent study on freshwater pearl mussel *Hyriopsis schlegelii*, calmodulin was found significantly up-regulated during pearl sac formation, suggesting that it might facilitate pearl sac formation (Peng et al., 2018). Similarly, we also found that calmodulin was highly up-regulated during pearl sac formation in *P. fucata*, suggesting their potential role in the development of pearl sac (Fig. 3.5j).

On the other hand, nacreous layer and both layers forming genes were down-regulated during the formation of pearl sac (Fig. 3.6 and Fig. 3.7). However, the increased expression of nacre forming genes immediately after grafting is because the grafts were

prepared from nacre secreting mantle. Thus, it is expected to be a simple continuation of the mineralizing activity of the graft. After the maturation of pearl sac, nacre forming genes were up-regulated with the highest expression during 1m (Fig. 3.6a-h), suggesting the accomplishment of nacreous layer formation. A previous study explained that the nacreous layer formed on the nucleus 35 days after grafting (Liu et al., 2012). However, nacreous deposition is not linear (Blay et al., 2017) throughout the pearl formation process and the highest deposition rate was observed during the first 3 months of culture (Fig. 9b, 10b) (Blay et al., 2017). In a prior study on the expression of MSI60, N19, N16, Pif80 and nacrein in pearl sac, the highest expression was detected on day 25, whereas the expression was relatively lower between 15 and 25 days, indicating their involvement in the appearance of the round flat tablets during pearl formation in *P. fucata* (Liu et al., 2012). In another study from 3 months to 9 months of culture, the relative expressions of Pif, MSI60 and pearlin were significantly higher at 3 months culture than at 6 or 9 months (Blay et al., 2018). The increase or decrease in gene expression may be linked to the calcification rate, which marks their contribution to the gradual formation of the nacreous layer surrounding the nucleus. Nacre weight and thickness is significantly correlated with pearlin, Pif177 and MSI60 gene expression levels (Blay et al., 2018). On the other hand, the low expression of genes like aspein and shematrin can result in a top quality pearl by inhibiting the prismatic layer formation (Blay et al., 2018).

CHAPTER 4

Microstructural characterization of surface depositions on pearls produced in *Pinctada fucata*

The content of this chapter was published as:

Mariom, S. Take, Y. Igarashi, K. Yoshitake, S. Asakawa, K. Maeyama, K. Nagai, S. Watabe and S. Kinoshita 2019. Gene expression profiles at different stages for formation of pearl sac and pearl in the pearl oyster *Pinctada fucata*. **BMC Genomics 20: 240**.

Abstract

During cultured pearl formation, soon after transplanting the outer epithelial cells of the mantle graft proliferate and form a pearl sac which secretes and deposits various shell matrix proteins (SMPs) surrounding the nucleus to form a lustrous pearl. In this study, we aimed to scrutinize the internal micro-crystal biomineralization of pearls mediated by the pearl sac. We collected the pearls at 1 and 3 months of culture. The surface depositions of the obtained pearls (6 at each time) were first observed using an optical microscope. The pearls were then cut in half and the transverse sections of the pearls were examined using a scanning electron microscope (SEM). Surface examination of 1 month pearls revealed the variation in the initial mineralization among the pearls. Moreover, the irregular surface of pearls illustrated that nacre deposition at the early stage was not uniform. But at 3 months, the pearl surface became smoother and more regular with a pearl lustre. Additionally, SEM imaging confirmed the deposition of nacreous layer encircling the nucleus at 1 month that we predicted from our previous expression studies of SMP genes. Microstructural analysis demonstrated two distinct pearl layers surrounding the nucleus. It was also noticeable that an initial organic layer was deposited onto the nucleus surface before the secretion of prismatic and nacreous layers. The thickness of organic material was variable among different pearls and even in different parts of the same pearl. There was considerable diversity in the structure of the prismatic layer compared to the regular brick-wall like structures of nacre. Unlike canonical mollusk shell, prismatic layer in pearl was made up of both aragonite and calcite prisms, organic materials and some unknown compounds though the overall composition was variable among the pearls. The study summarizes the mineralization sequence of pearl, where a heterogenous prismatic layer is secreted first and followed by nacreous layer.

4.1 Introduction

Pearl formation is a complex and precisely controlled process that is mainly regulated by the mantle tissue of mollusk (Kawakami, 1952; Taylor and Strack, 2008). It is commonly known that, the mineralization that occurs during cultured pearl formation is very similar to that of shell formation process in many aspects. The only distinguishing feature is the reversed sequence of the mineral layers i.e., the inside of the shell layers corresponds to the outside of the pearl layers (Kawakami, 1952; Taylor and Strack, 2008; Cuif et al., 2011). Thus the pearl layer is termed as the 'reversed shell'. The metabolic changes that occurs in the mineralizing epithelium during its differentiation into a pearl sac may results in the formation of a new mineralizing sequence that is comparable to the structure of the shell (Kawakami, 1952).

Cultivated pearls are made of a layer of nacre deposited onto the spherical nucleus. It takes almost two years to obtain a pearl with the desired nacre thickness (Gueguen et al., 2013). Moreover, not all the produced pearls are of good quality. The surface depositions regulated by the secretions of the mantle epithelium mainly determines the quality of the final pearl. Pearl surface deposition is a composite of an inorganic calcium carbonate with the organic secretions from the mollusk. The interplay between these organic matrix and inorganic minerals ($CaCO_3$) give the pearl layers a unique microstructural features, extraordinary mechanical stiffness, and fabulous optical properties (Addadi and Weiner, 1997; Marin and Luquet, 2004; Addadi et al., 2006; Meyers et al., 2008; Checa et al., 2009). The identification and functional characterization of the organic component of the shell provides a better understanding of the circumstances towards the formation of a lustrous pearl (Hare, 1963; Towe et al., 1966; Zhang and Zhang, 2006). Though extensive studies have been conducted to characterize the shell layers but, very little attention has been paid to the structural constitution of the pearl layers (Cuif et al., 2008,

2011). So, the study was aimed to examine the pearl layers in order to scrutinize the microstructural characterization of the surface aggregates on pearls secreted by the pearl sac epithelium.

4.2 Materials and Methods

4.2.1 Mantle grafting and pearl sample collection

Mantle grafting was performed by a skilled technician at the Mikimoto pearl farm, Mie, Japan. Two host oysters received graft from the same donor (Fig. 2.1a). We reared the oysters for three months after graft insertion and the pearl samples were collected at one month and three months of the culture. We collected six pearls at each sampling.

4.2.2 Microscopic observation of pearls

The surface depositions of the obtained pearls were observed using an optical microscope VHX-700F (Keyence) at Mikimoto pearl research laboratory. For SEM, the pearls were cut in half by ISOMET diamond cutter (BUEHLER) and embedded in Resin. Surface of embedded samples were polished with ECOMET polisher (BUEHLER) and aluminum oxide. After etching by NaOH, transverse sections of pearls were examined using a scanning electron microscope SU3500 (Hitachi) at Mikimoto Pharmaceutical Co. Ltd.

4.3. Results

4.3.1 Microscopic examination of pearl surface aggregates by optical microscopy

Microscopic observations were carried out to analyse the internal micro-crystal biomineralization of pearls mediated by the pearl sac epithelium. Clear morphological differences were observed among the pearls under the microscope (Fig. 4.1a). Surface examination of 1 month pearls revealed the variation in the initial mineralization activity among the pearls (Fig. 4.1a). Moreover, the irregular surface of pearls illustrated that nacre deposition at the early stage of pearl formation was not uniform throughout the surroundings of a given pearl (Fig. 4.1a). A visual change on the surface aggregates encircling the nucleus could be noticed at 3 months when the pearl surface became smoother and more regular with a pearl lustre (Fig. 4.1b).

4.3.2 Microstructural characterization of surface deposition on pearl by SEM

Scanning electron microscopic (SEM) imaging obtained from the cross section of pearls revealed two distinct pearl layers with clear cut differences in microstructures that were visible on the surface of the nucleus (Fig. 4.2). Microstructural analysis additionally demonstrated that an initial organic layer was deposited onto the nucleus surface before the secretion of prism and nacre (Fig. 4.2a,b). It was also noticeable that the thickness of organic material was variable among different pearls and even in different parts of the same pearl (Fig. 4.2a,b). A heterogeneous prismatic layer in contact with the initial organic layer was then accumulated onto the nucleus before the secretion of the outer aragonite nacreous layer. Unlike mollusk shell, prismatic layer in pearl was diversified. The overall composition of the epithelial secretion during the formation of prismatic layer is variable among the pearls (Fig. 4.2a,b). There was considerable diversity in the structure of the prismatic layer compared to the regular brick-wall like structures of nacre (Fig. 4.2a,b). Microstructural observation of surface depositions obtained from the pearls

at 1 month indicated the accumulation of significant amount of nacre confirming the deposition of nacreous layer encircling the nucleus by 1 month (Fig. 4.1a, 4.2a). Surface structure of 3 months pearls further suggested the significant increase in nacre tablets in the form of aragonite crystals towards the maturation of the nacreous layer (Fig. 4.1b, 4.2b).

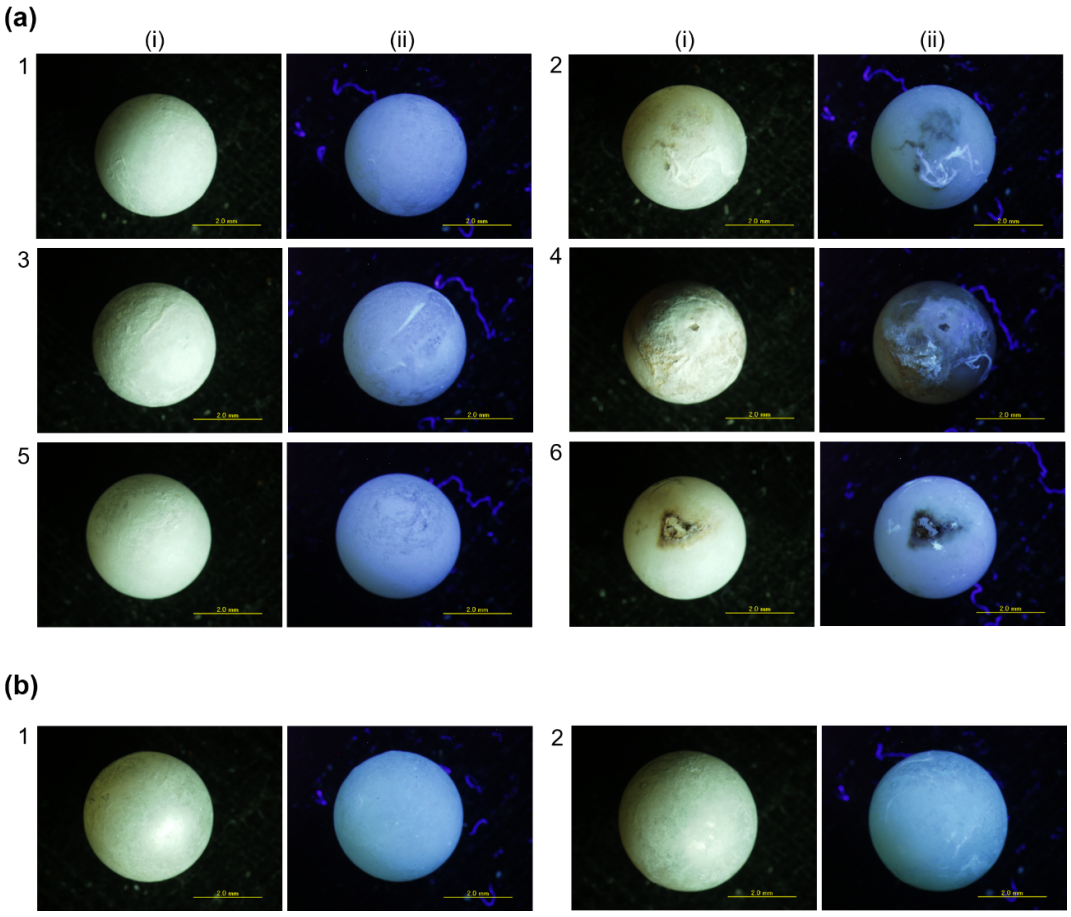

Figure 4.1. Microscopic images of surface depositions on pearl at (a) 1 month and (b) 3 months of grafting. (i) Normal microscopic image and (ii) UV fluorescence microscopic image. Different numbers 1-7 indicate different pearls. Scale bars 2.0 mm.

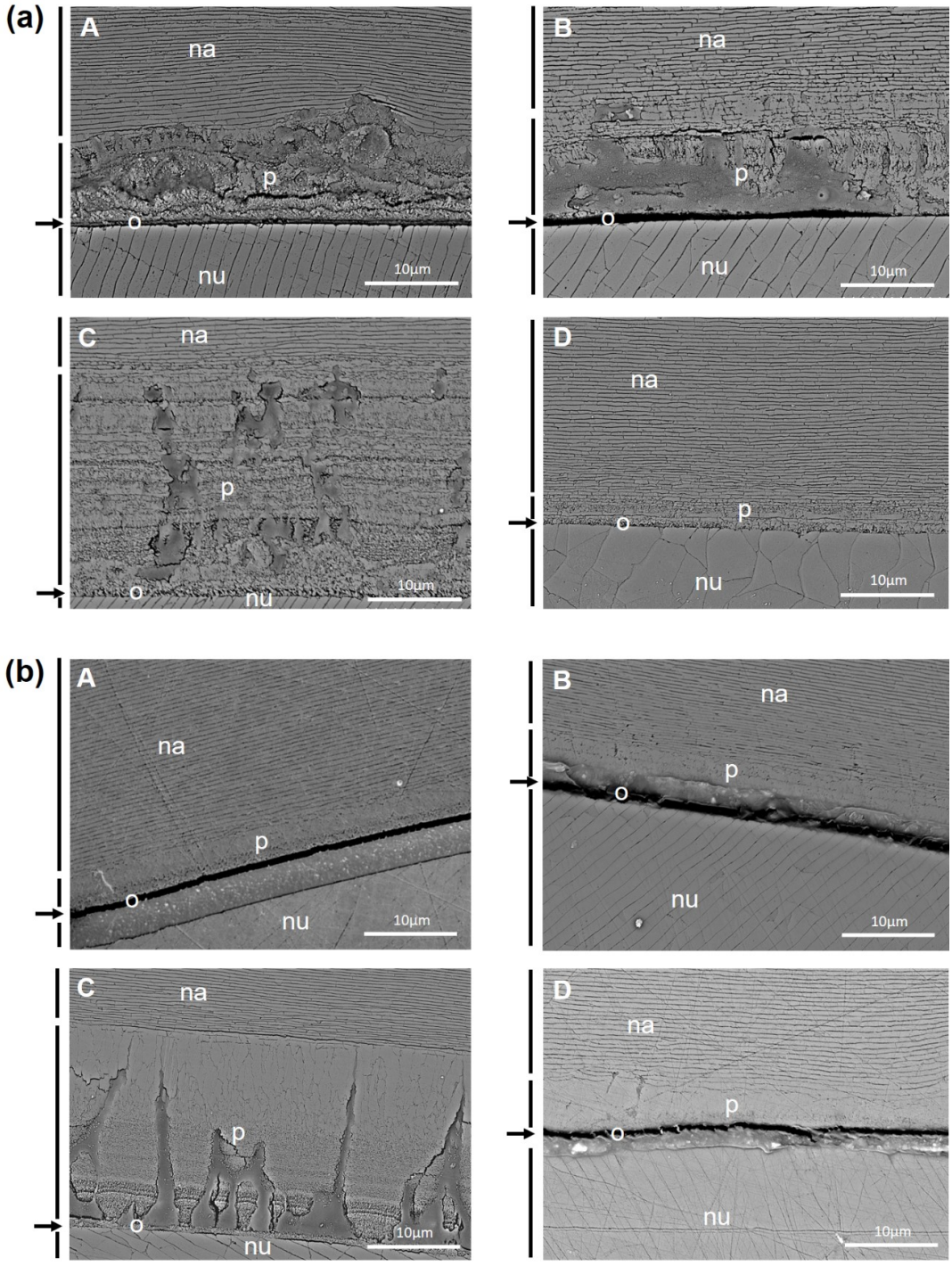

Figure 4.2. SEM images illustrating microstructural characterization of the pearl layers at (a) 1 month and (b) 3 months of grafting. nu: nucleus, o: organic layer indicated by black arrow, p: heterogeneous prismatic layer, na: nacreous layer. Uppercase letter A-D indicates different pearls. Scale bars: 10 µm.

4.4 Discussion

Pearl mineralization is considered as an interesting model to figure out the primary mechanisms of calcium carbonate mediated biomineralization in mollusk. Early mineralization activity among the pearls are quite discernible (Fig. 4.1, 4.2). During excessive cell proliferation, the in-depth modification of the epithelial cells responsible for mineralization may result in the variation in early mineral depositions (Cuif et al., 2008). Some previous studies also reported the differences in the morphology of the pearl-sac epithelial cells in relation to pearl structures (Nakahara and Machii, 1956; Aoki, 1966). Thus the initial mineralization of pearl is not simply the reappearance of the nacreous structures, rather it is more complex (Kawakami, 1952).

It has been hypothesized that, the newly formed epithelium starts its mineralizing activity by forming a microstructural sequence that is comparable to the initial shell microstructure of the young *Pinctada* (Kawakami, 1952). From the SEM imaging of pearls, it is worth noticing that the initial crystal development contains heterogeneous prism and organic material compared to the regular nacre structure that develops later on it (Fig. 4.2). Kawakami (1952) first observed the presence of non-nacreous materials onto the pearl surface under the nacreous layer. The inflammatory reaction of host oyster to the transplanted graft sometimes causes heavy accumulation of hemocytes in the wound sites leading to the undesirable secretion of organic layers on the pearl surface (Awaji and Machii, 2011). This organic layer is comparable to the periostracum layer of the shell which acts as a basis for the secretion of prism and nacre (Cuif et al., 2008; Awaji and Machii, 2011; Cuif et al., 2011; Nagai, 2013). It has also been previously reported that, many pearls contain radially oriented calcite structures beneath the nacreous surface, that is similar with that of the prisms existed in the outer shell layer of *Pinctada* (Kawakami, 1952; Taylor et al., 1969; Cuif et al., 2008, 2011; Checa et al.,

2013). Some other studies enlightened that the first deposition on the nucleus is either aragonitic (Cuif et al., 2008; Liu et al., 2012) or calcitic (Ma et al., 2007) prismatic layer in association with the organic layer detected from the cross section of the pearl. However, in addition to calcite and aragonite, vaterite can also be observed in pearls (Pe´rez-Huerta et al., 2014). It has therefore been suggested that the formation of prismatic structures in pearls may not be compared to the biomineral structures in shells in terms of crystal habit and crystallographic control (Cuif et al., 2008; Pe´rez-Huerta et al., 2014). Additionally, the prism in pearls possesses a strong correlation between crystallization and the formation of organic envelopes (Pe´rez-huerta et al., 2014). Furthermore, the prismatic layer surrounding the pearl is more complex than that of mollusk shell as it contains both aragonite and calcite crystals secreted simultaneously by the pearl sac epithelium (Cuif et al., 2008; Cuif et al., 2011). The nacreous material is then produced and deposited onto the nucleus (Fig. 4.2). Nacre is mostly built of aragonite crystals (95-99%) in the form of tablets along with some organic substances such as polysaccharides and proteins (Jackson et al., 1988; Zhang and Zhang, 2006). This organic material acts as a biological adhesive to arrange the aragonite tablets in a regular brick-wall like structure (Jackson et al., 1988; Zhang and Zhang, 2006).

The study summarizes the mineralization sequence of the cultivated pearl, where a periostracum-like layer is secreted first before the deposition of the prismatic and nacreous layer. SEM images also confirms the completion of the nacreous layer by 1 month that we predicted from the previous gene expression study (Fig. 4.2) (chapter 3). However, without mineralogical study we cannot conclude the exact composition of the heterogeneous prismatic layer. Therefore, further study is needed to know the exact composition of the prismatic layer and why does the prismatic layer vary from pearl to pearl.

CHAPTER 5

General Discussion

The pearl oyster, *P. fucata* is an attractive model mollusk for the biomineralization study. The availability of the whole genome and transcriptome has made it a suitable and popular model in this regard (Takeuchi et al., 2012; Takeuchi et al., 2016). Recently, RNA-seq, based on next generation sequencing technologies, has become a widely used tool to obtain transcriptomic information on genes of interest that are differentially expressed under certain conditions (Mortazavi et al., 2008; Qian et al., 2014; Huang et al., 2015b; Mazzitelli et al., 2017). In this study, we have generated 925 M sequencing reads from the mantle graft of the pearl oyster, *P. fucata*, and constructed a comprehensive expression profile of genes during the formation of pearl sac and pearl (Chapter 2-3). We also examined the surface structure of the produced pearl to verify the sequence of the deposited pearl layers (Chapter 4). In this chapter, the major findings obtained from the previous chapters has been integrated, interpreted and widely discussed.

5.1 Mantle grafting and pearl formation

Mantle grafting is the commonly practiced method to produce the cultured pearls. In this study, we performed mantle grafting to unravel the gene expression profiling as well as the molecular changes that occurs during different stages of cultured pearl formation. The important steps that we observed during the formation of cultured pearl in a 3 months grafting experiment is summarized in figure 5.1. We divided the whole process of pearl formation into two major events, one is the formation of pearl sac and another is the biomineralization of pearl (Figure 5.1).

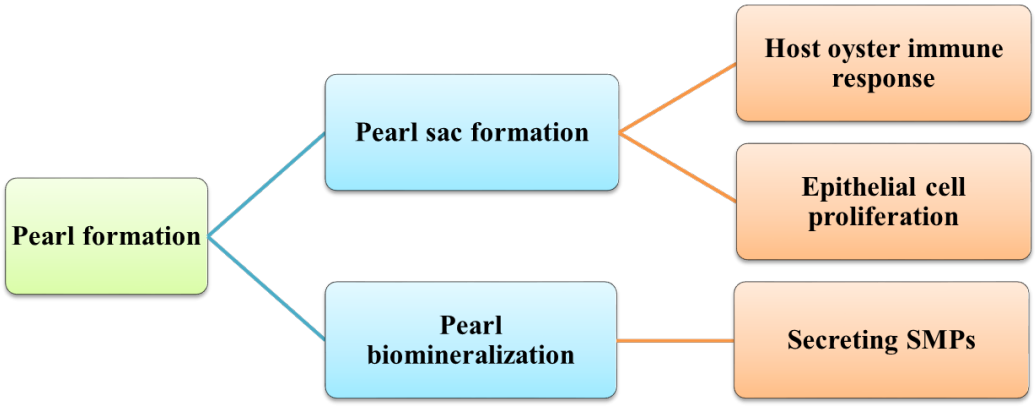

Figure 5.1. Outline of the major steps of pearl formation during 3 months grafting experiment.

5.1.1 Pearl sac formation

Pearl sac development is a complicated biological process which is resulted from the immune response of the host oyster to the transplanted mantle graft. Once the donor mantle graft and the nucleus is placed into the host oyster, the outer epithelial cells of the mantle graft tend to proliferate and differentiate into the pearl sac, the first important step of pearl formation. We demonstrated that the pearl sac was formed by two weeks of grafting during which two noticeable molecular changes occurred i.e., host oyster immune response and the proliferation of mantle epithelial cells (Fig. 5.1).

5.1.1.1 Host oyster immune response

Grafting process induces the immune response of the host oyster. Therefore, host oyster immune response to the transplanted graft is very important which essentially determines the acceptance or rejection of the nucleus. Pearl sac formation is generally regarded as a phenomenon identical to the epithelial regeneration observed in cutaneous wound healing process of mollusk (Armstrong et al., 1971; Awaji and Machii, 2011). In reaction to the wound healing process, the pearl sac was developed by 2 weeks of grafting which

is similar to the findings of a previous study (Awaji and Suzuki, 1995) (Fig. 2.4). The hemocytes of the host oyster also plays a key role during the process. The agranular hemocytes accumulate in the wound site and produce new extracellular matrix (ECM) on which new epithelium is formed (Mount et al., 2004; Li et al., 2016). However, access accumulation of hemocytes in the pearl sac has been reported to be a crucial factor potentially affecting the proper functioning of the pearl sac and thereby the pearl quality (Kishore and Southgate, 2016). Therefore, the interaction among cells, cytokines and ECM has been shown to be involved in the process of wound healing and control of cell proliferation in mollusks (Mount et al., 2004). In the present study, host immune response was mostly observed at 48 h – 1 w as indicated by the enriched immune pathways, which is also a crucial stage of pearl sac formation (Fig. 2.3). Moreover, we explored the key genes and pathways involved in the immunological changes that occur after graft transplantation (Fig. 2.3, Table 2.3). These results provide insight into the increased understanding of the immune reaction of the host oyster in response to accepting a transplant.

5.1.1.2 Proliferation of mantle epithelial cells

The outer epithelium of the mantle is a stable tissue that is mitotically inactive under normal condition and starts to proliferate vigorously upon injury (Awaji and Suzuki, 1995). The inner epithelial cells on the other hand, proliferate intermittently for the renewal of the tissue under normal condition (Awaji and Suzuki, 1995). However, during pearl formation, the external cells of the mantle graft become active after the grafting operation and start to proliferate and differentiate into a pearl sac. The cellular composition of the pearl sac is identical to the outer epithelium of the mantle pallial zone which is composed of mucous cells, cells containing large acidophilic granules and epidermal cells (Machi, 1968; Dix, 1973). From GO enrichment studies we observed that

the pearl sac formation was completed by 2 weeks of grafting (Fig. 2.4). We screened out a large number of genes that might play a significant role in the proliferation of mantle epithelial cells into the pearl sac (Table 2.4).

Literature claims, definitely the outer epithelia contains stem calls, though there is no direct evidence about the stem cell marker genes that contribute to the proliferation of mantle graft into pearl sac (Fang et al., 2008). However, in a prior study, the characteristic feature of stem cell was observed in the outer epithelia of the central zone of the mantle termed as 'proliferation hotspot' (Fang et al., 2008). The differential expression of several stem cell marker genes during the proliferation of mantle epithelial cells into pearl sac suggests their significant role in pearl sac development (Table 2.4). Moreover, these gene are widely expressed in *P. fucata* which further recommends their cell proliferation-related functions in different tissues (Fig. 2.6). As cell proliferation is the basis needs of almost all the cells, therefore, not only mantle but also other tissues such as gill, gonad and muscle express these identified cell proliferation-associated genes (Fig. 2.6). Additionally, higher expression of these genes in mantle again clarify their substantial role in pearl sac formation (Fig. 2.7) (Zhu et al., 2015; Cavelier et al., 2017).

5.1.2 Pearl biomineralization

Pearl formation like other biomineralization processes such as the biosynthesis of bone (Hoang et al., 2003), dental structures (Paine and Snead, 1997), diatom cell walls (Kröger et al., 2002) and mollusk shells (Falini et al., 1996), is also regulated by an extracellular organic matrix which is secreted by the mantle tissue of mollusk (Kawakami, 1952; Clark et al., 2010). The mineralization process that occurs during the formation of cultured pearl is identical to that of shell biomineralization (Kawakami, 1952; Taylor and Strack, 2008). Thus the role of the pearl sac in nacreous layer

biomineralization is speculated to mirror that of the oyster mantle. Previous studies on transcriptomic analysis of both the mantle and pearl sacs, and proteomics of shells and pearls have disclosed that the same genes and proteins are involved in their synthesis (Joubert et al., 2010; Jones et al., 2013, Li et al., 2015; Liu et al., 2015a). Therefore, the genes responsible for both the shell and pearl biomineralization are quite common. In this study, we reported 192 biomineralization-related genes that were expressed in the donor mantle and the later pearl sac, and accordingly involved in pearl biomineralization (Table 3.1).

Molluscan shells are mainly consists of calcium carbonate crystals surrounded and perfused by an organic matrix of proteins, lipids and polysaccharides (Lowenstam and Weiner, 1989; Zhang and Zhang, 2006; Furuhashi et al., 2009). The process is strictly regulated by the organic matrixes secreted from the mantle epithelium. And, different zones of mantle is responsible for constructing different layers of the shell, such as the inner nacreous layer is fabricated by the mantle pallium, while the outer prismatic layer is produced from the mantle edge (Runnegar, 1985; Marie et al., 2012). However, mantle epithelial cells are very complex in nature. Though in shell biomineralization, different cells secrete different proteins either in the form of prism or nacre but in pearl biomineralization same cell secretes both the prism and nacre (Marie et al., 2012). During pearl formation, the epithelial cells from the mantle are transported to the mineralization site in a way that typically occurs after some kind of injury, such as any shell damage (Armstrong et al., 1971; Awaji and Machii, 2011). Moreover, from the expression pattern of the SMPs, we observed that both the prismatic layer and the nacreous layer forming genes were secreted simultaneously by the pearl sac epithelium during the early stage of pearl mineralization (Fig. 3.5, 3.6). However, the genes that are highly expressed in the mantle are not necessarily also highly expressed in the pearl sac

explaining that the pearl formation process is much more complex than it is assumed (Wang et al., 2009; Inoue et al., 2009; Inoue et al., 2010; McGinty et al., 2012). Nacrein, EFCBP, N16 and MSI60 were found to express significantly higher in mantle than that of the pearl sac (Wang et al., 2009). On the other hand, N19 showed higher expression levels in the pearl sac whereas significantly lower in the mantle tissue (Wang et al., 2009). Moreover, the gene expression studies demonstrate the expression pattern of the biomineraliztion-related genes are not uniform throughout the pearl formation process (Fig. 3.4). Rather it indicates clearly distinct pattern between the earlier (before 1 week) and later stages (1 week to 3 months) of pearl formation (Fig. 3.3, 3.4).

The donor mantle pallium used as graft for cultured pearl production has been shown to secrete only the nacreous layer in shell formation (Sudo et al., 1997; Takeuchi and Endo, 2006; Taylor and Strack, 2008). But during pearl formation, it secretes both the prismatic layer and nacreous layer forming SMPs (Fig. 3.5, 3.6). The nacreous layer forming SMPs in a shell are therefore considered to be an important mediators for pearl formation (Bedouet et al., 2001, 2006). SMPs also act as an important regulator of $CaCO_3$ crystal formation and crystal growth. The precise role of the SMPs in cultured pearl formation has not been revealed yet. The identification and functional characterization of the organic component of the shell provides a better understanding of the circumstances towards the formation of a lustrous pearl. Recently, expression of some SMPs within the pearl sac as well as their potential influence on pearl formation has been examined (Wang et al., 2009; Inoue et al., 2009; Inoue et al., 2010; McGinty et al., 2012). Surprisingly, the expression patterns of SMPs have been found to vary between mantle and the pearl sac (Wang et al., 2009). Again, expression level is related to the quality of the pearl such as higher expression of MSI30 in pearl sac can yield a low quality pearl (Inoue et al., 2009). We also found variation among the expression levels of the SMPs

such as MSI31, KRMP, MSI60, pearlin, linkine, shematrin-1, MSI7 and nacrein expressed higher whereas calmodulin, prisilkin-39, lustrin A, perlucin, dermatopontin and mucoperlin expressed lower (Fig. 3.5, 3.6 and 3.7). Additionally, all the pearls that we obtained after 3 months were not of same quality. Therefore, the genes that regulate $CaCO_3$ supply should be present in high amount for the proper development of pearl, but sometimes shows lower expression (McGinty et al., 2012; Luyer et al., 2019). This indicates that the pearl sac cells probably rely on other sources for $CaCO_3$ supply. Possibly host oyster hemocytes have an influence in this regard during pearl biomineralization.

Though donor mantle primarily functions in pearl biomineralization but the surrounding host hemocytes may also possess a significant role (McGinty et al., 2012; Masaoka et al., 2013; Mount et al., 2004; Li et al., 2016; Huang et al., 2018). Some recent studies focused on the function of hemocytes in shell biomineralization. Heamocytes are involved in transporting the mineral ions to the site of biomineralization as well as in secreting extracellular matrix required for shell formation (Mount et al., 2004; Li et al., 2016; Huang et al., 2018; Ivanina et al., 2017; Ivanina et al., 2018). Despite the facts that hemocytes facilitate in shell formation but it is not well studied how they contribute in pearl formation. As the prepared donor mantle graft contains very little or no hemocytes, therefore, host oyster hemocytes surrounding the pearl sac can influence the pearl biomineralization. But from the present study, it is not possible to find out the role of the host hemocytes in pearl formation. Therefore, further study is needed to know the interactions between different types of biomineralizing cells of molluscs, such as mantle epithelial cells and hemocytes along with their potential specialization in the pearl biomineralization process.

5.1.2.1 Expression changes of SPMs and pearl surface depositions

In spite of having some valuable data obtained from the previous studies, they do not provide a general overview of how the epithelial secretion is organized in pearl since the onset of mineralization (Kawakami, 1952; Taylor et al., 1969; Ma et al., 2007; Cuif et al., 2008, 2011; Liu et al., 2012; Checa et al., 2013). In the present study, together with the expression profiling of the SMPs we also examined the pearl layers in order to characterize the surface aggregates on pearls which in turn determines the quality of the pearl. We have observed two major changes on the surface depositions of pearls that is correlated to our gene expression studies. One is the formation of heterogeneous prismatic layer that has been completed before 1 month and another is the deposition of homogeneous nacreous layer that develops later on the prismatic layer (Fig. 4.2). Furthermore, during the secretion of hetegeneous prismatic layer, we found the prismatic layer forming genes were up-regulated whereas the nacreous layer forming genes were down-regulated (Fig. 3.5, 3.6). On the otherhand, during nacreous layer formation, the genes involved in the formation of nacreous layer were up-regulated with very little or no expression of the prismatic layer forming genes (Fig. 3.5, 3.6).

Microstructural analysis of pearls additionally illustrates that they are essentially inside-out shells with an inner core organic layer that resembles a periostracum being encircled by a prismatic layer first and then an outermost nacreous layer (Fig. 4.2) (Taylor and Strack, 2008). However, this layering may be disrupted depending on the quality of the pearl. On the contrary, the pearl oyster shell usually consists of an outermost organic layer termed as periostracum, and two distinct $CaCO_3$ polymorphs, the outer calcitic prismatic layer and the inner aragonitic nacreous layer (Cuif et al., 2011). Typically, periostracum is a thin proteinaceous layer covering the outer surface of the molluskan

shell which also dictates the type of $CaCO_3$ polymorph that will be deposited in the shell (Saleuddin and Petit, 1983).

The periostracum and prismatic layer secreted only once during the early stage of mineralization, whereas the nacreous layer secreted continuously upto the maturation of the pearl (Fig. 3.5, 3.6). Furthermore, the prismatic layer in pearl contains both aragonitic and calcitic material giving the layer a heterogeneous microstructure (Fig. 3.5, 3.6, 4.2) (Hongyan et al., 2007; Ma et al., 2007; Cuif et al., 2008; Liu et al., 2012). Kawakami (1952) first observed that many pearls contain radially oriented calcite crystals with respect to nucleus surface. These structures showed the similar mineralogical properties as in calcitic prisms existed in the shells of the genus *Pinctada* (Kawakami, 1952; Cuif et al., 2008; Checa et al., 2013).

During intense cell proliferation stage in-depth modification occurs in the mineralizing epithelial cells which may be responsible for the secretion of non-nacreous material (Kawakami, 1952). The nacreous material then deposits onto the nucleus and grows rapidly in a direction perpendicular to the matrix surface (Nudelman et al., 2006). Nacre forms the framework and is mainly composed of aragonite crystals (95-99%) together with organic material such as polysaccharides and proteins (Zhang and Zhang, 2006). Nacre and the organic substances together makes a matrix complex in a brick and mortar (BM) arrangement where the aragonite crystals act as bricks and the organic material act as a biological organic adhesive, therefore the mortar (Jackson et al., 1988; Zhang and Zhang, 2006). Nacre is a highly organized nanostructure and is arranged in a brick-wall like structure in bivalve mollusk (Fig. 4.2) (Gregoire, 1972; Checa et al., 2013). Though nacre is the most desirable layer for a good quality pearl, but cultivated pearls offer a

variety of combinations of structures and mineralogies (Cuif et al., 2011). In addition to aragonite and calcite, vaterite can also be present in pearls.

Pearl quality enhancement is a very crucial aspect in sustaining the pearl farms and is of great challenge. From our transcriptome study, we unraveled the genes involved in the formation of pearl sac that is one of the most important steps of pearl formation. The results obtained from this study will inevitably promote our understanding towards the phenomenon of the production of iridescent pearls by allografting.

References

Addadi, L., Joester, D., Nudelman, F., Weiner, S., 2006. Mollusk shell formation: a source of new concepts for understanding biomineralization processes. *Chem. Eur. J.* 12, 980-987.

Addadi, L., Weiner, S., 1997. A pavement of pearl. *Nature* 389, 912-915.

Alagarswami, K., 1987. Cultured pearls-production and quality, in: K. Alagarswami (Eds.), Pearl Culture, Central Marine Fisheries Research Institute, Cochin, pp. 105-113.

Ansai, S., Kinoshita, M., 2014. Targeted mutagenesis using CRISPR/Cas system in medaka. *Biol. Open* 3, 362-371.

Aoki, S., 1966. Comparative histological observations on the pearl-sac tissues forming nacreous, prismatic and periostracal pearls. *Nippon Suisan Gakkaishi* 32, 1-10.

Armstrong, D.A., Armstrong, J.L., Krassner, S.M., Pauley, G.B., 1971. Experimental wound repair in the black abalone, *Haliotis cracherodii*. *J. Invertebrate Pathol*. 17, 216-227.

Ausubel, F.M., 2005. Are innate immune signaling pathways in plants and animals conserved? *Nat. Immunol*. 6, 973-979.

Avruch, J., Khokhlatchev, A., Kyriakis, J.M., Luo, Z., Tzivion, G., Vavvas, D., 2001. Ras activation of the raf kinase: tyrosine kinase recruitment of the MAP kinase cascade. *Recent Prog Horm Res*. 56(1), 127-155.

Awaji, M., Machii, A., 2011. Fundamental studies on *in vivo* and *in vitro* pearl formation- contribution of outer epithelial cells of pearl oyster mantle and pearl sacs. *Aqua-BioScience Monographs* (ABSM) 4(1), 1-39.

Awaji, M., Suzuki, T., 1995. The pattern of cell proliferation during pearl sac formation in the pearl oyster. *Fish. Sci.* 61(5), 747-751.

Bédouet, L., Schuller, M.J., Marin, F., Milet, C., Lopez, E., Giraud, M., 2001. Soluble proteins of the nacre of the giant oyster Pinctada maxima and of the abalone Haliotis tuberculata: extraction and partial analysis of nacre proteins. *Comp. Biochem. Physiol. B Biochem. Mol. Biol*. 128(3), 389-400.

Bédouet, L., Rusconi, F., Rousseau, M., Duplat, D., Marie, A., Dubost, L., Le Ny, K., Berland, S., Péduzzi, J., Lopez, E., 2006. Identification of low molecular weight molecules as new components of the nacre organic matrix. *Comp. Biochem. Physiol. B Biochem. Mol. Biol*. 144(4), 5 32-43.

Beer, A.C., Southgate, P.C., 2000. Collection of pearl oyster (family Pteriidae) spat at Orpheus Island Great Barrier Reef (Australia). *J. Shellfish Res.* 19, 821-826.

Belcher, A.M., Wu, X.H., Christensen, R.J., Hansma, P.K., Stucky, G.D. Morse, D.E., 1996. Control of crystal phase switching and orientation by soluble mollusc-shell proteins. *Nature* 381, 56-58.

Bénédicte, L., Salmena, L., Bidère, N., Su, H., Matysiak-Zablocki, E., Murakami, K., 2007. Essential role for caspase-8 in toll-like receptors and NF-κB signaling. *J. Biol. Chem.* 282(10), 7416-7423.

Beniash, E., Ivanina, A., Lieb, N.S., Kurochkin, I., Sokolova, I.M., 2010. Elevated level of carbon dioxide affects metabolism and shell formation in oysters *Crassostrea virginica* (Gmelin). *Mar. Ecol. Prog. Ser*. 419, 95-108.

Bhattacharya, D., Marfo, C.A., Li, D., Lane, M., Khokha, M.K., 2015. CRISPR/Cas9: An inexpensive, efficient loss of function tool to screen human disease genes in Xenopus. *Dev. Biol.* 408, 196-204.

Blay, C., Planes, S., Ky, C.L., 2017. Donor and recipient contribution to phenotypic traits and the expression of biomineralisation genes in the pearl oyster model *Pinctada margaritifera*. *Sci. Rep.* 7(1), 2696.

Blay, C., Planes, S., Ky, C.L., 2018. Cultured pearl surface quality profiling by the shell matrix protein gene expression in the biomineralised pearl sac tissue of *Pinctada margaritifera*. *Mar. Biotechnol.* 20(4), 490-501.

Bray, N.L., Pimentel, H., Melsted, P., Pachter, L., 2016. Near-optimal probabilistic RNA-seq quantification. *Nat. Biotechnol.* 34(5), 525-527.

Carter, J., 1980. Environmental and biological controls of bivalve shell mineralogy and microstructure. In: Skeletal growth of aquatic organisms. Rhoads, D.C., Lutz, R.A. (Eds.), New York, Plenum Press, 69-113.

Cavelier, P., Cau, J., Morin, N., Delsert, C., 2017. Early gametogenesis in the Pacific oyster: new insights using stem cell and mitotic markers. *J. Exp. Biol.* 220, 3988-3996.

Chang, N., Sun, C., Gao, L., Zhu, D., Xu, X., Zhu, X., Xiong, J.W., Xi, J.J., 2013. Genome editing with RNA-guided Cas9 nuclease in zebrafish embryos. *Cell Res.* 23, 465-472.

Checa, A., 2000. A new model for periostracum and shell formation in Unionidae (Bivalvia, Mollusca). *Tissue Cell* 32, 405-416.

Checa, A.G., Cartwright, J.H.E. Willinger, M.G., 2009. The key role of the surface membrane in why gastropod nacre grows in towers. *Proc. Natl. Acad. Sci. U.S.A.* 106, 38-43.

Checa, A.G., Cartwright, J.H.E., Willinger, M.G., 2013. Mineral bridges in nacre revisited. In: Watabe, S., Maeyama, K., Nagasawa, H. (eds), Recent Advances in

Pearl Research. *Proc. International Symposium Pearl Res. 2011*. TERRAPUB, Tokyo, pp 109-123.

Chellam, A., Victor, A., Dharmaraj, S., Velayudhan, T., Rao, K.S., 1991. Pearl oyster farming and pearl culture. *FAO Corporate Doc. Repository*. http://eprints.cmfri.org.in/id/eprint/6847.

Chen, C., Fenk, L.A., de Bono, M., 2013. Efficient genome editing in *Ceanorhabditis elegans* by CRISPR-targeted homologous recombination. *Nucleic Acids Res.* 41, e193.

Chen, S., Lee, B., Lee, A.Y., Modzelewski, A.J., He, L., 2016 .Highly efficient mouse genome editing by CRISPR ribonucleoprotein electroporation of zygotes. *J. Biol. Chem.* 291, 14457-14467.

Chen, Y.F., Qian, G.Y., 2009. Studies on the formation of pearl sac in vitro of epithelial cells and tissue from mantle. *J. Hydroecol*. 2, 74-77.

Cho, S.W., Kim, S., Kim, J.M., Kim, J.S., 2013. Targeted genome engineering in human cells with the Cas9 RNA-guided endonuclease. *Nat. Biotechnol.* 31, 230-232.

Cho, S.W., Lee, J., Carroll, D., Kim, J.S., Lee, J. 2013. Heritable gene knockout in *Caenorhabditis elegans* by direct injection of Cas9-sgRNA ribonucleoproteins. *Genetics* 195, 1177-1180.

Choi, Y.H., Chang, Y.J., 2003. Gametogenic cycle of the transplanted-cultured pearl oyster, *Pinctada fucata martensii* (Bivalvia: Pteriidae) in Korea. *Aquaculture* 220, 781-790.

Clark, M.S., Thorne, M.A., Vieira, F.A., Cardoso, J.C., Power, D.M., Peck, L.S., 2010. Insights into shell deposition in the Antarctic bivalve *Laternula elliptica*: gene discovery in the mantle transcriptome using 454 pyrosequencing. *BMC Genomics* 11, 362.

Cochennec-Laureau, N., Montagnani, C., Saulnier, D., Fougerouse, A., Levy, P., Lo, C., 2010. A histological examination of grafting success in pearl oyster *Pinctada margaritifera* in French Polynesia. *Aquat. Living Resour.* 23, 131-140.

Cochennec-Laureau, N., Montagnani, C., Saulnier, D., Fougerouse, A., Levy, P., Lo, C.A., 2010. Histological examination of grafting success in pearl oyster *Pinctada margaritifera* in French Polynesia. *Aquat Living Resour.* 23, 131-140.

Cong, L., Ran, F.A., Cox, D., Lin, S., Barretto, R., Habib, N., Hsu, P.D., Wu, X., Jiang, W., Marraffini, L.A., Zhang, F., 2013. Multiplex genome engineering using CRISPR/Cas systems. *Science* 339, 819-823.

Crenshaw, M.A., 1972. The inorganic composition of molluscan extrapallial fluid. *Biol. Bull.* 143, 506-512.

Cuif, J.P., Ball, A.P., Dauphin, Y., Farre, B., Nouet, J., Perez-Huerta, A., Salomé, M., Williams, C.T., 2008. Structural, mineralogical and biochemical diversity in the lower part of the pearl layer of cultivated seawater pearls from Polynesia. *Microsc Microanal.* 14, 405-417.

Cuif, J.P., Dauphin, Y., Howard, L., Nouet, J., Rouziere, S., Salome, M., 2011. Is the pearl layer a reversed shell? A re-examination of the theory of pearl formation through physical characterizations of pearl and shell developmental stages in *Pinctada margaritifera*. *Aquat Living Resour.* 24, 41-424.

Dakin, W.J., 1913. Pearls. In: Giles, P., Litt, D., Seward, A.C. (Eds.), The Cambridge Manuals of Science and Literature. Cambridge University Press, London. 103 pp.

Dang, Y., Jia, G., Choi, J., Ma, H., Anaya, E., Ye, C., Shankar, P., Wu, H., 2015. Optimizing sgRNA structure to improve CRISPR–Cas9 knockout efficiency. *Genome Biol.* 16, 280.

Dickinson, G. H., Matoo, O. B., Tourek, R. T., Sokolova, I. M., Beniash, E., 2013. Environmental salinity modulates the effects of elevated CO2 levels on juvenile hard-shell clams, *Mercenaria mercenaria*. *J. Exp. Biol.* 216, 2607-2618.

Dix, T. G., 1973. Histology of the mantle and pearl sac of pearl oysters *Pinctada maxima* (Lamellibranchia). *J. Malacol. Soc. Aust.* 2, 365-375.

Du, X., Jiao, Y., Deng, Y.W., Wang, Q.H.R., 2010. Ultrastructure of the pearl sac cells of pearl oyster *Pinctada martensii*. *Acta Oceanol. Sin.* 32, 160-164.

Duan, J., Lu, G., Xie, Z., Lou, M., Luo, J., Guo, L., Zhang, Y., 2014. Genome-wide identification of CRISPR/Cas9 off-targets in human genome. *Cell Res.* 24, 1009-1012.

Eddy, L., Affandi, R., Kusumorini, N., Sani, Y., Manal, W., 2015. The pearl sac formation in male and female *Pinctada maxima* host oysters implanted with allograft saibo. *HAYATI J. Biosci.* 22, 122-129.

Ellis, S., Haws, M., 1999. Producing pearls using the black-lip pearl oyster (*Pinctada margaritifera*). *Aquafarmer Inf. Sheet.* 8 pp.

Falini, G., Albeck, S., Weiner, S., Addadi, L., 1996. Control of aragonite or calcite polymorphism by mollusk shell macromolecules. *Science*. 271, 67-69.

Fang, Z., Feng, Q., Chi, Y., Xie, L., Zhang, R., 2008. Investigation of cell proliferation and differentiation in the mantle of *Pinctada fucata* (Bivalve, Mollusca). *Mar Biol.* 153, 745-754.

Fougerouse, A., Rousseau, M., Lucas, J.S., 2008. Soft tissue anatomy, shell structure and biomineralization. In: Southgate, P.C, Lucas, A.B. (Eds.), The pearl oyster. Elsevier, Amsterdam, 77-99 pp.

Fu Y, Foden, J.A., Khayter, C., Maeder, M.L., Reyon, D., Joung, J.K., Sander, J.D., 2013. High-frequency off-target mutagenesis induced by CRISPR-Cas nucleases in human cells. *Nat. Biotechnol.* 31, 822-826.

Fu, D., Zhang, Y., Xiao, S., Yu, Z., 2011. The first homolog of a *TRAF7* (TNF receptor associated factor 7) gene in a mollusk, *Crassostrea hongkongensis*. *Fish Shellfish Immunol.* 31, 1208-1210.

Funabara, D., Ohmori, F., Kinoshita, S., Koyama, H., Mizutani, S., Ota, A., Osakabe, Y., Nagai, K., Maeyama, K., Okamoto, K., Kanoh, S., Asakawa, S., Watabe, S., 2014. Novel genes participating in the formation of prismatic and nacreous layers in the pearl oyster as revealed by their tissue distribution and RNA interference knockdown. *PLoS One*. 9(1), e84706.

Funakoshi, S., 2000. Studies on the classification, structure and function of hemocytes in bivalves. *Bull. Natl. Res. Inst. Aquaculture* 29, 1-103.

Furuhashi, T., Schwarzinger, C., Miksik, I., Smrz, M., Beran, A., 2009. Molluscan shell evolution with review of shell calcification hypothesis. *Comp. Biochem. Physiol. B Biochem. Mol. Biol.* 154, 351-371.

Gao, J., Chen, Y., Yang, Y., Liang, J., Xie, J., Liu, J., Li, S., Zheng, G., Xie, L., Zhang, R., 2016. The transcription factor Pf-POU3F4 regulates expression of the matrix protein genes aspein and prismalin-14 in pearl oyster (*Pinctada fucata*). *FEBS J.* 283(10), 1962-1978.

Garcia-Gasca, A., Ochoa-Baez, J.R.I., Betancourt, M., 1994. Microscopic anatomy of the mantle of the pearl oyster *Pinctada magatianica* (Hanley, 1856). *J. Shellfish Res.* 13, 85-92.

Gasiunas, G., Barrangou, R., Horvath, P., Siksnys, V., 2012. Cas9-crRNA ribonucleoprotein complex mediates specific DNA cleavage for adaptive immunity in bacteria. *PNAS* 109, E2579-E2586.

Gervis, M.H., Sims, N.A., 1992. The biology and culture of pearl oysters (Bivalvia: Pteriidae). International Centre for Living Aquatic Resources Management (ICLARM) Studies and Reviews, 21: 49 pp.

Grabherr, M.G., Haas, B.J., Yassour, M., Levin, J.Z., Thompson, D.A., Amit, I., Adiconis, X., Fan, L., Raychowdhury, R., Zeng, Q., Chen, Z., Mauceli, E., Hacohen, N., Gnirke, A., Rhind, N., di Palma, F., Birren, B.W., Nusbaum, C., Lindblad-Toh, K., Friedman, N., Regev, A., 2011. Full-length transcriptome assembly from RNA-seq data without a reference genome. *Nat Biotechnol.* 29, 644-652.

Gratz, S.J., Cummings, A.M., Nguyen, J.N., Hamm, D.C., Donohue, L.K., Harrison, M.M., Wildonger, J., O'Connor-Giles, K.M., 2013. Genome engineering of Drosophila with the CRISPR RNA-guided Cas9 nuclease. *Genetics* 4, 1029-1035.

Gregoire, C., 1972. Structure of the molluscan shell. In: Florkin, M., Scheer, B.T. (Eds.), Chemical Zoology. Academic Press, New York, 45-102 pp.

Gu, Z., Yin, X., Yu, C., Zhan, X., Shi, Y., Wang, A., 2016, Expression profiles of nine bio mineralization genes and their relationship with pearl nacre thickness in the pearl oyster, *Pinctada fucata martensii* Dunker. *Aquaculture Res.* 47, 1874-1884.

Gueguen, Y., Montagnani, C., Joubert, C., Marie, B., Belliard, C., Tayale, A., Fievet, J., Levy, P., Piquemal, D., Marin, F., Moullac, G.L., Ky, C.L., Garen, P., Lo, C., Saulnier, D., 2013. Characterization of molecular processes involved in the pearl formation in *Pinctada margaritifera* for a sustainable development of pearl

farming industry in French Polynesia. In: Watabe, S., Maeyama, K., Nagasawa, H. (Eds.), Recent advances in pearl research -Proceedings of the International Symposium on Pearl Research, 2011. 184-194 pp.

Gyrd-Hansen, M., Meier, P., 2010. IAPs: from caspase inhibitors to modulators of NF-κB, inflammation and cancer. *Nat. Rev. Cancer.* 10, 561-574.

Haszprunar, G., Wanninger, A., 2012. Molluscs. *Curr. Biol.* 22, 510-514.

Haynes, L.M., Moore, D.D., Kurt-Jones, E.A., Finberg, R.W., Anderson, L.J., Tripp, R.A., 2001. Involvement of toll-like receptor 4 in innate immunity to respiratory syncytial virus. *J. Virol.* 75, 10730-10737.

Herbst, R.S., 2004. Review of epidermal growth factor receptor biology. *Int. J. Radiat. Oncol. Biol. Phys.* 59, Suppl 2, 21-26.

Hoang, Q.Q., Sicheri, F., Howard, A.J., Yang, D.S., 2003. Bone recognition mechanism of porcine osteocalcin from crystal structure. Nature, 425(6961), 977-980.

Hongyan, M.A., Beili, Z., LEE, I.S., Zuolu, Q., Zhangfa, T., Shuheng, Q.I.U., 2007. Aragonite observed in the prismatic layer of seawater-cultured pearls. *Front. Mater. Sci. China* 1(3), 326-329.

Hsu, P.D., Scott, D.A., Weinstein, J.A., Ran, F.A., Konermann, S., Agarwala, V., Li, Y., Fine, E.J., Wu, X., Shalem, O., Cradick, T.J., Marraffini, L.A., Bao, G., Zhang, F., 2013. DNA targeting specificity of RNA-guided Cas9 nucleases. *Nat. Biotechnol.* 31, 827-832.

Huang, B., Zhang, L., Du, Y., Li, L., Qu, T., Meng, J., Zhang, G., 2014. Alternative splicing and immune response of *Crassostrea gigas* tumor necrosis factor receptor associated factor 3. *Mol. Biol. Rep.* 41, 6481-6491.

Huang, B., Zhang, L., Du, Y., Li, L., Tang, X., Zhang, G., 2016. Molecular characterization and functional analysis of tumor necrosis factor receptor-associated factor 2 in the Pacific oyster. *Fish Shellfish Immunol.* 48, 12-19.

Huang, D.X., Wei, G.J., He, M.X., 2015a. Cloning and gene expression of signal transducers and activators of transcription (*STAT*) homologue provide new insights into the immune response and nucleus graft of the pearl oyster *Pinctada fucata*. *Fish Shellfish Immunol.* 47, 847-854.

Huang, L., Li, G.Y., Mo, Z.L., Xiao, P., Li, J., Huang, J., 2015b. *De Novo* assembly of the Japanese flounder (*Paralichthys olivaceus*) spleen transcriptome to identify putative genes involved in immunity. *PLoS One* 10(2), e0117642.

Huang, J., Li, S., Liu, Y., Liu, C., Xie, L., Zhang, R., 2018. Hemocytes in the extrapallial space of *Pinctada fucata* are involved in immunity and biomineralization. *Sci. Rep.* 8, 4657.

Huang, X.D., Liu W.G., Guan, Y.Y., Shi, Y., Wang, Q., Zhao, M., Wu, S.Z., He, M.X., 2012a. Molecular cloning, characterization and expression analysis of tumor necrosis factor receptor-associated factor 3 (*TRAF3*) from pearl oyster *Pinctada fucata*. *Fish Shellfish Immunol.* 33, 652-658.

Huang, X.D., Liu, W.G., Guan, Y.Y., Shi, Y., Wang, Q., Zhao, M., Wu, S.Z., He M.X., 2012b. Molecular cloning and characterization of class I *NF-κB* transcription factor from pearl oyster (*Pinctada fucata*). *Fish Shellfish Immunol.* 33:659-666.

Ikmi, A., McKinney, S.A., Delventhal, K.M., Gibson, M.C., 2014. TALEN and CRISPR/Cas9-mediated genome editing in the early branching metazoan *Nematostella vectensis*. *Nat. Commun.* 5, 5486.

Imler, J.L., Zheng, L., 2004. Biology of toll receptors: lessons from insects and mammals. J. Leukoc. *Biol.* 75, 18-26.

Inoue, N., Ishibashi, R., Ishikawa, T., Atsumi, T., Aoki, H., Komaru, A., 2011. Can the quality of pearls from the Japanese pearl oyster (*Pinctada fucata*) be explained by the gene expression patterns of the major shell matrix proteins in the pearl sac?. *Mar. Biotechnol. (NY)* 13(1), 48-55.

Ivanina, A.V., Borah, B.M., Vogts, A., Malik, I., Wu, J., Chin, A.R., Almarza, A.J., Kumta, P., Piontkivska, H., Beniash, E., Sokolova, I.M., 2018. Potential trade-offs between biomineralization and immunity revealed by shell properties and gene expression profiles of two closely related *Crassostrea* species. *J. Exp. Biol.* 221, jeb183236.

Ivanina, A.V., Falfushynska, H.I., Beniash, E., Piontkivska, H., Sokolova, I.M., 2017. Biomineralization-related specialization of hemocytes and mantle tissues of the Pacific oyster *Crassostrea gigas*. *J. Exp. Biol.* 220, 3209-3221.

Jackson, A.P., Vincent, J.F.V., Turner, R.M., 1988. The mechanical design of nacre. *Proc. R. Soc. Lond. B* 23, 415-440.

Jasin, M., Haber, J.E., 2016. The democratization of gene editing: Insights from site-specific cleavage and double-strand break repair. *DNA Repair (Amst.)* 44, 6-16.

Jiang, W., Bikard, D., Cox, D., Zhang, F., Marraffini, L.A., 2013. RNA-guided editing of bacterial genomes using CRISPR-Cas systems. *Nat. Biotechnol.* 31, 233–239.

Jiao, Y., Tian, Q.L., Du, X.D., Wang, Q.H., Huang, R.L., Deng, Y.W., Shi, S.L., 2014. Molecular characterization of tumor necrosis factor receptor-associated factor (*TRAF6*) in pearl oyster *Pinctada martensii*. *Genet. Mol. Res.* 13(4), 10545-10555.

Jinek, M., Chylinski, K., Fonfara, I., Hauer, M., Doudna, J.A., Charpentier, E., 2012. A programmable dual-RNA-guided DNA endonuclease in adaptive bacterial immunity. *Science* 337, 816-821.

Jinek, M., Jiang, F., Taylor, D.W., Sternberg, S.H., Kaya, E., Ma, E., Anders, C., Hauer, M., Zhou, K., Lin, S., Kaplan, M., Iavarone, A.T., Charpentier, E., Nogales, E., Doudna, J.A., 2014. Structures of Cas9 endonucleases reveal RNA-mediated conformational activation. *Science* 343, 1247997.

Jones, D.B., Jerry, D.R., Forêt, S., Konovalov, D.A., Zenger, K.R., 2013. Genome-wide SNP validation and mantle tissue transcriptome analysis in the silver-lipped pearl oyster, *Pinctada maxima. Marine Biotechnol.* 15(6), 647–658.

Joubert, C., Piquemal, D., Marie, B., Manchon, L., Pierrat, F., Zanella-Cléon, I., Cochennec-Laureau, N., Gueguen, Y., Montagnani, C., 2010. Transcriptome and proteome analysis of *Pinctada margaritifera* calcifying mantle and shell: focus on biomineralization. *BMC Genomics* 11, 613.

Kamat, S., Su, X., Ballarini, R., Heuer, A.H., 2000. Structural basis for the fracture toughness of the shell of the conch *Strombus gigas*. *Nature* 405, 1036-1040.

Kanzok, S.M., Hoa, N.T., Bonizzoni, M., Luna, C., Huang, Y., Malacrida, A.R., Zheng, L., 2004. Origin of toll-like receptor-mediated innate immunity. *J. Mol. Evol.* 58, 442-448.

Kawakami, I.K., 1952. Studies on pearl formation. On the regeneration and transformation of the mantle piece in the pearl oyster. *Mem Fac Kyushu Univ (Ser E)* 1, 83-89.

Kawakami, I.K., 1953. Studies on pearl-sac formation II. The effect of water temperature and freshness of transplant on pearl-sac formation. *Ann. Zool. Japan* 26, 217-223.

Kiefert, L., McLaurin-Moreno, D., Arizmendi, E., Hanni, H.A., Elen, S., 2004. Cultured pearls from the Gulf of California, Mexico. *Gems Gemmology* 40, 26-38.

Kim, S., Kim, D., Cho, S.W., Kim, J., Kim, J.S., 2014. Highly efficient RNA-guided genome editing in human cells via delivery of purified Cas9 ribonucleoproteins. *Genome Res.* 24, 1012-1019.

Kinoshita, S., Wang, N., Inoue, H., Maeyama, K., Okamoto, K., Nagai, K., Kondo, H., Hirono, I., Asakawa, S., Watabe S., 2011. Deep sequencing of ESTs from nacreous and prismatic layer producing tissues and a screen for novel shell formation-related genes in the pearl oyster. *PLoS ONE* 6, e21238.

Kishore, P., Southgate, P.C., 2016. A detailed description of pearl-sac development in the black-lip pearl oyster, *Pinctada margaritifera* (Linnaeus 1758). *Aquac. Res.* 47, 2215-2226.

Kong, Y., Jing, G., Yan, Z., Li, C., Gong, N., Zhu, F., Li, D., Zhang, Y., Zheng, G., Wang, H., Xie, L., Zhang, R., 2009. Cloning and characterization of prisilkin-39, a novel matrix protein serving a dual role in the prismatic layer formation from the oyster *Pinctada fucata*. *J. Biol. Chem.* 284(16), 10841-10854.

Kotani, H., Taimatsu, K., Ohga, R., Ota, S., Kawahara, A., 2015. Efficient multiple genome modifications induced by the crRNAs, tracrRNA and Cas9 protein complex in zebrafish. *PLoS One* 10, e0128319.

Kripa, V., Mohamed, K.S., Appukuttan, K.K., Velayudhan, T.S., 2007. Production of Akoya pearls from the southwest coast of India. *Aquaculture* 262, 347-354.

Krishna, M., Narang, H., 2008. The complexity of mitogen-activated protein kinases (MAPKs) made simple. *Cell Mol. Life Sci.* 65, 3525-3544.

Kröger, N., Lorenz, S., Brunner, E., Sumper, M., 2002. Self-assembly of highly phosphorylated silaffins and their function in biosilica morphogenesis. *Science* 298(5593), 584-586.

Ky, C., Broustal, F., Koua, M.S., Quillien, V., Beliaeff, B., 2018. Donor effect on cultured pearl nacre development and shell matrix gene expression in *Pinctada margaritifera* reared in different field sites. *Aquac. Res.* 49, 1934-1943.

Lee, J.S., Kwak, S.J., Kim, J., Kim, A.K., Noh, H.M., Kim, J.S., Yu, K., 2014. RNA-guided genome editing in *Drosophila* with the purified Cas9 protein. *G3 (Bethesda)* 4, 1291-1295.

Lemaitre, B., Nicolas, E., Michaut, L., Reichhart, J.M., Hoffmann, J.A., 1996. The dorsoventral regulatory gene cassette spatzle/toll/cactus controls the potent antifungal response in *Drosophila* adults. *Cell* 86, 973-983.

Lewis, T.S., Shapiro, P.S., Ahn, N.G., 1998. Signal transduction through MAP kinase cascades. *Adv. Canc. Res.* 74, 49-139.

Li, C., Qu, T., Huang, B., Ji, P., Huang, W., Que, H., Li, L., Zhang, G., 2015. Cloning and characterization of a novel caspase-8-like gene in *Crassostrea gigas*. Fish Shellfish Immunol. 46, 486-492.

Li, H., Zhang, B., Fan, S., Liu, B., Su, J., Yu, D., 2017. Identification and Differential Expression of Bio mineralization Genes in the Mantle of Pearl Oyster *Pinctada fucata*. *Marine Biotechnology* 19(3): 266-276.

Li, S., Liu, C., Huang, J., Liu, Y., Zhang, S., Zheng, G., Xie, L., Zhang, R., 2016. Transcriptome and biomineralization responses of the pearl oyster *Pinctada fucata* to elevated CO2 and temperature. *Sci Rep.* 6, 18943.

Li, S., Liu, Y., Huang, J., Zhan, A., Xie, L., Zhang, R., 2017. The receptor genes *PfBMPR1B* and *PfBAMBI* are involved in regulating shell biomineralization in the pearl oyster *Pinctada fucata*. Sci Rep. 7, 9219.

Li, S., Liu, Y., Liu, C., Huang, J., Zheng, G., Xie, L., 2016. Hemocytes participate in calcium carbonate crystal formation, transportation and shell regeneration in the pearl oyster *Pinctada fucata*. *Fish Shellfish Immunol.* 51, 263-270.

Liu, C., Li, S., Kong, J., Liu, Y., Wang, T., Xie, L., Zhang, R., 2015a. In-depth proteomic analysis of shell matrix proteins of *Pinctada fucata*. *Sci Rep.* 5, 17269.

Liu, J., Yang, D., Liu, S., Li, S., Xu, G., Zheng, G., Xie, L., Zhang, R., 2015b. Microarray: a global analysis of biomineralization related gene expression profiles during larval development in the pearl oyster, *Pinctada fucata*. *BMC Genomics* 16, 325.

Liu, X., Li, J., Xiang, L., 2012. The role of matrix proteins in the control of nacreous layer deposition during pearl formation. *Proc. R. Soc. B.* 279, 1000-1007.

Liu, X., Li, J., Xiang, L., Sun, J., Zheng, G., Zhang, G., Wang, H., Xie, L., Zhang, R., 2012. The role of matrix proteins in the control of nacreous layer deposition during pearl formation. *Proc. Biol. Sci.* 279, 1000-1007.

Livak, K.J., Schmittgen, T.D., 2001. Analysis of relative gene expression data using realtime quantitative PCR and the 2^{DDCT} CT method. *Methods* 25, 402-408.

Love, M.I., Huber, W., Anders, S., 2014. Moderated estimation of fold change and dispersion for RNA-seq data with DESeq2. *Genome Biol.* 15, 550.

Lowenstam, H.A., 1981. Minerals formed by organisms. *Science* 211, 1126.

Lowenstam, H.A., Weiner, S., 1989. On Bio mineralization. Oxford University Press, London. pp. 7-23.

Luyer, J.L., Auffret, P., Quillien, V., Leclerc, N., Reisser, C., Vidal-Dupiol, J., Ky, C.L., 2019. Whole transcriptome sequencing and bio mineralization gene architecture associated with cultured pearl quality traits in the pearl oyster, *Pinctada margaritifera*. *BMC Genomics* 20, 111.

Ma, H., Zhang, B., Lee, I.S., Qin, Z., Tong, Z., Qiu, S., 2007. Aragonite observed in the prismatic layer of seawater cultured pearls. *Front. Mater. Sci. Chin.* 1, 326-329.

Machii, A., 1968. Histological studies on the pearl sac formation. *Bull. Nat. Pearl Res. Lab.* 13, 1489-1539.

Machii, A., Nakahara, H., 1957. Studies on the histology of the pearl-sac, II. On the speed of the pearl-sac formation different by season. *Bull. Nat. Pearl. Res. Lab.* 2, 107-112.

Mali, P., Yang, L., Esvelt, K.M., Aach, J., Guell, M., DiCarlo, J.E., Norville, J.E., Church, G.M., 2013. RNA-guided human genome engineering via Cas9. *Science* 339, 823-826.

Marie, B., Joubert, C., Tayalé, A., Zanella-Cléon, I., Belliard, C., Piquemal, D., Cochennec-Laureau, N., Marin, F., Gueguen, Y., Montagnani, C., 2012. Different secretory repertoires control the biomineralization processes of prism and nacre deposition of the pearl oyster shell. *Proc. Natl. Acad. Sci.* 109, 20986-20991.

Marin, F., Luquet, G., 2004. Molluscan shell proteins. *Comptes Rendus Palevol* 3, 469-492.

Masaoka, T., Samata, T., Nogawa, C., Baba, H., Aoki, H., Kotaki, T., Nakagawa, A., Sato, M., Fujiwara, A., Kobayashi T., 2013. Shell matrix protein genes derived from donor expressed in pearl sac of Akoya pearl oysters (*Pinctada fucata*) under pearl culture. *Aquaculture* 384, 56-65.

Matlins, A., 2001. The pearl book: the definitive buying guide – how to select, buy, care for and enjoy pearls. Gemstone Press, 3-19 pp.

Mazzitelli, J.Y., Bonnafe, E., Klopp, C., Escudier, F., Geret, F., 2017. *De novo* transcriptome sequencing and analysis of freshwater snail (*Radix balthica*) to

discover genes and pathways affected by exposure to oxazepam. *Ecotoxicology* 26, 127-140.

McGinty, E.L., Evans, B.S., Taylor, J.U., Jerry, D.R., 2010. Xenografts and pearl production in two pearl oyster species, *P. maxima* and *P. margaritifera*: effect on pearl quality and a key to understanding genetic contribution. *Aquaculture* 302, 175-181.

McGinty, E.L., Zenger, K.R., Jones, D.B., Jerry, D.R., 2012. Transcriptome analysis of biomineralisation-related genes within the pearl sac: host and donor oyster contribution. Mar. Genomics. 5, 27-33.

McGinty, E.L., Zenger, K.R., Taylor, J.U., Evans, B.S., Jerry, D.R., 2011. Diagnostic genetic markers unravel the interplay between host and donor oyster contribution in cultured pearl formation. *Aquaculture* 316, 20-24.

McIlwain, D.R., Berger, T., Mak, T.W., 2013. Caspase functions in cell death and disease. *Cold Spring Harb Perspect Biol.* 5, a008656.

Meyers, M.A., Lin, A.Y., Chen, P., Muyco, J., 2008. Mechanical strength of abalone nacre: role of the soft organic layer. *J Mech Behav Biomed Mater* 1, 76-85.

Miyamoto, H., Miyashita, T., Okushima, M., Nakano, S., Morita, T., Matsushiro, A., 1996. A carbonic anhydrase from the nacreous layer in oyster pearls. *Proc. Natl. Acad. Sci. USA* 93, 9657-9660.

Miyamoto, H., Miyoshi, F., Kohno, J., 2005. The carbonic anhydrase domain protein nacrein is expressed in the epithelial cells of the mantle and acts as a negative regulator in calcification in the mollusc *Pinctada fucata*. *Zoolog. Sci.* 22, 311-315.

Miyashita, T., Takagi, R., Miyamoto, H., Matsushiro, A., 2002. Identical carbonic anhydrase contributes to nacreous or prismatic layer formation in *Pinctada fucata* (Mollusca: Bivalvia). *Veliger* 45, 250-255.

Miyazaki, Y., Nishida, T., Aoki, H., Samata, T., 2010. Expression of genes responsible for biomineralization of *Pinctada fucata* during development. *Comparative Biochemistry and Physiology, Part B* 155, 241-248.

Mohamed, K.S., Kripa, V., Velayudhan, T.S., Appukuttan, K.K., 2006. Growth and biometric relationships of the pearl oyster, *Pinctada fucata* (Gould) on transplanting from the Gulf of Mannar to the Arabian Sea. *Aquaculture Research* 37, 725-741.

Mojica, F.J., Diez-Villasenor, C., Garcia-Martinez, J., Almendros, C., 2009. Short motif sequences determine the targets of the prokaryotic CRISPR defence system. *Microbiology* 155, 733-740.

Montagnani, C., Marie, B., Marin, F., Belliard, C., Riquet, F., Tayalé, A., Zanella-Cléon, I., Fleury, E., Gueguen, Y., Piquemal, D., Cochennec-Laureau, N., 2011. Pmarg-pearlin is a matrix protein involved in nacre framework formation in the pearl oyster *Pinctada margaritifera*. *Chembiochem.* 12, 2033-2043.

Moreno-Mateos, M.A., Vejnar, C.E., Beaudoin, J.D., Fernandez, J.P., Mis, E.K, Khokha, M.K., Giraldez, A.J., 2015. CRISPRscan: designing highly efficient sgRNAs for CRISPR-Cas9 targeting *in vivo*. *Nat. Methods.* 12 (10): 982-988.

Mortazavi, A., Williams, B.A., McCue, K., Schaeffer, L., Wold, B., 2008. Mapping and quantifying mammalian transcriptomes by RNA-seq. *Nat. Methods* 5, 621-628.

Mount, A.S., Wheeler, A.P., Paradkar, R.P., Snider, D., 2004. Hemocyte mediated shell mineralization in the eastern oyster. *Science* 304, 297-300.

Nagai, K., 2013. A history of the cultured pearl industry. *Zoolog. Sci.* 30(10), 783-93.

Nagai, K., 2013. The iridescence of pearls and the cultured-pearl industry. In S. Watabe, K. Maeyama, Nagasawa, H. (Eds.), Recent advances in pearl research (pp. 19–35). Tokyo, Japan Terrapub.:

Nakahara, H & Machii, A, 1956, Studies on the histology of the pearl sac. I. Histological observations of pearl-sac tissues which produce normal and abnormal pearls. *Bull. Natl. Pearl Res. Lab.* 1, 10-13 (in Japanese with English abstract).

Nakahara, H., Bevelander, G., 1971. The formation and growth of the prismatic layer of *Pinctada radiata*. *Calcif. Tissue Res.* 7, 31-45.

Nishimasu, H., Ran, F.A.A., Hsu, P.D.D., Konermann, S., Shehata, S.I.I., Dohmae, N., Ishitani, R., Zhang, F., Nureki, O., 2014. Crystal structure of Cas9 in complex with guide RNA and target DNA. *Cell* 156, 935-949.

Niu Y, Shen, B., Cui, Y., Chen, Y., Wang, J., Wang, L., Kang, Y., Zhao, X., Si, W., Li, W., Xiang, A.P., Zhou, J., Guo, X., Bi, Y., Si, C., Hu, B., Dong, G., Wang, H., Zhou, Z., Li, T., Tan, T., Pu, X., Wang, F., Ji, S., Zhou, Q., Huang, X., Ji, W., Sha, J., 2014. Generation of gene-modified cynomolgus monkey via Cas9/RNA-mediated gene targeting in one-cell embryos. *Cell* 156, 836-843.

Nogawa, C., Obara, M., Ozawa, M., Sato, A., Watanabe, A., Yamazaki, R., Yamada, D., Akiniwa, K., Samata, T., 2008. Characterization of organic matrix components of pearl oyster, *Pinctada fucata* and their implications in shell formation Frontiers of Material Science in China, 2: 156. of marine bivalves. Springer, Dordrecht, pp 73-93.

Nudelman, F., Gotliv, B.M., Addadi, L., Weiner, S., 2006. Mollusk shell formation: Mapping the distribution of organic matrix components underlying a single aragonitic tablet in nacre. J. Structural Biology 153, 176-187.

Ohashi, K., Burkart, V., Flohé, S., Kolb, H., 2000. Cutting edge: heat shock protein 60 is a putative endogenous ligand of the toll-like receptor-4 complex. *J. Immunol.* 164, 558-561.

Ohmori, F., Kinoshita, S., Funabara, D., Koyama, H., Nagai, K., Maeyama, K., Okamoto, K., Asakawa, S., Watabe, S., 2018. Novel isoforms of N16 and N19 families implicated for the nacreous layer formation in the pearl oyster *Pinctada fucata*. *Mar. Biotechnol.* 20, 155-167.

Okumura, T., Suzuki, M., Nagasawa, H., Kogure, T., 2012. Microstructural variation of biogenic calcite with intracrystalline organic macromolecules. *Cryst. Growth Des.* 12, 224-230.

Ota, S., Hisano, Y., Muraki, M., Hoshijima, K., Dahlem, T.J., Grunwald, D.J., Okada, Y., Kawahara, A., 2013. Efficient identification of TALEN-mediated genome modifications using heteroduplex mobility assays. *Genes Cells* 18, 450-458.

Paine, M.L., Snead, M.L., 1997. Protein interactions during assembly of the enamel organic extracellular matrix. *J. Bone Miner. Res.* 12(2), 221-227.

Pattanayak, V., Lin, S., Guilinger, J.P., Ma, E., Doudna, J.A., Liu, D.R., 2013. High-throughput profiling of off-target DNA cleavage reveals RNA-programmed Cas9 nuclease specificity. *Nat. Biotechnol.* 31, 839-843.

Pauley, G.B., Heaton, L.H., 1969. Experimental wound repair in the freshwater mussel *Anodonta oregonensis*. *J. Invertebrate Pathol.* 13, 241-249.

Pe´rez-Huerta, A., Cuif, J., Dauphin, Y., Cusack, M., 2014. Crystallography of calcite in pearls. *European Journal of Mineralogy* 26, 507-516.

Peng, K., Liu, F., Wang, J., Hong, Y., 2018. Calmodulin highly expressed during the formation of pearl sac in freshwater pearl mussel (*Hyriopsis schlegelii*). *Thalassas: An International Journal of Marine Sciences* 34(1), 219.

Perry, K.J., Henry, J.Q., 2015. CRISPR/Cas9-mediated genome modification in the Mollusc, *Crepidula fornicate*. *Genesis* 53, 237-244.

Petit, H., Davis, W.L., Jones, R.G., Hagler, H.K., 1980. Morphological studies on the calcification process in the fresh-water mussel *Amblema*. *Tissue Cell* 12, 13-28.

Pimentel, H., Bray, N.L., Puente, S., Melsted, P., Pachter, L., 2017. Differential analysis of RNA-seq incorporating quantification uncertainty. *Nat. Methods* 14(7), 687-690.

Qian, X., Ba, Y., Zhuang, Q.F., Zhong, G.F., 2014. RNA-seq technology and its application in fish transcriptomics. OMICS 18, 98-110.

Qu, F., Xiang, Z., Xiao, S., Wang, F., Li, J., Zhang, Y, Qin, Y., Yu, Z., 2017. c-Jun N-terminal kinase (JNK) is involved in immune defense against bacterial infection in *Crassostrea hongkongensis*. *Dev. Comp. Immunol.* 67, 77-85.

Qu, F., Xiang, Z., Zhang, Y., Li, J., Xiao, S., Zhang, Y., Mao, F., Ma, H., Yu, Z., 2016. A novel p38 MAPK indentified from *Crassostrea hongkongensis* and its involvement in host response to immune challenges. *Mol. Immunol.* 79, 113-124.

Qu, T., Huang, B., Zhang, L., Li, L., Xu, L., Huang, W., Li, C., Du, Y., Zhang, G., 2014. Identification and functional characterization of two executioner caspases in *Crassostrea gigas*. *PLoS One* 9, e89040.

Riedl, S.J., Shi, Y., 2004. Molecular mechanisms of caspase regulation during apoptosis. *Nat. Rev. Mol. Cell Biol.* 5, 897-907.

Ries, J. B., Cohen, A.L., McCorkle, D.C., 2009. Marine calcifiers exhibit mixed responses to CO2-induced ocean acidification. *Geology* 37, 1131-1134.

Roach, J.C., Glusman, G., Rowen, L., Kaur, A., Purcell, M.K., Smith, K.D, Hood, L.E., Aderem, A., 2005. The evolution of vertebrate toll-like receptors. *Proc. Natl. Acad. Sci.* 102, 9577-9582.

Rouet, P., Smih, F., Jasin, M., 1994. Introduction of double-strand breaks into the genome of mouse cells by expression of a rare-cutting endonuclease. *Mol. Cell. Biol.* 14, 8096-8106.

Rudin, N., Sugarman, E., Haber, J.E., 1989. Genetic and physical analysis of double-strand break repair and recombination in *Saccharomyces cerevisiae*. *Genetics* 122, 519-534.

Ruiz-Rubio, H., Acosta-Salmón, H., Olivera, A., Southgate, P.C., Rangel-Dávalos, C., 2006. The influence of culture method and culture period on quality of half-pearls ('mabé') from the winged pearl oyster *Pteria sterna*, Gould, 1851. *Aquaculture* 254, 269-274.

Runnegar, B., 1985. Shell microstructures of Cambrian mollusc replicated by phosphate. *Alcheringa* 9, 245-257.

Saleuddin, A.S.M., Petit, H.P., 1983. The mode of formation and the structure of the periostracum. In: Saleuddin ASM, Wilbur KM (eds). Mollusca Vol. 4, Physiology Part 1. Academic Press, New York, 199–234.

Samata, T., Hayashi, N., Kono, M., Hasegawa, K., Horita, C., Akera, S., 1999. A new matrix protein family related to the nacreous layer formation of *Pinctada fucata*. *FEBS Lett.* 462, 225-229.

Saruwatari, K., Matsui, T., Mukai, H., Nagasawa, H., Kogure, T., 2009. Nucleation and growth of aragonite crystals at the growth front of nacres in pearl oyster, *Pinctada fucata*. *Biomaterials* 30(16), 3028–3034.

Schmitt, N., Marin, F., Thomas, J., Plasseraud, L., Demoy-Schneider, M., 2018. Pearl grafting: Tracking the biological origin of nuclei by straightforward immunological methods. *Aquac. Res.* 49, 692-700.

Scoones, R.J.S., 1990. Research on practices in the Western Australian cultured pearl industry. Fishing industry research project and development council project. NP12. July 1987 to June 1990. Broome Pearl Pty. Ltd. And MG Kailis Group of Companies. 74 pp.

Scoones, S.J.R., 1996. The development of the pearl sac in *Pinctada maxima* (Jameson,1901) (Lamellibranchia: Pteriidae) and the implications for the quality of cultured pearls. MSc Thesis, The University of Western Australia. Perth, 89 p.

See N. Landman et al., *Pearls* (2001).

Shah, S.A., Erdmann, S., Mojica, F.J., Garrett, R.A., 2013. Protospacer recognition motifs: mixed identities and functional diversity. *RNA Biol.* 10, 891-899.

Shen, X., Belcher, A.M., Hansma, P.K., Stucky, G.D., Morse, D.E., 1997. (Title). *J. Biol. Chem.* 272, 32472-32481.

Shigeta, M., Sakane, Y., Iida, M., Suzuki, M., Kashiwagi, K., Kashiwagi, A., Fujii, S., Yamamoto, T., Suzuki, K.T., 2016. Rapid and efficient analysis of gene function using CRISPRCas9 in Xenopus tropicalis founders. *Genes to Cells* 21, 755-771.

Shuman, S., Glickman, M.S., 2007. Bacterial DNA repair by non-homologous end joining. *Nat. Rev. Microbiol.* 5, 852-861.

Silke, J., Meier, P., 2013. Inhibitor of apoptosis (IAP) proteins–modulators of cell death and inflammation. *Cold Spring Harb Perspect Biol.* 5, a008730.

Skelton, P.W., Benton, M.J., 1993. Mollusca: rostroconchia, scaphopoda and bivalvia. In: Benton M.J. (Eds.), The Fossil Record 2. Chapman & Hall, London: 237-263 pp.

Slaymaker, I.M., Gao, L., Zetsche, B., Scott, D.A., Yan, W.X., Zhang, F., 2016. Rationally engineered Cas9 nucleases with improved specificity. *Science* 351, 84-88.

Sminia, T., Pietersma, K., Scheerboom, J.E.M., 1973. Histological and ultrastructural observations on wound healing in the freshwater pulmonate *Lymnaea stagnalis*. *Z. Zellforsch.* 41, 561-573.

Song, L.S., Wang, L.L., Zhang, H., Wang, M.Q., 2015. The immune system and its modulation mechanism in scallop. *Fish Shellfish Immunol.* 46, 65-78.

Southgate, P.C., Lucas, J.S., 2008. The pearl oyster. Oxford: Elsevier, 544 p.

Strack, E., 2008. Introduction. In: Southgate, P.C., Lucas, J.S. (Eds.), The pearl oyster. Elsevier Press, Oxford, 1-35 pp.

Sudo, S., Fujikawa, T., Nagakura, T., Ohkubo, T., Sakaguchi, K., Tanaka, M., Nakashima, K., Takahashi, T., 1997. Structures of mollusk shell framework proteins. *Nature* 387, 563-564.

Sun, J., Xu, G., Wang, Z., Li, Q., Cui, Y., Xie, L., Zhang, R., 2015. The effect of NF-κB signalling pathway on expression and regulation of nacrein in pearl oyster, *Pinctada fucata*. *PLoS One* 10(7), e0131711.

Sun, L., Huan, P., Wang, H., Liu, F., Liu, B., 2014. An *EGFR* gene of the Pacific oyster *Crassostrea gigas* functions in wound healing and promotes cell proliferation. Mol. Biol. Rep. 41(5), 2757-2765.

Suzuki, M., Murayama, E., Inoue, H., Ozaki, N., Tohse, H., Kogure, T., Nagasawa, H., 2004. Characterization of prismalin-14, a novel matrix protein from the prismatic layer of the Japanese pearl oyster (*Pinctada fucata*). *Biochem. J.* 382, 205-213.

Suzuki, M., Nagasawa, H., 2013. Mollusk shell structures and their formation mechanism. *Can. J. Zool.* 91, 349-366.

Suzuki, M., Saruwatari, K., Kogure, T., Yamamoto, Y., Nishimura, T., Kato, T., Nagasawa, H., 2009. An acidic matrix protein, Pif, is a key macromolecule for nacre formation. *Science* 325, 1388–1390.

Suzuki, T., Funakoshi, S. 1992. Isolation and a fibronectin-like molecule from a marine bivalve, *Pinctada fucata*, and its secretion by amebocytes. *Zool. Sci.* 9, 541-550.

Suzuki, T., Yoshinaka, R., Mizuta, S., Funakoshi, S., Wada, K., 1991. Extracellular matrix formation by amebocytes during epithelial regeneration in the pearl oyster *Pinctada fucata*. *Cell Tissue Res.* 266, 75-82.

Takeda, K., Akira, S., 2005. Toll-like receptors in innate immunity. *Int. Immunol.* 17, 1-14.

Takeuchi, T., Endo, K., 2006. Biphasic and dually coordinated expression of the genes encoding major shell matrix proteins in the pearl oyster *Pinctada fucata*. *Mar. Biotechnology* 8, 52-61.

Takeuchi, T., Kawashima, T., Koyanagi, R., Gyoja, F., Tanaka, M., Ikuta, T., Shoguchi, E., Fujiwara, M., Shinzato, C., Hisata, K., Fujie, M., Usami, T., Nagai, K., Maeyama, K., Okamoto, K., Aoki, H., Ishikawa, T., Masaoka, T., Fujiwara, A., Endo, K., Endo, H., Nagasawa, H., Kinoshita, S., Asakawa, S., Watabe, S., Satoh, N., 2012. Draft genome of the pearl oyster *Pinctada fucata*: a platform for understanding bivalve biology. *DNA Res*. 19(2), 117-130.

Takeuchi, T., Koyanagi, R., Gyoja, F., Kanda, M., Hisata, K., Fujie, M., Goto, H., Yamasaki, S., Nagai, K., Morino, Y., Miyamoto, H., Endo, K., Endo, H., Nagasawa, H., Kinoshita, S., Asakawa, S., Watabe, S., Satoh, N., Kawashima, T., 2016. Bivalve-specific gene expansion in the pearl oyster genome: implications of adaptation to a sessile lifestyle. *Zoological Lett*. 2, 3.

Takeuchi, T., Sarashina, I., Iijima, M., Endo, K., 2008. *In vitro* regulation of $CaCO_3$ crystal polymorphism by the highly acidic molluscan shell protein aspein. *FEBS Lett.* 582, 591-596.

Tanguy, A., Guo, X., Ford, S.E., 2004. Discovery of genes expressed in response to *Perkinsus marinus* challenge in Eastern (*Crassostrea virginica*) and Pacific (*C. gigas*) oysters. *Gene* 338,121-131.

Tayale, A., Gueguen, Y., Treguier, C., Le Grand J.L., Cochennec-Laureau, N., Montagnani, C., Ky, C.L., 2012. Evidence of donor effect on cultured pearl quality from a duplicated grafting experiment on *Pinctada margaritifera* using wild donors. *Aquat. Living Resour.* 25, 269-280.

Taylor, J.D., Kennedy, W.J., 1969. The influence of the periostracum on the shell structure of bivalve molluscs. *Calcif. Tissue Res.* 3, 274-283.

Taylor, J.J., 2002. Producing golden and silver south sea pearls from Indonesian hatchery reared *Pinctada maxima*, in: World Aquaculture 2002 Book of Abstracts. Beijing, P. R. Of China, Apr 23-27, World Aquaculture Society, Baton Rouge LA.

Taylor, J.J., Strack, E., 2008. Pearl production. In: Southgate PC, Lucas JS, editors. The pearl oyster. Amsterdam: Elsevier, p. 273-302.

Torrey, R.D., Sheung, B., 2008. The pearl market. In: Southgate, P.C., Lucas, J.S., (Eds.). The pearl oyster. Elsevier, Amsterdam, 357-365 pp.

Tsan, M.F., Gao, B., 2004. Heat shock protein and innate immunity. *Cell Mol. Immunol.* 1(4), 274-279.

Van Noort, J.M., Bsibsi, M., Nacken, P., Gerritsen, W.H., Amor, S., 2012. The link between small heat shock proteins and the immune system. *Int. J. Biochem. Cell Biol.* 44, 1670-1679.

Varshney, G.K., Pei, W., LaFave, M.C., Idol, J., Xu, L., Gallardo, V., Carrington, B., Bishop, K., Jones, M., Li, M., Harper, U., Huang, S.C., Prakash, A., Chen, W., Sood, R., Ledin, J., Burgess, S.M., 2015. High-throughput gene targeting and phenotyping in zebrafish using CRISPR/Cas9. *Genome Res.* 25, 1030-1042.

Vejnar C.E., Moreno-Mateos M.A., Cifuentes, D., Bazzini, A.A., Giraldez, A.J., 2016 Optimized CRISPR–Cas9 system for genome editing in zebrafish. *Cold Spring Harb. Protoc.* doi: 10.1101/pdb.prot086850.

Velayudhan, T.S., Chellam, A., Dharmaraj, S., Victor, A.C.C., Alagarswami, K., 1994. Histology of the mantle and pearl-sac formation in the Indian pearl oyster *Pinctada fucata* (Gould). *Indian J Fish.* 41(2), 70-75.

Wada, K., 1968. Mechanism of growth of nacre in bivalvia. *Bull. Natl. Pearl Res. Lab.* 13, 1561–1596.

Wada, K., Komaru, A., 1996. Color and weight of pearls produced by grafting the mantle tissue from a selected population for white shell color of the Japanese pearl oyster *Pinctada fucata martensii* (Dunker). *Aquaculture* 142(1), 25-32.

Wada, K.T., Temkin, I., 2008. Taxonomy and Phylogeny. In: Southgate, P.C., Lucas, J.S. (Eds.). The Pearl Oyster. Elsvier, Amsterdam, 37-66 pp.

Waller, T.R., 1980. SEM of the shell and mantle in the order Arcoida (Mollusca, Bivalvia). Smithson. Contrib. Zool. No. 313. pp. 1–58.

Wang, L., Song, X., Song, L., 2018a. The oyster immunity. *Dev. and Comp. Immunol.* 80, 99-118.

Wang, M., Wang, L., Jia, Z., Yi, Q., Song, L., 2018b. The various components implied the diversified toll-like receptor (TLR) signaling pathway in mollusk *Chlamys farreri*. *Fish Shellfish Immun.* 74, 205-212.

Wang, M., Yang, J., Zhou, Z., Qiu, L., Wang, L., Zhang, H., Gao, Y., Wang, X., Zhang, L., Zhao, J., Song, L., 2011. A primitive toll-like receptor signaling pathway in mollusk Zhikong scallop *Chlamys farreri*. *Dev. Comp. Immunol.* 35, 511-520.

Wang, M.Q., Wang, L.L., Guo, Y., Sun, R., Yue, F., Yi, Q.L., Song, L., 2015. The broad pattern recognition spectrum of the toll-like receptor in mollusk Zhikong scallop *Chlamys farreri*. *Dev. Comp. Immunol.* 52, 192-201.

Wang, N., Kinoshita, S., Riho, C., Maeyama, K., Nagai, K., Watabe, S., 2009. Quantitative expression analysis of nacreous shell matrix protein genes in the process of pearl biogenesis. *Comp. Biochem. Physiol.* B 154, 346-350.

Wang, W., Wu, Y., Lei, Q., Liang, H., Deng, Y., 2017. Deep transcriptome profiling sheds light on key players in nucleus implantation induced immune response in the pearl oyster *Pinctada martensii*. *Fish Shellfish Immunol.* 69, 67-77.

Wang, W., Zhang, T., Wang, L., Xu, J., Li, M., Zhang, A., Qiu, L., Song, L., 2016a. A new non-phagocytic TLR6 with broad recognition ligands from Pacific oyster *Crassostrea gigas*. *Dev. Comp. Immunol.* 65, 182-190.

Ward, F., 1995. Pearls. Gem Book Publishers, 64 pp.

Watabe, N., 1965. Studies on shell formation. XI crystal–matrix relationships in the inner layer of mollusk shells. *J. Ultrastruct. Res.* 12, 351-370.

Watabe, N., 1983. Shell repair. In: Saleuddin ASM, Wilbur KM (eds). Mollusca Vol. 4, Physiology Part 1. Academic Press, New York, 289-316.

Wei, J., Liu, B., Fan, S., Li, H., Chen, M., Zhang, B., Su, J., Meng, Z., Yu, D., 2017a. Differentially expressed immune-related genes in hemocytes of the pearl oyster *Pinctada fucata* against allograft identified by transcriptome analysis. *Fish Shellfish Immunol.* 62, 247-256.

Wei, J., Fan, S., Liu, B., Zhang, B., Su, J., Yu, D., 2017b. Transcriptome analysis of the immune reaction of the pearl oyster *Pinctada fucata* to xenograft from *Pinctada maxima*. *Fish Shellfish Immunol.* 67, 331-345.

Wu, Y., Liang, H., Wang, Z., Lei, Q., Xia, L., 2017. A novel toll-like receptor from the pearl oyster *Pinctada fucata martensii* is induced in response to stress. *Comp. Biochem. Physiol. B Biochem. Mol. Biol.* 214, 19-26.

Xiang, Z., Qu, F., Qi, L., Zhang, Y., Tong, Y., Yu, Z., 2013. Cloning, characterization and expression analysis of a caspase-8 like gene from the Hong Kong oyster, *Crassostrea hongkongensis*. *Fish Shellfish Immunol.* 35, 1797-1803.

Xie, C., Mao, X., Huang, J., Ding, Y., Wu, J., Dong, S., Kong, L., Gao, G., Li, C.Y., Wei, L., 2011. KOBAS 2.0: a web server for annotation and identification of enriched pathways and diseases. Nucleic Acids Res. 39, W316-W322.

Xie, L., Zhang, R., 2009. Cloning and characterization of prisilkin-39, a novel matrix protein serving a dual role in the prismatic layer formation from the oyster *Pinctada fucata*. *J. Biol. Chem.* 284, 10841-10854.

Xin, L.S., Wang, M.Q., Zhang, H., Li, M.J., Wang, H., Wang, L.L., Song, L., 2016. The categorization and mutual modulation of expanded MyD88s in *Crassostrea gigas*. *Fish Shellfish Immunol.* 54, 118-127.

Yan, F., Jiao, Y., Deng, Y., Du, X., Huang, R., Wang, Q., Chen, W., 2014. Tissue inhibitor of metalloproteinase gene from pearl oyster *Pinctada martensii* participates in nacre formation. *Biochem. Biophys. Res. Commun.* 450, 300-305.

Yano, M., Nagai, K., Morimoto, K., Miyamoto, H., 2007. A novel nacre protein N19 in the pearl oyster *Pinctada fucata*. *Biochem. Biophys. Res. Commun.* 326, 158-163.

Yano, M., Nagain, K., Morimoto, K., Miyamoto, H., 2006. Shematrin: a family of glycine-rich structural proteins in the shell of the pearl oyster *Pinctada fucata*. *Comp. Biochem. Physiol. B: Biochem. Mol. Biol.* 144, 254-262.

Yukihira, H., Klumpp, D.W., 2006. The pearl oysters, *Pinctada maxima* and *Pinctada margaritifera*, respond in different ways to culture in dissimilar environments. *Aquaculture* 252(2-4), 208-224.

Zhang, C., Zhang, R., 2006. Matrix proteins in the outer shells of molluscs. *Mar. Biotechnology* 8, 572-586.

Zhang, H., Huang, X., Shi, Y., Liu, W., He, M., 2018. Identification and analysis of an *MKK4* homologue in response to the nucleus grafting operation and antigens in the pearl oyster, *Pinctada fucata*. *Fish Shellfish Immunol.* 73, 279-287.

Zhang, L.L., Li, L., Guo, X.M., Litman, G.W., Dishaw, L.J., Zhang, G.F., 2015. Massive expansion and functional divergence of innate immune genes in a protostome. *Sci. Rep.* 5, 8693.

Zhang, Y., He, X., Yu, F., Xiang, Z., Li, J., Thorpe, K.L., Yu, Z., 2013. Characteristic and functional analysis of toll-like receptors (TLRs) in the lophotrocozoan, *Crassostrea gigas*, reveals ancient origin of TLR-mediated innate immunity. *PLoS One* 8, e76464.

Zhang, Y., Xie, L., Meng, Q., Jiang, T., Pu, R., Chen, L., Zhang, R., 2003. A novel matrix protein participating in the nacre framework formation of pearl oyster *Pinctada fucata*. *Comp. Biochem. Physiol. B: Biochem. Mol. Biol.* 135, 565-573.

Zhang, Y.L., Dong, C., 2005. MAP kinases in immune responses. *Cell Mol. Immunol.* 2(1), 20-27.

Zhao, M., He, M., Huang, X., Wang, Q., 2014. A homeodomain transcription factor gene, *PfMSX*, activates expression of pif gene in the pearl oyster *Pinctada fucata*. *PLoS One* 9(8), e103830.

Zhao, M., Shi, Y., He, M., Huang, X., Wang, Q., 2016. PfSMAD4 plays a role in biomineralization and can transduce bone morphogenetic protein-2 signals in the pearl oyster *Pinctada fucata*. *BMC Dev. Biol.* 16, 9.

Zhao, X., Wang, Q., Jiao, Y., Huang, R., Deng, Y., Wang, H., Du, X., 2012. Identification of genes potentially related to biomineralization and immunity by transcriptome analysis of pearl sac in pearl oyster *Pinctada martensii*. *Mar. Biotechnol. (NY)* 14, 730-739.

Zheng, Q., Wang, X.J., 2008. GOEAST: a web-based software toolkit for Gene Ontology enrichment analysis. *Nucleic Acids Res.* 36, W358-W363.

Zheng, X., Cheng, M., Xiang, L., Liang, J., Xie, L., Zhang, R., 2015. The AP-1 transcription factor homolog Pf-AP-1 activates transcription of multiple biomineral proteins and potentially participates in *Pinctada fucata* biomineralization. *Sci. Rep.* 5, 14408.

Zhu, C., Southgate, P., Li, T., 2019. Production of pearls. In: Smaal, A. et al (eds) Goods and services.

Zhu, W., Fan, S., Huang, G., Zhang, D., Liu, B., Bi, X., Yu, D., 2015. Highly expressed *EGFR* in pearl sac may facilitate the pearl formation in the pearl oyster, *Pinctada fucata*. *Gene* 566(2), 201-211.

Zou, J., Wang, R., Li, R., Kong, Y., Wang, J., Ning, X., Zhang, L., Wang, S., Hu, X., Bao, Z., 2015. The genome-wide identification of mitogen-activated protein kinase kinase (*MKK*) genes in Yesso scallop *Patinopecten yessoensis* and their expression responses to bacteria challenges. *Fish Shellfish Immunol.* 45, 901-911.